MASTER'S THESIS

Model-Based Closed-Loop Control of SCR Based DeNOx Systems

For obtaining the degree of
Master of Science in Engineering (MSc.)

Submitted at the University of Applied Science Technikum Kärnten

Degree Program System Design

under the guidance of
FH-Prof. Dipl.-Ing. Dr. Wolfgang Werth

in cooperation with

under the guidance of
Dipl.-Ing. Dr. Christian Roduner

presented by

Dipl.-Ing.(FH) Bernd Hollauf
0710528005

Villach, September 2009

Acknowledgements

This master's thesis was conducted at AVL - List GmbH in Graz (Austria) from November 2008 to September 2009. It was part of the state - aided R & D project B01 / T01 "*Advanced & Alternative Diesel Propulsion Systems: Emission Reduction & Fuel Economy Improvement*".

First of all I would like to thank my supervisors, FH - Prof. Dr. Wolfgang Werth and Dr. Christian Roduner for the excellent guidance through the work on this interesting topic and for their helpful comments on the text. Special thanks to Christian for the many insightful conversations during the development of the ideas within this thesis.

Further I would like to thank Dr. Holger Hülser, the head of the Advanced Software and Electronics Department at AVL, for giving me the possibility to carry out this thesis at AVL.

For their support, their interest and cooperation in this promising field of research I sincerely thank Dipl. - Ing. Michael Glensvig, Dipl. - Ing. Petr Micek, Dr. Martin Schüßler, Dr. Ingo Allmer, Dr. Bernd Breitschädel, Dipl. - Ing.(FH) Thomas Sacher and the entire MOBEO project team at AVL.

Finally, my sincere thanks goes to my best friends Florian, Michael and Patrick for their encouragement and distraction. Above all I express my profound appreciation to my girlfriend Elisabeth for her understanding, patience and happiness even during hard times of this study.

This master's thesis is dedicated to my parents, Caroline and Dietmar Hollauf.

They began my education.
They motivated me to continue it.
They will always contribute to it.

Model-based Closed-Loop Control of SCR Based DeNOx Systems

Ever more stringent emission legislation for vehicles all over the world imposes new challenges in the field of pollutant emissions aftertreatment technologies, their control and diagnosis. A key technology for CI engines to meet future emission standards is Selective Catalytic Reduction (SCR) of nitrogen oxides (NO_x) emissions by means of aqueous urea solution (AdBlue^{TM}). Today, the SCR technology is well known for stationary applications and was already introduced in the past for mobile applications in order to avoid Exhaust Gas Recirculation (EGR) technology which causes fuel economy penalty. Nevertheless, in the future for even more stringent emission standards, a combination of both, EGR and SCR technology will be obligatory to achieve the required low NO_x emission levels. However, the appliance of SCR systems for mobile applications has to overcome the problem of achieving optimal reduction rates of NO_x emissions under the constraints of minimal reducing agent consumption and minimal ammonia (NH_3) breakthrough. Unfortunately, SCR in mobile applications has to face more challenges than compared to stationary applications. Some of these are, for example, lower system temperatures, dynamic operating conditions or limitations in weight and size of the SCR catalyst. In order to minimize the performance losses due to these unfavourable boundary conditions, a high quality control strategy for SCR catalysts is necessary.

Therefore, to face these challenges, a model - based control strategy for SCR systems is developed within this thesis. In order to investigate the important properties of the SCR catalyst, basic experiments using a zeolite - based SCR catalyst on an engine test bed are performed at the beginning. Based on the resultant observations, the requirements for SCR control and the entire control concept are derived. The developed structure of the control algorithm is built in a modular way, which allows the appliance of the control algorithm on various aftertreatment system configurations. Core of the control concept is an one - dimensional control - oriented SCR catalyst model which is verified with a sophisticated simulation model and test bed measurements. Based on this verified SCR model, a control of the ammonia loading surface coverage of the catalyst is developed. In order to adjust in a fast and uncomplicated way the tradeoff between optimal NO_x reduction rates and resultant NH_3 breakthrough, an integrated calibration procedure is developed for the entire control algorithm. At the end of this thesis, the important results of the verification of the entire control concept on an engine test bed under real conditions are presented.

The achieved results within this thesis show that the developed model - based control concept for SCR systems for mobile applications is usable under real conditions and achieves adequate NO_x reduction rates in a transient test cycle. Moreover, the outcome and documented experiences of this work provide a verified control concept for SCR systems, which can be used as a basis for further developments.

Key words: Selective catalytic reduction, Exhaust gas aftertreatment, AdBlue^{TM} Catalytic converter, Model - based control, Control - oriented model

Contents

List of Figures

List of Tables

Abbreviations, Chemical Species and Symbols

Abbreviations

BIBO	–	*Bounded - Input / Bounded - Output*
CI	–	*Compression Ignition*
COM	–	*Control Oriented Model*
CPSI	–	*Cells Per Square Inch*
DCU	–	*Dosing Control Unit*
DOC	–	*Diesel Oxidation Catalyst*
DPF	–	*Diesel Particulate Filter*
EAS	–	*Exhaust Gas Aftertreatment System*
ECU	–	*Engine Control Unit*
EGR	–	*Exhaust Gas Recirculation*
ETC	–	*European Transient Cycle*
FTIR	–	*Fourier - Transform - Infrared - Spectroscopy*
FTP	–	*Federal Test Procedure*
GSA	–	*Geometric Surface Area*
ICE	–	*Internal Combustion Engine*
IMC	–	*Internal Model Control*
LNT	–	*Lean NO_x Trap*
NSR	–	*Nominal Stoichiometric Ratio*
OBD	–	*On Board Diagnostics*
ODE	–	*Ordinary Differential Equation*
OFA	–	*Open Frontal Area*
PDE	–	*Partial Differential Equation*
RPS	–	*Rapid Prototyping System*
SCR	–	*Selective Catalytic Reduction*
SESAM	–	*System for Emission Sampling And Measurement*
SI	–	*Spark Ignition*
SISO	–	*Single - Input / Single - Output*
TWC	–	*Three Way Catalyst*

Chemical Species

$(NH_2)_2CO$	–	*Urea*
CH_4	–	*Methane*
CO	–	*Carbon monoxide*
CO_2	–	*Carbon dioxide*
Cu	–	*Copper*
Fe	–	*Iron*
H_2O	–	*Water*
HC	–	*Hydrocarbons*
$HNCO$	–	*Isocyanic acid*
N_2	–	*Nitrogen*
NH_3	–	*Ammonia*
NO	–	*Nitric oxide*
NO_2	–	*Nitrogen dioxide*
NO_x	–	*Nitrogen oxide*
PM	–	*Particulate Matter*
TiO_2	–	*Titanium dioxide*
V_2O_5	–	*Vanadium pentoxide*
WO_3	–	*Tungsten trioxide*

Symbols

α	–	*Feedratio*	$[-]$
α_c	–	*Heat transfer coefficient to ambient*	$[W/(m^2 \cdot K)]$
β	–	*Tradeoff index*	$[-]$
δ	–	*Monolith total wall thickness*	$[m]$
δ_{Wall}	–	*Monolith wall thickness*	$[m]$
δ_{Wc}	–	*Washcoat thickness*	$[m]$
ϵ	–	*Coverage dependency*	$[-]$
ϵ_g	–	*Open frontal area of monolith*	$[-]$
η	–	*Conversion efficiency*	$[\%]$
γ	–	*Anti - windup weighting factor*	$[-]$
λ	–	*Excess - air ratio*	$[-]$
ω_0	–	*Eigenfrequency of 2^{nd} order system*	$[rad/s]$
ρ	–	*Density*	$[kg/m^3]$
τ	–	*Time constant*	$[s]$
θ	–	*Surface coverage fraction*	$[-]$
Θ	–	*Surface density*	$[mol/m^2]$
θ_{crit}	–	*Critical surface coverage fraction of ammonia*	$[-]$
υ_{ij}	–	*Stoichiometric coefficient of species i in reaction j*	$[-]$
$\bar{\theta}$	–	*Mean surface coverage fraction*	$[-]$
$\bar{x}$	–	*Mean substance amount fraction*	$[mol/mol]$
$\mathbf{\Gamma}$	–	*Stoichiometric matrix*	$[-]$
$\mathbf{\Lambda}$	–	*Coefficient matrix*	$[var.]$
$\theta_{\mathbf{NH_3}}$	–	*Surface coverage fraction of NH_3 (vector)*	$[-]$
$\tilde{\mathbf{c}}_\mathbf{i}$	–	*Combined concentration vector*	$[kmol/m^3]$
$\tilde{\mathbf{T}}_\mathbf{c}$	–	*Combined temperature vector*	$[K]$
$\mathbf{a_R}$	–	*Reactive surface area (matrix)*	$[m^2/m^3]$
$\mathbf{c_i}$	–	*Concentration of reactant i (vector)*	$[kmol/m^3]$
$\mathbf{I}$	–	*Unit matrix*	$[-]$
$\mathbf{r}$	–	*Reaction rate (vector)*	$[kmol/m^2]$
$\mathbf{T_c}$	–	*Catalytic converter temperature (vector)*	$[K]$
$\overset{*}{m}$	–	*Mass flow*	$[kg/s]$
$\overset{*}{n}$	–	*Molar flow*	$[kmol/s]$
$\overset{*}{Q}$	–	*Heat flow*	$[W]$
a	–	*Surface*	$[m^2]$
A	–	*Temperature dependency of NO oxidation*	$[-]$
a_R	–	*Reactive surface area of catalyst*	$[m^2/m^3]$
c	–	*Concentration*	$[kmol/m^3]$
c_p	–	*Heat capacity*	$[J/(kg \cdot K)]$
$CPSI$	–	*Monolith cells density*	$[1/in^2]$
d	–	*Diameter*	$[m]$
d	–	*Damping factor of 2^{nd} order system*	$[-]$

E	–	*Activation temperature of the reaction*	$[K]$
J	–	*Cost function*	$[ppm]$
k	–	*Gain*	[var.]
K	–	*Frequency factor of the reaction*	[var.]
K_{equ}	–	*Temperature dependent equilibrium constant*	$[m^{1.5}/kmol^{0.5}]$
k_p	–	*Controller gain*	$[-]$
l	–	*Length*	$[m]$
m	–	*Mass*	$[kg]$
M	–	*Molecular weight*	$[kg/kmol]$
M_p	–	*Overshoot of* $2^n d$ *order system*	$[-]$
n	–	*Number of CSTR cells in flow direction*	$[-]$
N	–	*Model order*	$[-]$
p	–	*Pressure*	$[Pa]$
p	–	*Individual weighting factor for* $x_{NO_x,ds}$	$[-]$
q	–	*Individual weighting factor for* $x_{NH_3,ds}$	$[-]$
r	–	*Reaction rate*	$[kmol/m^2]$
R	–	*Universal gas constant*	$[J/(K \cdot kmol)]$
s	–	*Monolith repeat thickness*	$[m]$
S	–	*Surface site*	$[-]$
T	–	*Temperature*	$[K]$
T_i	–	*Integral time constant*	$[s/rad]$
t_r	–	*Rising - time*	$[s]$
t_T	–	*Time delay*	$[s]$
v	–	*Flow velocity*	$[m/s]$
V	–	*Volume*	$[m^3]$
x	–	*Substance amount fraction*	$[mol/mol]$
x	–	*Axial position in flow direction*	$[m]$

Subscripts

AB	–	*AdBlue*
ad	–	*Adsorption*
Air	–	*Air*
Amb	–	*Ambient*
C	–	*Catalytic converter*
$crit$	–	*Critical*
d	–	*Desired*
de	–	*Desorption*
ds	–	*Downstream*
EG	–	*Exhaust gas*
equ	–	*Equilibrium*
fst	–	*Fast*
g	–	*Gas phase*
i	–	*Reactant* i
I	–	*First*
II	–	*Second*
j	–	*Reaction rate* j
k	–	k^{th} *cell of CSTR cascade*
lin	–	*Linearised*
max	–	*Maximum*
$norm$	–	*Normalised*
ox	–	*Oxidation*
R	–	*Material production due to reaction*
ref	–	*Reference variable*
slw	–	*Slow*
std	–	*Standard*
us	–	*Upstream*
$Wall$	–	*Wall*
Wc	–	*Washcoat*

Chapter 1

Introduction

This chapter should lead the reader to the main topic of this thesis, the control of an SCR system. Firstly some general remarks are given on internal combustion engines (ICE), their pollutants and entailed exhaust gas aftertreatment and introduces the selective catalytic reduction (SCR) technology for ICE. The intention is to show, beginning from the basics of ICE, the need of such a sophisticated technology to overcome the problem of environmental pollution and to meet future emission legislations.

1.1 General Remarks on IC Engines

Today and in the near future ICE are still the most used nonelectrical drives in modern industry. Their enormous field of applications makes them to an essential component in our daily life. ICE are utilised nearly through all power ratings either for stationary or mobile applications. Some few examples of common use of ICE are [1]:

- Stationary applications
  - Power and heat supply stations
  - Emergency power supplies
  - Power sets
- Mobile applications
  - On - road: passenger cars, commercial vehicles, buses, motorbikes
  - Off - road: agricultural engines, construction machines, etc.
  - Locomotives
  - Aircraft
  - Watercraft

Besides the stationary applications, which are also a huge global industry, the real strength of ICE is in the field of mobile applications. In 2004 more than 827 million vehicles were

registered worldwide and towards 2010 this value will increase up to 1 billion [2]. This growing need of mobility in industrialised countries as well as in emerging markets entails challenges with exhaustible raw materials and increasing pollutants in the atmosphere. To face these problems, worldwide emission standards were defined for ICE by legislation. Therefore, in the last decades the minimisation of fuel consumption[1] and reduction of pollutant emissions at the same or often better performance were the main driving forces for ICE development.

Arising concepts like hybrid systems (combination of ICE with electric motor) in any kind of gradation[2] or all - electric systems seem to be promising and are the right and only way towards the zero - emission vehicle in the long term. Unfortunately, such concepts are too expensive nowadays and do not have not the same power - to - weight ratio and operating range available as comparable pure ICE systems [4]. Hence the ICE will not lose importance in the foreseeable future. The challenge in development of future ICE will be to meet tougher emission standards and to best possible handle the conflict of objectives in

- Fuel economy
- Pollutant emissions
- Convenience and driving dynamics

with respect to customers needs and demands.

1.1.1 Principle of Operation

Characteristic feature common to all commercially successful ICE is the generation of power by converting chemical energy, which is bound in a fuel, into heat and the heat thus produced into mechanical work. The conversion of chemical energy into heat is accomplished by combustion of the fuel using an oxidiser (usually air) in a combustion chamber. Afterwards mechanical work is generated by expansion of the burned air / fuel mixture due to high pressures in the combustion chamber, thus directly applying a force to a movable component of the engine, the piston. The crank mechanism converts the reciprocating movement of the piston in a rotatory motion of the crankshaft. These kind of engines are called reciprocating-piston engines with internal combustion in the literature [5]. In order to get continuous mechanical work out of this procedure, this process is carried out in a cyclic manner several times per seconds in several combustion cambers, called cylinders, of the engine. This causes the crankshaft to turn and to achieve a usable torque.

Table 1.1 shows a principal classification of internal combustion engines with respect to DIN 1940 [6].

[1] Less fuel consumption leads directly to lower carbon dioxide (CO_2) emissions [1].
[2] Distinction between: Micro -, Mild -, Full -, Plug - In - Hybrid [3].

	Internal Combustion Engines	
Induction System	self-inducted / forced-inducted engine	
Mixture Formation	exterior mixture formation (mixture induction) e.g. carburetter engine, intake-manifold injector engine, gas engine	interior mixture formation (air induction) Injection in combustion chamber
Combustion Chamber	Normally one-piece	one-pice: direct injection engine subdivided: prechamber engine swirl-chamber engine
Ignition	Spark ignition (SI) (Otto engine)	Compression ignition (CI) (Diesel engine)
Operating Method	Four-stroke, two-stroke procedure (or Wankel procedure)	

Table 1.1: Classification of internal combustion engines

This kind of classification is very abstract and not often used in daily life. Commonly known is the division of ICE by their ignition, spark ignition (SI) and compression ignition (CI) engines. Both concepts have advantages and disadvantages compared to each other. A brief overview of this is given in table 1.2.

	Spark ignition engines (Otto engine)	Compression ignition engines (Diesel engine)
Advantages	- simple design - high power density - extremly efficient exhaust-gas purification using three-way catalytic converter (TWC)	- very low fuel consumption - long service life - easy to supercharge (Keyword "Downsizing")
Disadvantages	- poor part-load efficency - low fuel efficency	- high pollutant emissions (TWC concept possible) - noisy - engine runs rough

Table 1.2: Comparison of SI and CI engines

According to [7], pollutant emission of SI engines in combination with TWC [3] is or soon will be a “problem solved“ such that the focus of research and development efforts on

[3]Generally, catalytic converters are materials which either increase or decrease chemical reactions without changing of its own properties [6].

the field of SI engines will be redirected towards the improvement of fuel economy (CO_2 emission reduction).

On the other hand, CI engines have a large potential to become much cleaner in the future. Basically, there are two approaches for further reduction of fuel consumption and pollutant emissions of CI engines. One approach is engine modifications, such as

- Exhaust gas turbocharging
- Exhaust gas recirculation (EGR)
- Injection parameter modifications

This is just a brief overview. Investigations on possible engine modifications for simultaneous optimisation of performance and reduction of pollutant emissions are a huge and very exciting area of research in today's automotive industry. With respect to the focus and straightforwardness of this thesis, please refer to [1] [5] [6] [7] [8] for more detailed information on this topic.

The other approach is to reduce pollutant emissions after the engine by applying so-called "exhaust gas aftertreatment systems" (EAS). The next section (1.1.2) provides more detailed information about exhaust gas aftertreatment for CI engines.

1.1.2 Exhaust Gas Aftertreatment for CI Engines

Above-mentioned engine modifications to reduce engine-out[4] emissions and fuel consumption had the benefit in the past to save EAS and therefore a lot of costs. For future tougher emission legislations, engine modifications alone will not be sufficient to meet the needed low pollutant emission with adequate fuel consumption. Thus exhaust gas aftertreatment for CI engines will become more and more important. However a well tuned combination of both, engine modifications and exhaust gas aftertreatment, will be needed to optimise the tradeoff between fuel consumption and pollutant emissions.

Generally, the main harmful exhaust gas components of CI engines are [6]:

- **Hydrocarbons (HC):**
  Caused by incomplete combustion of fossil fuels. They appear in a great variety in the exhaust gas, e.g. methane (CH_4). They are mostly carcinogenic and strong-smelling.
- **Carbon monoxide (CO):**
  Caused by incomplete oxidation of carbon. It is a colourless, inodorous and flavourless gas. Very toxic.

[4] In general, engine-out means the position after the engine, normally after exhaust gas turbocharger, and before EAS.

- **Nitrogen oxide (NO_x):**
  Side product of combustion at high temperatures. NO_x are defined as the sum of nitric oxide (NO) and nitrogen dioxide (NO_2). Nitric oxide is a colourless, inodorous and flavourless gas. Whereas nitrogen dioxide is red - brown, toxic and strong - smelling.

- **Particulate matter (PM):**
  Strong local air deficiency at high temperatures leads to soot particles. They consist mainly of solid carbon. Particulate matter is strong - smelling, carcinogenic and can cause sight obscuration.

Compared to SI engines, CI engines work with excess air during the combustion. Unfortunately this leads to the problem that the TWC concept does not work with CI engines (refer to [5] [7] [8]). Nevertheless, other effective methods for emission purification for CI engines using EAS were developed in the past.

EAS for CI engines consist basically of different catalytic converters[5], typically one for each harmful component which has to be reduced. Generally it can be said, that more or less the same assembly is used for all kinds of catalysts. Modern catalysts consist mostly of a temperature - resistant honeycomb[6] made of ceramic or metal. On this carrier material the so - called washcoat is applied in order to enlarge the surface of the catalyst ($\approx 15000\,m^2$) and therefore to make it more effective. The catalytic material itself is added to the washcoat and is typically precious metal, like platinum or rhodium. The structure of a modern ceramic catalyst is shown in figure 1.1 [6].

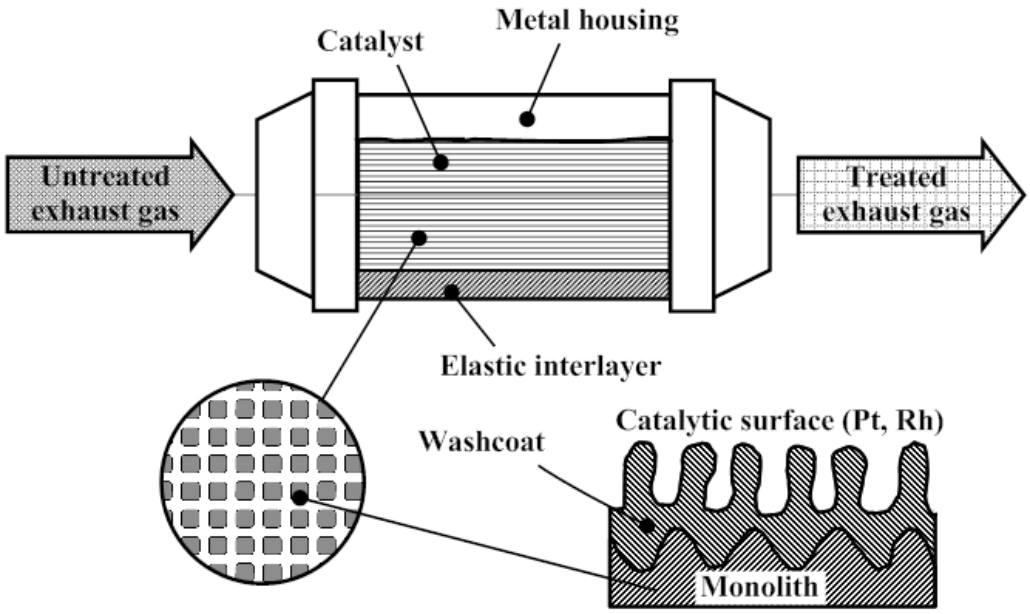

Figure 1.1: Structure of a typical ceramic exhaust catalyst

[5]The term *catalyst* will be used further (shortform).
[6]Often also called *monolith*.

With respect to the above - mentioned harmful engine - out emissions, the following catalyst devices are commonly used in CI engine EAS in order to meet today's and future emissions standards:

- **Diesel oxidation catalyst (DOC):**
  DOC are two - way catalysts. This means they have two simultaneous tasks, the oxidation of CO and HC to CO_2 and H_2O. In contrast, three - way catalysts in SI engines additionally reduce NO_x. But this is due to the working principle of CI engines (excess air) not possible. In addition, DOC also reduce attached hydrocarbons on particles. This leads further to a reduction of PM emissions itself. DOC are also used to oxidise NO to NO_2. Therefore the ratio between NO_2 and NO will be increased. This fact causes a better efficiency of subsequent catalysts like DPF or SCR.

- **Diesel particulate filter (DPF):**
  DPF are applied to remove particulate matter (PM) and soot from the exhaust gas. They are very effective (85% up to 99.9% separation rate of particulate matter [1]) and are commonly designed as ceramic or steel - wool filters. DPF have to be regenerated[7] either continuously (catalytically) or periodically (fuel injection). Drawbacks of DPF are increased fuel consumption of the engine caused by higher back pressure and limited lifetime of the filter itself due to ash accumulation.

- **Lean NO_x trap (LNT):**
  LNT are so - called DeNOx[8] Systems for lean - combustion (CI) engines and are used for reduction of NO_x emissions from the exhaust gas. Their working principle is similar to DPF apart from the fact that they are accumulating NO_x. The cumulated NO_x are regenerated periodically under rich conditions[9]. Drawbacks of LNT are low NO_x reduction (max. 50% conversion efficiency [1]) and the poisoning by sulphur.

- **Selective catalytic reduction (SCR) catalyst:**
  SCR catalysts are also DeNOx Systems for lean - combustion engines. In contrast to LNT, SCR continuously removes NO_x emissions from the exhaust gas by using a reducing agent. DeNOx systems based on SCR achieve high NO_x reduction rates beginning from 80% up to 98% [4]. Detailed information on SCR is given later on in section 1.2.

Of course, every combination of the mentioned catalyst devices can be mounted in the tailpipe of the engine. But not every combination makes sense and also the order of the catalysts in the EAS is important [9].

The main problem of CI engines is the high engine - out emissions of the pollutants NO_x and PM. Unfortunately there is a tradeoff between NO_x and PM emissions. This means, tuning a CI engine to minimum NO_x emissions causes high PM emissions and vice versa.

[7] Regeneration is a process of removing the accumulated soot from the filter.

[8] Reduction of NO_x is shortly called "DeNOx".

[9] Rich condition contains excess of fuel during combustion ($\lambda < 1$). On the opposite, lean condition contains excess of air ($\lambda > 1$).

Therefore, depending on the applied engine modifications, e.g. PM emissions engine - out meet the legislation limit (e.g. Euro V)[10], an EAS should be applied which reduces the resultant high NO_x emissions. A reasonable EAS for this case will be a combination of DOC and a SCR - catalyst connected in series.

1.2 Introduction to SCR

Purification of nitrogen oxide (NO_x) emissions using the principle of selective catalytic reduction (SCR) is known now for several decades. It is an established DeNOx technology since the 1970s for stationary applications such as fossil fuel power plants, refinery heaters or coal - fired cogeneration plants [11]. Coming up with tougher emission standards for mobile diesel applications, especially for heavy - duty vehicles (e.g. Euro V, Euro VI, US2010), the SCR technology was adapted for the use with CI engines. Unfortunately, SCR in mobile applications has to face more challenges than compared to stationary applications. Some of the main challenges are:

- Low operating temperatures
- Higher dynamics in exhaust mass flow
- Permanent change of operating conditions
- Limits in weight and size of SCR catalyst

Thus SCR catalysts in mobile applications need a high quality control strategy to achieve sufficient NO_x reduction rates. However, the application of SCR technology in CI engines brings a lot of advantages. It allows engine modifications straightened to low fuel consumption and low PM emissions. Such an engine adjustment would lead to high engine - out NO_x emissions, which can afterwards be reduced by the SCR system (refer to section 1.1.2).

1.2.1 Process Description

SCR uses ammonia (NH_3) as reducing agent in order to reduce NO_x emissions in the exhaust gas. The resultant exhaust gas species after the reduction process are harmless nitrogen (N_2) and water (H_2O). Since pure NH_3 is toxic and difficult to store on board of a vehicle, various possible reducing agents with more convenient properties have been investigated in the past [12]. Of these investigations, the most promising and today mostly used reducing agent is an eutectic aqueous solution with 32.5% urea ($(NH_2)_2CO$), called AdBlue™ [11]. Because of the fact that the final needed reactive species for SCR is ammonia, the drawback when using reducing agents like AdBlue™ is that there is an additional need for conditioning after its injection into the tailpipe. Therefore, the SCR process for mobile applications can be separated in two areas:

[10] For detailed information on emission standards refer to [10].

[11] Composition of AdBlue™ is standardised by DIN 70070/AUS 32 [11].

- Decomposition of urea / water solution (AdBlue^{TM}) to ammonia
- Reduction of nitrogen oxide due to SCR mechanism

A general scheme of an SCR system for mobile applications is shown in figure 1.2

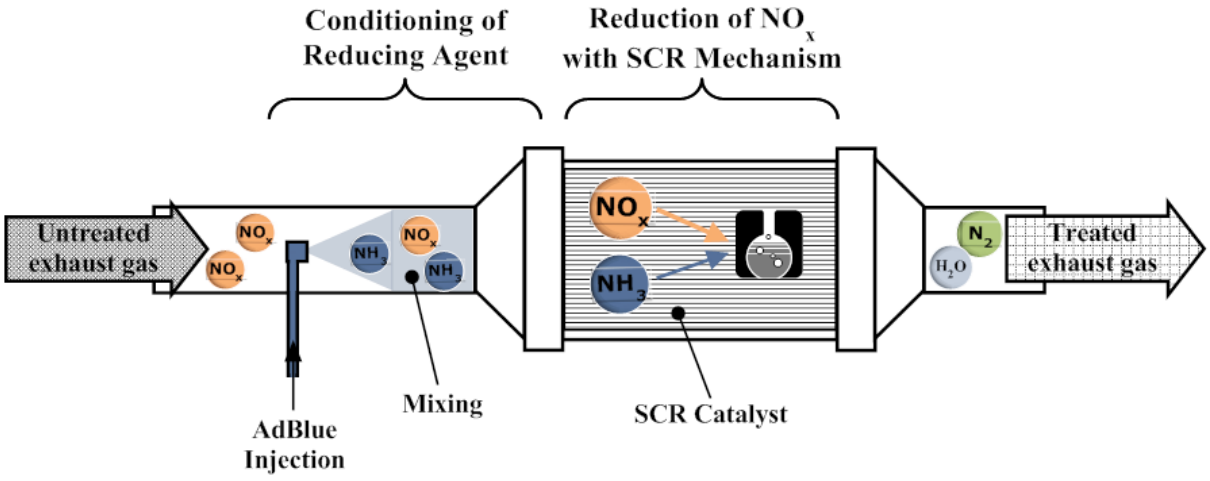

Figure 1.2: General scheme of an AdBlue^{TM} based SCR System

In general, commonly used SCR catalysts are vanadia - based or zeolite - based SCR catalysts. In the past, mostly vanadia - based, especially $V_2O_5/WO_3 - TiO_2$, catalysts were used. A drawback of vanadia - based catalysts is that they can resist temperature above 650°C only for a short time until they deactivate and release vanadia species in the atmosphere. Therefore, more and more zeolite - based SCR catalysts, like Fe - ZSM5 or Cu - ZSM5 are used and investigated. The main advantage of zeolite - based catalysts is that they are more temperature resistant with similar NO_x reduction efficiency compared to vanadia - based SCR catalysts[13].

1.2.2 Dominant Chemical Reactions

As already mentioned, the SCR process can be separated in two areas. The first set of reaction kinetics (equations 1.1 to 1.3) describes the decomposition of the reducing agent AdBlue^{TM} to ammonia. Afterwards, the second set of reaction kinetics (equations 1.4 to 1.6) describes the reduction of NO_x itself by the SCR mechanism.

Primarily, AdBlue^{TM}, consisting of urea ($(NH_2)_2CO$) and water (H_2O), is dosed into the exhaust gas where it immediately evaporates. The urea particles melt[12] and decompose thermally in the exhaust stream into NH_3 and isocyanic acid ($HNCO$). This kind of reaction is called thermolysis [11] in literature and can be described by

$$(NH_2)_2CO(molten) \rightarrow NH_3(gaseous) + HNCO(gaseous). \tag{1.1}$$

[12]Melting point of urea: 132.7 - 135°C.

In a second step, the generated isocyanic acid in combination with water is further decomposed by the so called hydrolysis according to

$$HNCO + H_2O \rightarrow NH_3 + CO_2 \tag{1.2}$$

and produces a second molecule of NH_3. Both reactions (equations 1.1 and 1.2) can be combined together to an overall reaction kinetics which describes the decomposition of urea to ammonia given by

$$(NH_2)_2CO(molten) + H_2O(gaseous) \rightarrow 2NH_3(gaseous) + CO_2(gaseous). \tag{1.3}$$

According to this equation, out of one molecule urea, two molecules ammonia can be produced. Because of the fact that urea melts at temperatures above 135°C, no dosing of reducing agent should be done at temperatures below this threshold. This may foul and deactivate the SCR catalyst presumably due to the production of polymeric species which mask the catalyst surface [11].

The second set of reaction kinetics describes the reduction of NO_x itself by the SCR mechanism. Under normal operating conditions, an SCR catalyst can be described with three dominant chemical reaction kinetics (equations 1.4, 1.5, 1.6). The first and simplest variant of the NO_x reduction in combination with NH_3 is the so - called "standard SCR" reaction:

$$4NH_3 + 4NO + O_2 \rightarrow 4N_2 + 6H_2O. \tag{1.4}$$

According to this equation, only nitric oxide (NO) attends the reaction scheme and will be therefore reduced. The "standard SCR" consumes one mole NH_3 per mole NO. The kinetically favoured SCR reaction is the so - called "fast SCR" reaction and is about ten times faster than equation 1.4:

$$4NH_3 + 2NO + 2NO_2 \rightarrow 4N_2 + 6H_2O. \tag{1.5}$$

The "fast SCR" again consumes one mole NH_3 per mole NO_x and converts as much NO as NO_2. Due to the fact that equation 1.5 is very fast and therefore favoured, an equimolar composition of NO and NO_2 is preferred in the exhaust gas upstream the SCR catalyst. Usually the ratio of NO_2/NO_x in raw exhaust gas of CI engines is in ranges between 0% and 30%. Thus, a DOC is applied upstream the SCR catalyst to increase the NO_2/NO_x ratio up to 50%.

For higher NO_2/NO_x ratios, in case when an overdesigned DOC is placed upstream of the SCR catalyst or if all NO is consumed, the so - called "slow SCR" reaction becomes kinetically favoured:

$$8NH_3 + 6NO_2 \rightarrow 7N_2 + 6H_2O \tag{1.6}$$

The "slow SCR" is much slower than the "fast SCR" reaction and even slower than the "standard SCR" reaction. Therefore its not preferred to have higher NO_2/NO_x ratios than 50% in the exhaust gas upstream the SCR catalyst.

1.3 Motivation and Objectives of the Thesis

1.3.1 Motivation

SCR is a key technology for CI engines to meet tougher future emission standards. The field of possible applications of SCR systems is nearly through all power ratings beginning from passenger cars (PC) up to heavy - duty trucks (HD) and nonroad diesel engines. Today, SCR technology already allows depending on the severity of the emission standard the fulfilment of it, by simultaneous significant fuel economy improvement. By contrast, the competing EGR technology would cause fuel economy penalty. Thus SCR may be more attractive, especially for commercial vehicles where fuel economy is essential. Nevertheless, in the future for even tougher emission standards a combination of both EGR and SCR technology will be obligatory to achieve low NO_x emissions.

From today's point of view, NO_x reduction rates of approximately 85-95% will be need to achieve the required emission levels for NO_x [14]. While for stationary applications such high reduction rates of NO_x are usual, mobile applications have to face more challenges to achieve this performance as well (refer to section 1.2). However, DeNOx is not the only criteria for an SCR catalyst. Also an excellent selectivity regarding NO_x and urea as well as low ammonia slip[13] are needed. Ammonia slip is an undesired secondary emission of the SCR process and will also be limited by emission legislation in the future and causes reducing agent economy penalty.

In order to face all the challenges and requirements of SCR technology for mobile applications, a high quality control algorithm is needed, which considers the dynamics, limits and changing operating conditions of the SCR catalyst as well as the desired control objective.

1.3.2 Objectives

Based on the motivation for this thesis (refer to section 1.3.1), the objectives are defined as follows:

- Development of a state - of - the - art control algorithm for SCR catalysts for mobile applications.
- Control algorithm should allow highest NO_x reduction rates in stationary as well as in dynamic operating conditions.
- Reducing agent consumption and ammonia slip should be kept on a minimum level by the control algorithm.
- Integrated calibration procedure allowing fast and optimal adjustment of the NO_x reduction versus reducing agent consumption tradeoff according to the desired control objective.
- Modular structure of the control algorithm to allow application on various EAS configurations (e.g. different sensor or hardware layouts).

[13] Ammonia slip denotes the breakthrough of ammonia downstream the SCR catalyst.

- Entire control algorithm concept should be verified under real conditions on an engine test bed with an adequate EAS.

It has to be mentioned that it is not an objective of this thesis to deliver a fully verified and fixed - point implemented SCR control algorithm for mass production for an embedded system, like an engine control unit (ECU) as final result. This goal would exceed by far the framework of a thesis. Rather the outcomes and documented experiences of this thesis should provide a verified control concept for SCR catalysts which can be used as a basis for further developments.

The here presented thesis is conducted within the state - aided R & D project B01 / T01 "*Advanced & Alternative Diesel Propulsion Systems: Emission Reduction & Fuel Economy Improvement*".

1.4 Structure of the Thesis

The thesis is structured in following six chapters:

(i) Chapter 1, **Introduction**:
This chapter should lead the reader to the main topic of this thesis, the control of an SCR system. Firstly some general remarks are given on internal combustion engines (ICE), their pollutants and entailed exhaust gas aftertreatment and introduces the selective catalytic reduction (SCR) technology for ICE. The intention is to show, beginning from the basics of ICE, the need of such a sophisticated technology to overcome the problem of environmental pollution and to meet future emission legislations.

(ii) Chapter 2, **Control Concept Definition for SCR Systems**:
The intention of this chapter is to show the investigation of the control concept based on fundamental test bed experiments. At the beginning, general remarks on control theory are given and a common used SCR system with available sensors and actuators is shown. For completeness, also a brief overview of today's already existing control strategies is given. Afterwards basic experiments and main observations are shown and based on these the derivation of the ideal control concept. At the end, the defined control concept with its properties is discussed in detail.

(iii) Chapter 3, **Control - Oriented Catalytic Converter Model**:
Main topic of this chapter is the development of the control - oriented SCR model, which is the core of the investigated control concept from chapter 2. Firstly, a general introduction to chemical reaction engineering is given. Based on this, a detailed description of the derivation of the SCR catalyst equations is made and the considered chemical reaction schemes are discussed. In addition, a useful implementation of the derived catalyst model in a modelling tool is shown. At the end, the verification of the developed SCR model using engine test bed measurements and results from an other simulation model is discussed.

(iv) Chapter 4, **Realisation of Model - Based Control Concept**:
The intention of this chapter is to show how the defined control concept from chapter 2 is conducted and furthermore how the control algorithm is parametrised for the application on the real system. At the beginning, basic experiments with the derived SCR catalyst model are shown. The outcomes of these experiments are discussed and used as input for the controller design. Afterwards, the controller design is performed using the so - called *inward approach*. Based on this, the determination of the optimal reference values for the loading control is shown. Finally, the main outcomes of the chapter are summarised and discussed.

(v) Chapter 5, **Experimental Results**:
The intention of this chapter is to illustrate the validity and the performance of the developed control concept for SCR systems within this thesis. Therefore, the main important test bed results of the model - based control strategy are shown. At the beginning, a short overview of the experimental setup itself is given. Finally, the performance of the loading control of the SCR catalyst in transient engine test cycles is shown and the results are discussed.

(vi) Chapter 6, **Summary and Outlook**: At the end of this thesis, a summary of the main points, outcome and made experiences during the work on this topic is given. Also an outlook for further developments based on the investigations shown here is discussed.

The appendix contains more detailed information on simulation results, test bed measurements and parameter sets. The enclosed CD - ROM contains an online version of this thesis in PDF - format.

Chapter 2

Control Concept Definition for SCR Systems

The intention of this chapter is to show how the control concept is investigated based on fundamental test bed experiments. At the beginning, general remarks on control theory are given and a common used SCR system with available sensors and actuators is shown. For completeness, also a brief overview of today's already existing control strategies is given. Afterwards basic experiments and observations are shown and based on these the derivation of the ideal control concept. At the end, the defined control concept with its properties is discussed in detail.

2.1 Control of an SCR System in General

In order to control a SCR catalyst optimally, an adequate control approach has to be investigated. Thus the entire SCR system has to be analysed regarding its properties and system characteristics. In general, SCR systems are catalytic converters and therefore chemical reactors. In control theory the field of controlling chemical reactors, like SCR catalysts, is named generally *process control*. This notation comes from chemical engineering, because in this discipline many control tasks have to deal with the problem of control of feed materials[1] which react in a chemical process to the desired products [15].

Basically, apart from the concrete control problem, *process control* in general has to consider two major dynamic effects when controlling a chemical reactor. Firstly, the change of concentrations upstream and inside the chemical reactor and secondly the dependency of reaction rates on temperature as well as on residence time. In the special case of control of an SCR catalyst for mobile applications, both effects are strongly present and have to be considered in the control design. As a result, the information of these dynamic effects has to be available for an optimal control of the SCR catalyst.

Furthermore, every industrial chemical process has the objective, to produce economically a desired product or behaviour of the chemical reactor by applying of adequate actuating signals at given operating conditions. This requirement should be best possible

[1] In chemical engineering feed materials are denoted as *educt*.

accomplished for stationary as well as in dynamic operating conditions. In the case of the control of an SCR catalyst the control objectives are clearly defined as:

- Achievement of highest possible NO_x reduction rates
- Lowest NH_3 slip and therefore lowest reducing agent consumption (AdBlue^{TM})

For the purpose of illustration, in figure 2.1 a general chemical reactor with its important characteristic values is shown [16].

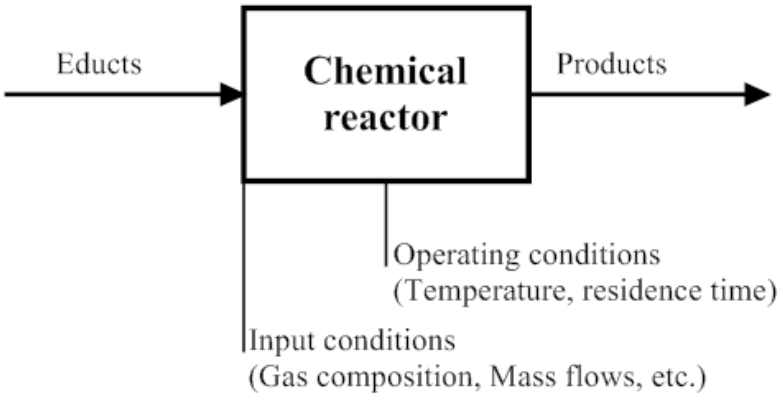

Figure 2.1: General scheme of a chemical reactor

2.1.1 System Layout

Generally, the problem of control of a chemical reactor like an SCR catalyst, underlies also the mode of action as every common control task. This means, at the beginning the boundary conditions have to be known, in order to define a suitable control concept for an SCR system. Basically, every control problem contains three important steps [15]:

1. **Measuring:**
   The control variable is measured either directly with a sensor, or indirectly calculated from other measurements using for example a mathematical model.
2. **Comparing:**
   The value of the control variable is quantitative compared with the desired reference value. Thus leads to the control error.
3. **Regulating:**
   Depending on the control error and the dynamical behaviour of the control plant, the actuating signal is determined by the controller.

Therefore, these elementary steps are also applied for the control of the SCR system. But at the moment no restrictions are made on the control variable, how the comparing is done and how the actuating signal is calculated. The only constraints which are considered right now, is the entire system layout with its available sensors and actuators. For that reason, figure 2.2 shows a general system layout for SCR systems.

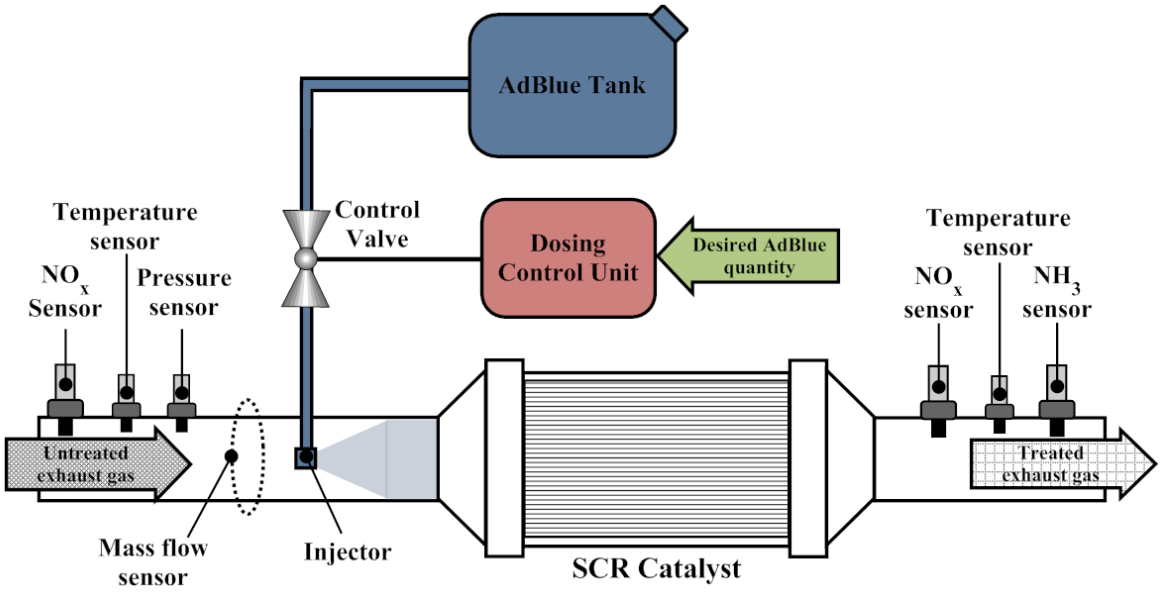

Figure 2.2: Ideal SCR system layout for mobile applications

2.1.1.1 Sensor Configuration

It has to be mentioned that the shown sensor layout in figure 2.2 is ideal and not realistic for applications in mass production. For instance, NO_x sensor, mass flow sensor or pressure sensor upstream the SCR catalyst are usually replaced by models due to cost reduction issues. Unfortunately, also the shown NH_3 sensor downstream the SCR catalyst, which should monitor the ammonia slip, is today still not available for mass production on the market. This fact will not change in the next years and therefore a closed - loop control concept based on a NH_3 sensor downstream the SCR catalyst seems not to be very promising [17].

Thus, a today common aspired sensor layout for control of SCR systems contains only a temperature sensor upstream and as feedback information and for on - board diagnostics (OBD) of the SCR catalyst a NO_x sensor downstream the SCR catalyst. However, this aspect has to be considered in the control concept definition with respect to economics and usage.

2.1.1.2 AdBlue™ Delivery System

The delivery system of AdBlue™ comprises according to figure 2.2 the *AdBlue™ Tank*, the *Dosing Control Unit* (DCU), the *Control Valve* and the *Injector*. Usually the entire control strategy and therefore the AdBlue™ quantity is calculated within the DCU. Apart from that, the DCU contains also low level drivers (e.g. control of valves to deliver the exact desired injection quantity in the exhaust) and monitoring routines (e.g. monitoring of AdBlue™ quality, Tank level, plugging of pump, etc.). Such an entire AdBlue™ delivery system is for instance the so - called *Denoxtronic* from the company BOSCH[2].

[2]For detailed information regarding the *Denoxtronic* refer to [18].

For the investigations on the test bed within this work, also the AdBlue^{TM} delivery system *Denoxtronic* from BOSCH is used. Because of the fact that the focus of the thesis is on the development of an SCR control strategy, the *Denoxtronic* is just used as an intelligent actuator. This means, all control algorithms for AdBlue^{TM} calculation within the DCU are bypassed and only the desired quantity of AdBlue^{TM} is delivered to the *Denoxtronic* via a CAN[3] interface. Therefore, the actuating variable of the developed control algorithm is represented by a demand injection quantity of AdBlue^{TM} which will be sent to the DCU. In figure 2.2 this is symbolised using the green arrow. A detailed description of the exact experimental setup used on the engine test bed is given later on in chapter 5.

2.1.2 Existing Control Systems

Today already several control algorithms and strategies for control of an SCR system are available on the market. Most of the developed control strategies in the past are using empirical approaches based on pre - programmed maps and are often only available as open - loop dosing algorithms. Drawbacks of these pure empirical dosing algorithms are mainly the high degree of freedom in the parametrisation of the empirical models. Therefore a lot of expert knowledge is needed for parametrisation of the models as well as time consuming measurement effort on an engine test bed which causes high costs. For sure these approaches were sufficient in the past to control the SCR system and to fulfil the needed emission standards, e.g. Euro IV/V [14]. A typical example for a map - based control strategy for SCR catalysts is the *Denoxtronic* from BOSCH which is introduced in section 2.1.1.2.

For completeness and illustration, in figure 2.3 a simplified overview of a generic map - based open - loop control strategy is given [17]. From the figure it can be seen that this kind of control strategy contains three main components, a map - based engine - out NO_x prediction model, a tailpipe NO_x target and a open - loop control part. The desired NO_x reduction is calculated by the difference between the engine - out NO_x emissions and the tailpipe target. Using a nominal stoichiometric ratio (NSR) between NO_x reduction and needed AdBlue^{TM} amount, a desired dosing quantity is calculated. This quantity is further corrected by the catalyst temperature in order to avoid undesired ammonia slip.

Generally, such map - based approaches for control algorithms are commonly used in control units in automotive industry. As already above mentioned, a major drawback of such an approach is the high calibration effort needed on an engine test bed.

In order to fulfil future emission standards more sophisticated control algorithms for SCR control will be needed. For example such algorithms will contain model - based approaches and will use closed - loop control based on a NO_x sensor downstream of the SCR catalyst. A first control concept based on this was introduced by [19].

It has to be mentioned that currently open - loop dosing strategies are already able to achieve high NO_x reduction rates with low ammonia slip. But closed - loop approaches make the control more robust against tolerances, achieve better performance especially in transient operating conditions and can be used for in-use compliance requirements.

[3] Controller Area Network.

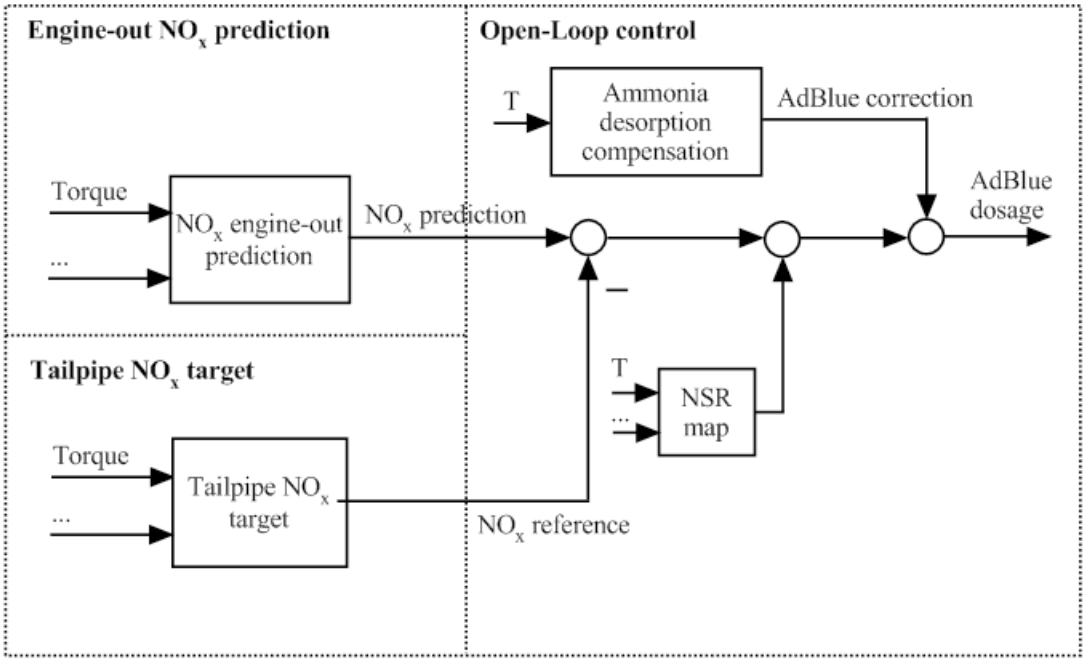

Figure 2.3: Generic map - based open loop control strategy for an SCR system

Moreover, closed - loop control strategies have the potential to reduce essential calibration effort on an engine test bed and therefore costs [17].

2.2 Basic Experiments and Observations

In order to investigate important system properties of an SCR catalysts which have to be considered in the control concept, several fundamental experiments on the engine test bed are performed. Focus of the test bed research is on stationary and especially transient system behaviour of the SCR catalyst. The shown investigations are made on a zeolite - based SCR catalyst (Fe - ZSM5) from *Johnson Matthey* with a total catalyst volume of 2.47l. Note, zeolite - based SCR catalysts are typically used today for SCR systems in mobile applications.

2.2.1 Fundamental Relations

According to the dominant SCR reaction, the "standard SCR" (refer to equation 1.4), a stoichiometric factor α can be defined as

$$\alpha = \frac{\overset{*}{n}_{NH_3,us}}{\overset{*}{n}_{NO_x,us}}. \tag{2.1}$$

This stoichiometric factor α is called *feedratio*[4]. It can be seen from equation 2.1 that ideally a equimolar ratio of $\alpha = 1$ is needed to reduce all NO_x molecules. For sure, this value is ideal, because if for example the "slow SCR" reaction (refer to equation 1.6) becomes dominant, the feedratio has to be increased. Furthermore, from the decomposition of urea to ammonia (refer to equation 1.3) it is known that out of one molecule urea, two molecules ammonia can be produced. Therefore it can be written,

$$\alpha = \frac{\overset{*}{n}_{NH_3,us}}{\overset{*}{n}_{NO_x,us}} = \frac{2 \cdot \overset{*}{n}_{(NH_2)_2CO,us}}{\overset{*}{n}_{NO_x,us}}. \tag{2.2}$$

Because of the fact that AdBlue^{TM} is standardised (refer to section 1.2.1) the amount of urea molecules in the urea / water solution can be calculated with

$$\overset{*}{n}_{(NH_2)_2CO,us} = 0.325 \cdot \frac{1}{M_{(NH_2)_2CO}} \cdot \overset{*}{m}_{AB,us}. \tag{2.3}$$

The amount of NO_x molecules upstream the SCR catalyst can be calculated based on the NO_x substance amount fraction in the exhaust molar flow according to

$$\overset{*}{n}_{NO_x,us} = \frac{1}{M_{EG}} \cdot \overset{*}{m}_{EG} \cdot x_{NO_x,us}. \tag{2.4}$$

The information on NO_x fraction in the exhaust can be delivered either by an engine - out NO_x model or a NO_x sensor. Further, for simplicity it is assumed that $M_{EG} = M_{AIR}$. This simplification is acceptable especially for CI engines, which are usually operated with air excess. Finally, combining equations 2.2, 2.3 and 2.4 together, the needed stoichiometric mass flow of AdBlue^{TM} for a chosen feedratio and measured NO_x fraction upstream the SCR catalyst can be calculated with

$$\overset{*}{m}_{AB,us} = \alpha \cdot \frac{1}{2 * 0.325} \cdot \frac{M_{(NH_2)_2CO}}{M_{AIR}} \cdot \overset{*}{m}_{EG} \cdot x_{NO_{x,us}}. \tag{2.5}$$

Apart from the stoichiometric calculation of the needed AdBlue^{TM} quantity for NO_x reduction, also evaluation criteria for the SCR catalyst performance have to be defined. A commonly used way to assess the performance of a chemical reactor is its conversion efficiency with respect to a specific educt. For the SCR catalyst it can be defined regarding NO_x conversion according to

$$\eta_{NO_x} = \frac{\overset{*}{n}_{NO_x,us} - \overset{*}{n}_{NO_x,ds}}{\overset{*}{n}_{NO_x,us}} \cdot 100\%, \tag{2.6}$$

[4]Note, fluxes in equations are explicitly denoted by using "$*$".

and regarding NH_3 conversion according to

$$\eta_{NH_3} = \frac{\overset{*}{n}_{NH_3,us} - \overset{*}{n}_{NH_3,ds}}{\overset{*}{n}_{NH_3,us}} \cdot 100\% \tag{2.7}$$

Instead of η_{NH_3} often also the ammonia slip downstream the SCR catalyst $x_{NH_3,ds}$ is used in order to evaluate the performance of the SCR catalyst.

2.2.2 Experimental Investigations

In order to investigate important system properties of an SCR catalyst, several experiments on the engine test bed are made. To assess the stationary and dynamic behaviour of the SCR, step responses and ramp signals are applied on the real system. Since from equation 2.5 the relation between NO_x upstream the catalyst and stoichiometric needed AdBlue^{TM} mass flow is known, thus the step responses and ramp signals are conducted using the stoichiometric ratio α for changing the urea dosing quantity. All experiments are performed at several stationary operating conditions of the SCR catalyst distributed over its operating range. Stationary operating conditions are defined as following:
No change of

- Exhaust mass flow, $\frac{d}{dt}\overset{*}{m}_{EG,us}(t) = 0$
- Temperature, $\frac{d}{dt}T_{EG,us}(t) = 0$
- Pressure, $\frac{d}{dt}p_{EG,us}(t) = 0$
- NO_x fraction, $\frac{d}{dt}x_{NO_x,us}(t) = 0$

Table 2.1 gives an overview of all stationary operating points (OP 1 to OP 6) where the different step responses are performed.

		OP 1	OP 2	OP 3	OP 4	OP 5	OP 6
Exhaust mass flow, $m_{EG,us}$	[kg/h]	200,26	222,00	255,05	327,88	356,91	470,62
Temperature, $T_{EG,us}$	[°C]	224	299	348	398	453	438
Temperature, T_{Amb}	[°C]	23	24	25	25	26	26
Pressure, $p_{EG,us}$	[Pa]	101849	104645	107302	113116	116792	127344
NO_x fraction, $x_{NOx,us}$	[ppm]	230	453	421	449	585	576
NO_2/NO_x ratio	[%]	47	58	43	27	12	22

Table 2.1: Stationary operating points for experimental investigations

For all experiments at the operating points, the gas composition downstream the SCR catalyst is measured using a *SESAM FTIR* measurement device from AVL - List GmbH. *SESAM FTIR* allows to measure NO, NO_2, NH_3 (important for the SCR process) and

many more gas species independently (for more detailed information refer to [20]). Additionally two commercially available NO_x sensors from Siemens VDO are used up - and downstream the SCR catalyst. Based on the NO_x sensor information upstream the SCR catalyst the stoichiometric needed AdBlue^{TM} mass flow depending on α is calculated. The NO_x sensor information downstream the SCR catalyst is further compared with *SESAM FTIR* NO_x measurement, because the Siemens sensor is foreseen for the use in SCR control algorithm, which will be shown later on.

In figure 2.4 such a step response for operating point OP 3 is shown. In this experiment, a feedratio step from $\alpha = 0 \rightarrow 0.8$ is applied.

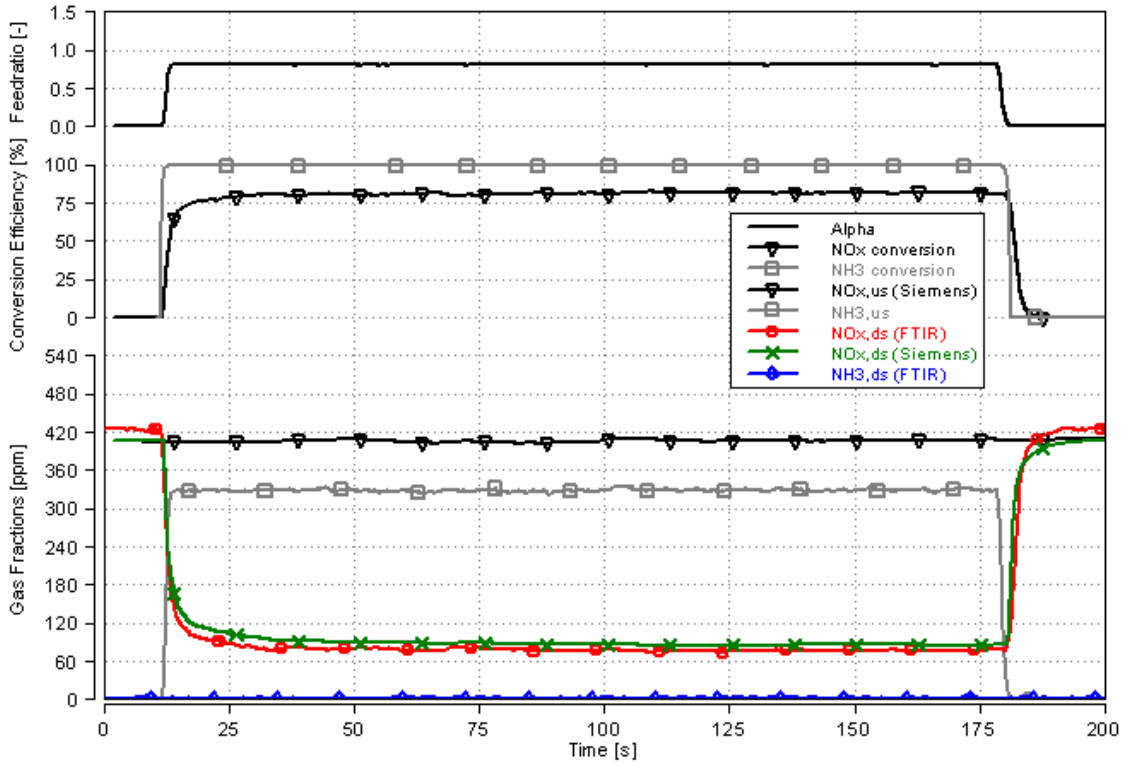

Figure 2.4: Step response for $\alpha = 0 \rightarrow 0.8$ in OP 3

From this experiment can be seen that when the feedratio step is applied at $t \approx 11\,\text{s}$, the NO_x fraction downstream the SCR immediately decreases and reaches a stationary level after a time period of $\Delta t \approx 22\,\text{s}$. The two NO_x signals downstream the SCR from FTIR and Siemens correspond very well to each other. The seen offset errors between them are negligible. Furthermore, after the dynamic phase at the beginning, a stationary NO_x conversion efficiency of $\eta_{NO_x} \approx 81\,\%$ can be achieved. Since a feedratio of $\alpha = 0.8$ is applied in this experiment, no ammonia slip downstream the SCR occurs ($x_{NH_3,ds} = 0\,\text{ppm}$). Thus the NH_3 conversion efficiency is $\eta_{NH_3} = 100\,\%$. Assuming for this operating point a plant behaviour for $\alpha \rightarrow x_{NO_x,ds}$ of first order with time delay, the characteristic values for dynamic behaviour with $\tau = 1.14\,\text{s}$ and $t_T = 1.3\,\text{s}$ are identified. Since time constant and time delay are in the same order of magnitude, this fact has to be considered for stability reasons when applying a classical closed - loop control using the NO_x sensor,

which does not consider the time delay.

In order to force also NH_3 slip, two further step responses in each operating point using higher feedratios are performed. The first applied step of those is done using $\alpha = 0 \rightarrow 1$ shown in figure 2.5.

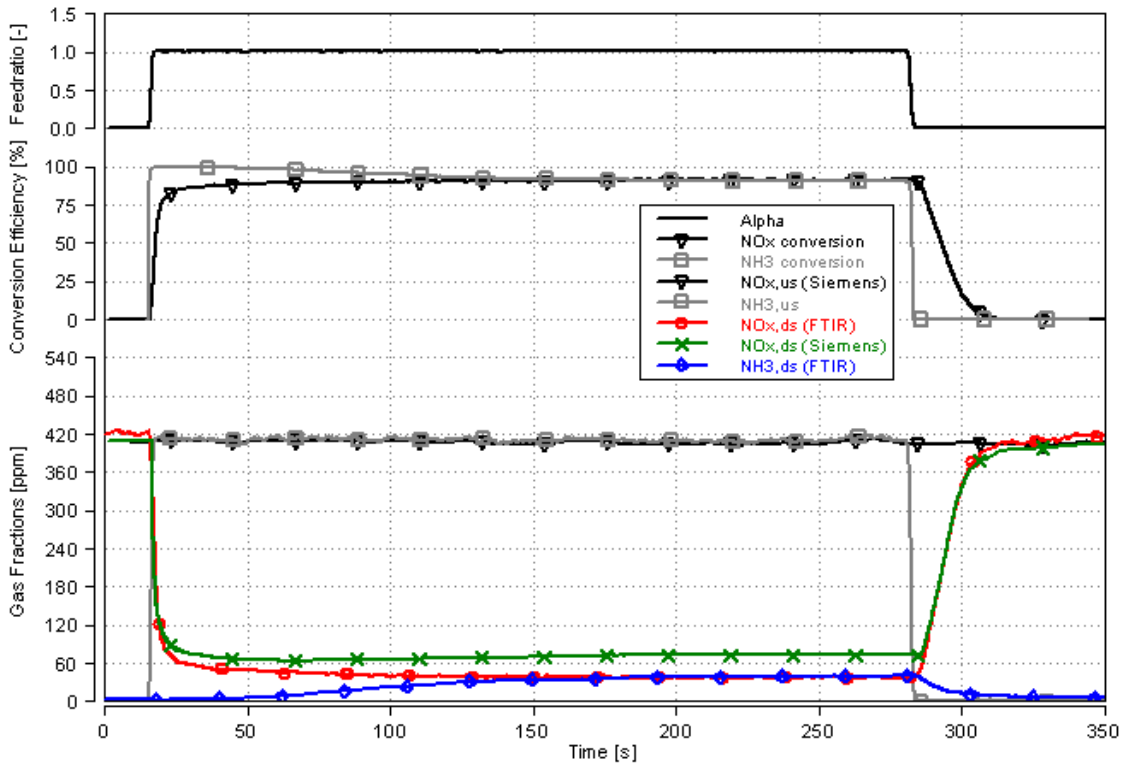

Figure 2.5: Step response for $\alpha = 0 \rightarrow 1.0$ in OP 3

As it can be seen, using stoichiometric dosing of $\alpha = 1$ a significant NH_3 slip downstream the SCR catalyst occurs. The NH_3 slip needs quite longer to become stationary than the NO_x level, $\Delta t \approx 100\,\text{s}$. This behaviour is an evidence for a storage behaviour of the SCR catalyst regarding NH_3. This assumption seems to be valid, because when the dosing quantity is shut off at $t \approx 280\,\text{s}$ the NO_x level downstream the SCR increases much more slower than it decreases when the dosing quantity is switched on at $t \approx 15\,\text{s}$. According to this observation this leads to the conclusion that the adsorption of NO_x on the catalyst surface is negligible [21]. Furthermore, due to the higher feedratio, the stationary NO_x conversion efficiency can be increased to $\eta_{NO_x} \approx 91\,\%$. This value is equal to η_{NH_3} due to the same gas fractions of NO_x and NH_3 downstream the SCR. This is because of appliance of equimolar dosing quantity of $\alpha = 1$ and a NO_2/NO_x ratio around $50\,\%$ upstream the SCR catalyst.

From the figure a further interesting effect can be seen. The Siemens NO_x sensor has a cross-sensitivity to NH_3 in the exhaust gas. This property of the NO_x sensor is also documented in the manufacturers data from Siemens VDO [22]. Of course when using the NO_x sensor for feedback control this constraints has to be considered, because when NH_3 slip occurs, also a sign change of the closed-loop system happens.

The effect of NO_x sensor cross-sensitivity to NH_3 can be even more seen in figure 2.6. In this experiment a feedratio step from $\alpha = 0 \rightarrow 1.2$ is shown in OP 3.

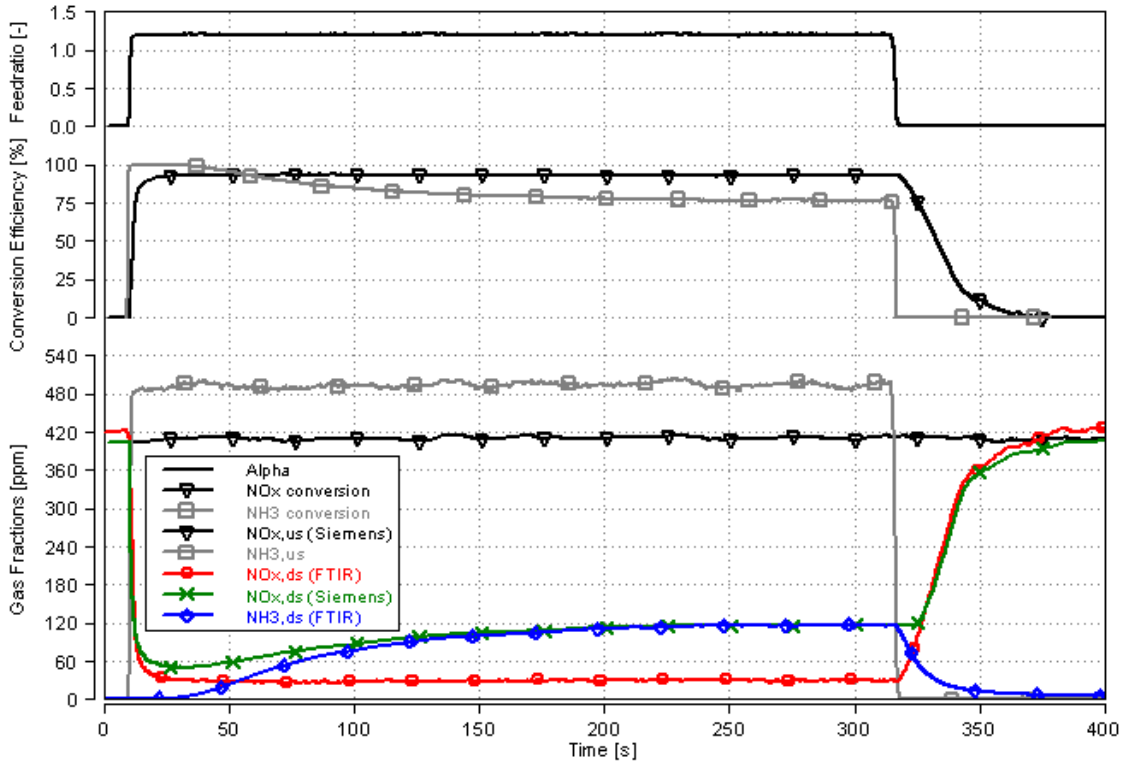

Figure 2.6: Step response for $\alpha = 0 \rightarrow 1.2$ in OP 3

As it can be seen in the figure, at this high feedratio $\alpha > 1$ a high NH_3 slip occurs. The SCR catalyst can only adsorb a limited amount of NH_3 on its surface. The amount of NH_3 which can be stored is mainly depending on the temperature and residence time of the exhaust gas and is a equilibrium of ammonia adsorption and desorption [21]. Furthermore it can be seen, although the dosing quantity is increased by 20% compared to figure 2.5, η_{NO_x} does not increase significantly. This fact indicates that the NO_x reduction is more or less independent on the ammonia surface loading above a certain value [13] [21]. The NO_x conversion efficiency for $\alpha = 1.2$ in OP 3 is $\approx 92\,\%$ for stationary conditions. On the other hand, η_{NH_3} decreases due to the high NH_3 slip of $x_{NH_3,ds} = 120\,\text{ppm}$ to $\eta_{NH_3} \approx 76\,\%$ (at $t \approx 300\,\text{s}$). As already mentioned, the NO_x sensor cross-sensitivity to NH_3 is very dominant in this experiment. According to the Siemens NO_x sensor, at $t \approx 300\,\text{s}$ a NO_x fraction of $x_{NO_x,ds} = 120\,\text{ppm}$ occurs. This value is in effect the NH_3 fraction measured by FTIR.

Further figures of the experiments at the other five operating points are documented in the appendix A.1. All of them are showing similar behaviour of the SCR catalyst as here discussed for OP 3.

Table 2.2 gives a summary of the SCR performance for all six operating points where the step responses are performed. Again, for identification of the characteristic values for

dynamic operating conditions, a plant behaviour of first order with time delay using the transfer function

$$G(s) = \frac{1}{\tau \cdot s + 1} \cdot e^{-s \cdot t_T} \tag{2.8}$$

is assumed. The important parameters for the time response of the system are identified for the plants $\alpha \rightarrow x_{NO_x,ds}$ and $\alpha \rightarrow x_{NH_3,ds}$.

			OP 1	OP 2	OP 3	OP 4	OP 5	OP 6
Feedratio step, α		[-]	0 → 1.25	0 → 1.0	0 → 1.0	0 → 1.0	0 → 1.0	0 → 1.0
Exhaust mass flow, $m_{EG,us}$		[kg/h]	200,26	222,00	255,05	327,88	356,91	470,62
Temperature, $T_{EG,us}$		[°C]	224	299	348	398	453	438
NO_2/NO_x ratio		[%]	47	58	43	27	12	22
NO_x Plant Parameter	Conversion, η_{NOx}	[%]	69,50	88,80	90,70	86,00	84,00	83,50
	Time constant, τ	[s]	26,20	6,40	1,18	0,65	0,55	0,50
	Delay Time, t_T	[s]	3,10	1,70	1,40	0,90	0,52	0,91
NH_3 Plant Parameter	Conversion, η_{NH3}	[%]	65,60	95,50	90,50	82,00	80,00	74,00
	Time constant, τ	[s]	314,00	87,70	65,60	32,80	16,30	8,70
	Delay Time, t_T	[s]	82,00	45,00	33,00	9,30	6,50	4,20

Table 2.2: Summary of important SCR plant parameters

As it can be seen in the table, the dynamic behaviour of the SCR catalyst changes significant with its operating point. Generally, a tendency of time constant and time delay for both plants depending on exhaust mass flow and temperature can be seen. With increasing temperature or exhaust mass flow, the time constant and the time delay decreases. Further, the dynamic behaviour of NH_3 is much slower compared to NO_x. This is an indication of the storage behaviour of the catalyst regarding NH_3. As already above mentioned, the time delays in the system are significant compared to its time constants in all operating points.

Considering a typically measurement error of 2 - 3% of FTIR and Siemens NO_x sensor, a decreasing trend in conversion efficiency towards higher exhaust mass flow regarding η_{NO_x} and η_{NH_3} can be seen. For OP 1, although the applied feedratio step is higher ($\alpha = 0 \rightarrow 1.25$) the reduction rates of NH_3 and NO_x are significant lower as compared to the other operating points. Because of this, it is assumable that the temperature $T_{EG,us} = 224\,°C$ in OP 1 is too low for achieving higher conversion rates. Generally, the observation holds that the performance of the SCR catalyst significant changes over its operating range.

For additional investigations, in an extra operating point a stepwise increase of the feedratio is applied to evaluate the SCR catalyst performance over a wide α range. Figure 2.7 shows the result. In this experiment the feedratio is varied by $\Delta\alpha = 0.1$ from $\alpha = 0.5 \rightarrow 1.1$.

As it can be seen in the figure, with increasing α and therefore also increasing NH_3 surface loading, the NO_x fraction downstream the SCR decreases. At the beginning, for α - steps

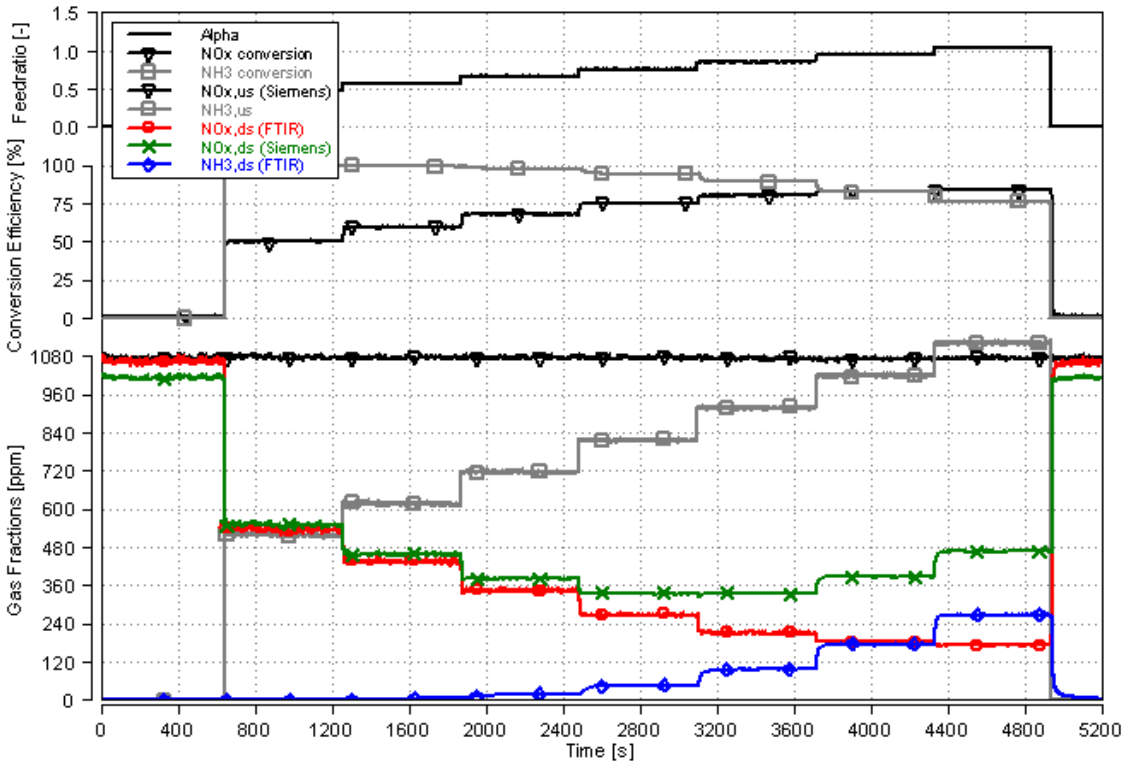

Figure 2.7: System response by stepwise increase of feedratio

0.5, 0.6 and 0.7 the achieved NO_x reduction with every increased α-step is high. When the NH_3 slip becomes significant, at α-steps 0.8, 0.9, 1.0 and 1.1, the NO_x reduction capability saturates and the NH_3 slip increases more and more. From this behaviour it can be seen that there is a tradeoff between achievable NO_x reduction and resultant NH_3 slip depending on applied α and resultant NH_3 surface loading. This means for dynamic operating condition of the SCR that its performance regarding NO_x and NH_3 conversion efficiency is limited to this stationary tradeoff.

2.2.3 Summary of the Observations

Based on the experimental investigations from section 2.2.2 following important observations are made regarding the stationary and dynamic behaviour of the SCR catalyst:

- Feedratio variations upstream the SCR catalyst are showing mutual influence on NO_x and NH_3 fractions downstream the SCR catalyst.
  - For $\alpha < 1$ the occurring NH_3 slip downstream the SCR is negligible.
  - For $\alpha \geq 1$ the NH_3 slip increases significantly, while additional NO_x reduction is poor. A saturation effect can be observed regarding NO_x reduction.
- NH_3 is adsorbed by the SCR catalyst surface for the reduction process, while the adsorption of NO_x is negligible.

- The storage capacity of the SCR catalyst regarding NH_3 is strongly dependent on the temperature and residence time of the exhaust gas in the catalyst.
- For stationary operating conditions (as defined in section 2.2.2) the resultant NH_3 surface loading due to an applied feedratio α, determines the tradeoff between NO_x conversion efficiency and NH_3 slip downstream the SCR.
- The stationary performance of the SCR catalyst regarding NO_x conversion at certain NH_3 slip is strongly dependent on feedratio and on its operating point.
- The performance of the SCR catalyst in dynamic operating conditions is limited to the stationary tradeoff between achievable NO_x conversion and resultant NH_3 slip.
- Time delays in the SCR systems are significant compared to the time constants.
- The Siemens NO_x sensor has a significant cross - sensitivity to NH_3.

These observations based on the Fe - ZSM5 SCR catalyst derived from the above described experiments agree mainly with the results and conclusions presented in the literature regarding this topic. For more detailed information on SCR catalyst characterisation and investigations of their physiochemical properties refer to [12],[13], [21], [23] and [24].

2.3 Requirements for the Control of an SCR System

Since the important system properties of the SCR catalysts are mainly known, these are considered in the requirement definition for the control concept of the entire SCR system. Based on the objectives for this thesis (section 1.3.2), the described system layout (section 2.1.1) and important experimental observations (section 2.2.3) following requirements are derived:

- **General Requirements:**
  - The control algorithm should achieve a reasonable SCR catalyst performance for stationary and transient operating conditions.
  - A integrated and systematic calibration procedure should be available for the entire control algorithm, to allow fast and best possible its parametrisation.
  - The structure of the control algorithm should be build up modular, in order the allow the appliance of the control algorithm on various EAS configuration (e.g. with or without NO_x sensor downstream the SCR catalyst).
- **Requirements due to System Layout:**
  - A commercially available NO_x sensor downstream the SCR catalyst should be used as feedback information.
  - NH_3 sensor downstream the SCR is currently not promising for commercial usage and will be therefore not used in the control algorithm. But later implementation of the NH_3 sensor in the control structure should be possible.

  - Control algorithm should deliver the desired AdBlue^{TM} quantity for dosing to the AdBlue^{TM} delivery system (*Denoxtronic*).

- **Requirements due to experimental observations:**
  - The tradeoff between achievable NO_x conversion and resultant NH_3 slip should be considered for stationary as well as for dynamic operating conditions.
  - Due to the fact that the NH_3 surface loading in the catalyst has mutual influence on NO_x and NH_3 fractions downstream the SCR, the actual NH_3 loading of the catalyst should be considered.
  - The different performance of the SCR catalyst regarding NO_x conversion at certain NH_3 slip over its entire operating range should be considered.
  - When applying closed - loop control, the cross - sensitivity of the commercial NO_x sensor regarding NH_3 should be considered.
  - The significant time delays in the SCR system, which limit the transient performance when applying closed - loop control, should be compensated using model - based approaches (refer to [25], [15]).

2.4 Control Concept for the SCR System

Based on the stated requirements regarding control of an SCR system, a control concept is defined in the following. As already mentioned, for every stationary operating point of the SCR catalyst, a optimal feedratio α according to the desired tradeoff between NO_x conversion and NH_3 slip can be determined. Based on the chosen stationary feedratio automatically a corresponding ammonia surface coverage in the catalyst will be achieved. Therefore, if α is optimal also the resultant ammonia surface coverage is optimal according to the desired tradeoff. For transient operating conditions the optimal feedratio in an operating point differs from its stationary value, due to the fact that the actual state of the SCR catalyst (especially actual ammonia surface coverage) has to be considered. For example, the SCR catalyst is still able to achieve high conversion rates although $\alpha = 0$, because of remaining ammonia surface coverage. Therefore, for transient conditions the performance of the catalyst can only be optimised in the direction, to achieve fast and best possible the stationary determined ammonia loading which is optimal with respect to the desired NO_x conversion and NH_3 slip tradeoff. As a result, the ammonia surface coverage is chosen as control variable of the SCR catalyst, since it is the most important state of the catalyst in transient operating conditions. Moreover, using the ammonia surface coverage as control variable, it considers the existing tradeoff between NO_x conversion and NH_3 slip at once. Since higher ammonia loading in the catalyst leads to lower NO_x and higher NH_3 fractions downstream of it and vice versa (refer to figure 2.7). Because of the fact that the ammonia surface coverage is an important quantity of the SCR catalyst, the symbol θ_{NH_3} is introduced for it.

Due to the fact that the actual ammonia surface coverage θ_{NH_3} of the SCR is not measurable, the observer principle from control theory is used in order to obtain this information from the system. Generally a observer, more precisely a state observer, is a system that

models a real system in order to provide an estimate of its internal state [26]. The model of the system is typically a dynamic mathematical model which is implemented on a real-time computer. This mathematical model is adjusted during operation to the real system using sensor information. Further, the estimated states of the observer can be considered and used in the controller design. The idea of this kind of state observer bases on D. G. LUENBERGER [27], [28]. Today such a approach is often also called model-based control or internal model control (IMC) [15].

Figure 2.8 shows the observer approach adapted for the control of an SCR system. The variables of the SCR observer are denoted by a "hat", like e.g. $\hat{NO}_x$, in order to distinguish them from the variables of the real SCR system.

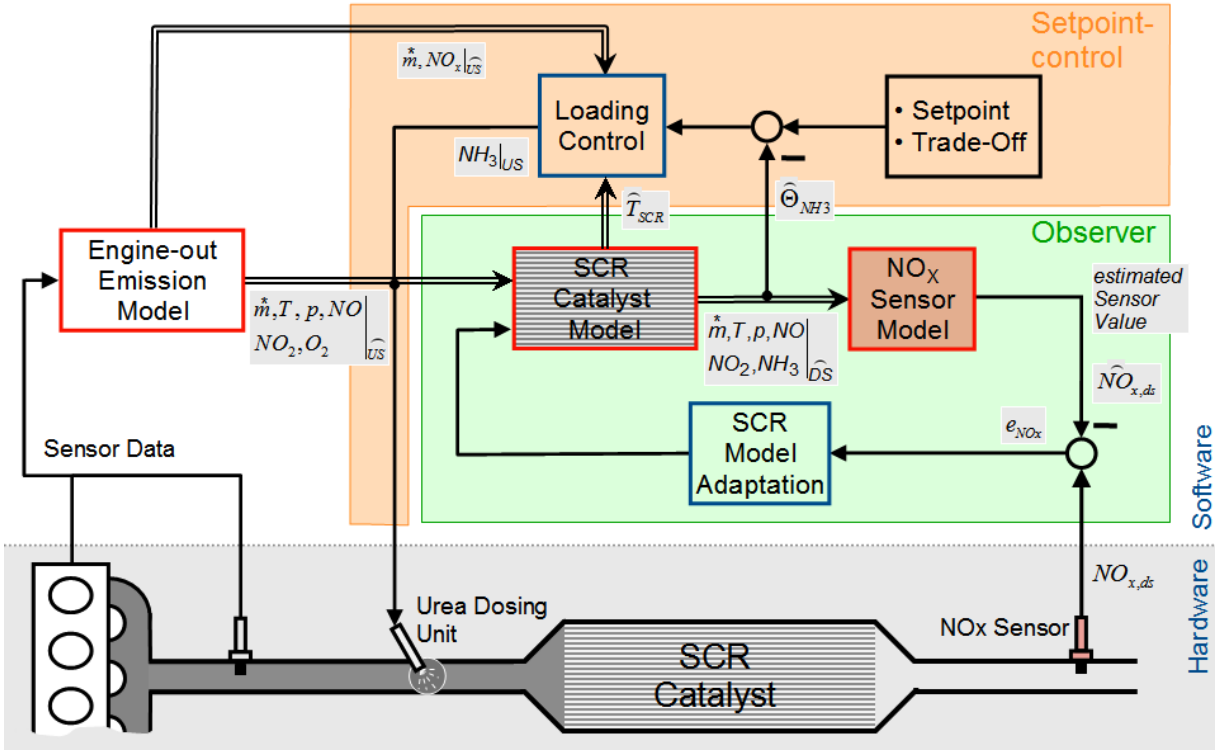

Figure 2.8: Observer-based control concept for an SCR system

As it can be seen in the figure, the control concept is build up modular consisting of several components. The important modules of the model-based control concept are:

- **Engine-out Emission Model**:
  This model provides the exhaust gas composition upstream the SCR catalyst needed for input in the control strategy. In concrete, the exhaust mass flow $\overset{*}{m}_{EG,us}$, the temperature $T_{EG,us}$, the pressure p_{EG}, us and the gas fractions $x_{NO,us}$, $x_{NO_2,us}$ and $x_{O_2,us}$ are required. The gas fraction $x_{NH_3,us}$ is the actuating signal out of the *Loading Control* and is therefore known. It has to be mentioned that the development and content of such an engine-out emission model is not scope of this thesis and therefore it is assumed that the needed input information is available anyhow. For

example, if the NO_x fraction information upstream the SCR is obtained from a sensor or a model, is for the control strategy itself not important.

- **SCR Catalyst Model:**
  Core of the model - based control concept is the *SCR Catalyst Model*. Aim of the model is to estimate the actual ammonia surface loading θ_{NH_3} of the real SCR catalyst best possible. Further, the SCR model delivers also the information of the gas composition downstream the real SCR catalyst. This information is used for adaptation of the SCR model using the NO_x sensor information downstream the SCR.

- NO_x **Sensor Model:**
  The NO_x *Sensor Model* is required for the adaptation of the SCR catalyst model to the real system. In order to compare the real NO_x sensor reading downstream the SCR with the estimated NO_x value, the important properties of the commercial NO_x sensor have to be considered, since the SCR catalyst model delivers an ideal gas composition information.

- **SCR Model Adaptation:**
  This module uses the information of the difference between the estimated and the real NO_x sensor reading and tries to adapt the SCR model according to this deviation in order to minimise it. The gained information of required adaptation signals for the SCR model can be further used for diagnostic purposes of the entire SCR system.

- **Loading Control:**
  The *Loading Control* module contains the controller for closed - loop control of the desired ammonia surface loading $\hat{\theta}_{NH_3}$ of the SCR catalyst model. As already mentioned, the actuating signal of the loading controller is the ammonia gas fraction $x_{NH_3,us}$. For appliance of this actuating signal on the real system, $x_{NH_3,us}$ is converted in a desired AdBlue^{TM} mass flow and sent to the AdBlue^{TM} delivery system.

- **Setpoint / Tradeoff:**
  The *Setpoint / Tradeoff* module delivers the optimal desired ammonia surface loading according to the wanted tradeoff between NO_x conversion and NH_3 slip.

It has to be mentioned, according to the required modularity of the control algorithm from section 2.3, the here shown observer - based concept also works without the NO_x sensor information downstream the SCR. In that case the control algorithm will operate as a model - based open loop control strategy, without the NO_x *Sensor Model* and the *SCR Model Adaptation* modules. Furthermore, if there is an NH_3 sensor available downstream the SCR, this information can be integrated in the control concept similar to the NO_x sensor information instead or additional to it.

Chapter 3

Control - Oriented Catalytic Converter Model

Main topic of this chapter is the development of the control - oriented SCR model, which is the core of the investigated control concept (refer to previous chapter). Firstly, a general introduction to chemical reaction engineering is given. Based on this, a detailed description of the derivation of the SCR catalyst equations is made and the considered chemical reaction schemes are discussed. In addition, a useful implementation of the derived catalyst model in a modelling tool is shown. At the end, the verification of the developed SCR model using engine test bed measurements and results from an other simulation model is discussed.

3.1 Chemical Reaction Engineering in General

Generally, the field of chemical reaction engineering deals mainly with the design and characterisation of chemical reactors to produce economical a desired product. In order to achieve this, reactor design uses information, knowledge and experience from a variety of disciplines like thermodynamics, chemical kinetics, fluid mechanics, heat transfer, mass transfer and economics. The primarily task in chemical reaction engineering is to get a "quantitative description" of the chemical reactor with its relevant properties of the chemical process and its performance. "Quantitative description" means in this case the usage of mathematical models which are describing the important functional relationships between relevant quantities which are important for the observed process [16]. Process relevant quantities for example are

- Concentrations of reactants (Composition)
- Relationship of reactants and products (Stoichiometry)
- Duration of reactions (Kinetics)
- Temperature, pressure, mass flow (Thermodynamics)
- Reaction volume

Using mass - and heat - balance for these process relevant quantities, the functional relationships, meaning mathematical models, can be derived. Figure 3.1 shows schematically the typically needed information for the modelling of a chemical reactor in order to predict its performance [29].

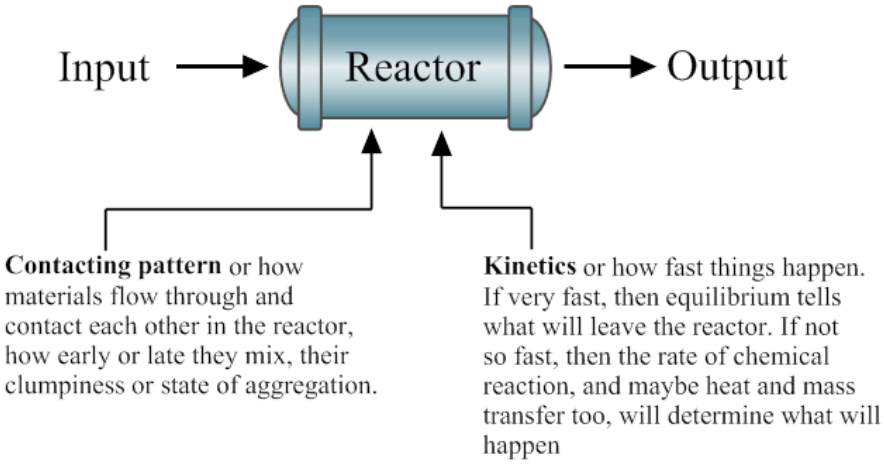

Figure 3.1: Information needed for modelling of an reactor

Therefore, to derive a reactor model (e.g. SCR catalyst), an expression has to be found which relates the input to output according to

$$output = f\,[input, kinetics, contacting] \tag{3.1}$$

This expression is also called the *performance equation*. If that functional relationship is known, a huge number of questions with respect to chemical engineering can be answered. For example, some of these questions are dealing with reactor design, comparison of reactors, simulation, optimisation or determination of kinetic parameters. In the case of the model - based control concept for SCR systems this relationship has also to be known.

3.1.1 Kinds of Ideal Chemical Reactors

As already mentioned, chemical processes occur in chemical reaction engineering typically in reactors. Therefore, to describe these reactors, ideal reactors were defined. Ideal reactors have in general three basic flow or contacting patterns [16], [29]:

- **Batch reactor(BR):**
  In a BR the reactants are initially charged into a tank. The reactants are well mixed and are left to react in the tank for a certain period. The resultant mixture is then discharged. This process is an unsteady - state operation where composition changes with time. However, at any instant the composition within the reactor is uniform. The BR can be characterised by its material - balance according to

$$\frac{d}{dt}n_i = \overset{*}{n}_{i,R}. \tag{3.2}$$

- **Plug flow reactor(PFR):**
  The PFR is also known as slug flow, piston flow, ideal tubular and unmixed flow reactor. This kind of reactor is characterised by the fact that the flow of the fluid through the reactor is orderly with no element of fluid overtaking or mixing with any other element ahead or behind. There may be only a lateral mixing of the fluid in a plug flow reactor. Therefore the residence time of the reactants is the same for all elements of the fluid. The material - balance for the PFR can be written as[1]

$$\frac{\partial}{\partial t}c_i + v \cdot \frac{\partial}{\partial x}c_i = \sum_j \nu_{ij} \cdot r_j. \tag{3.3}$$

- **Continuous stirred tank reactor(CSTR):**
  The CSTR, often also called mixed flow reactor, is a reactor which is characterised by well stirred and uniform distributed content. This means, within the reactor exists no spatially dependency regarding temperature and concentration of reactants. Therefore, the exit stream composition from this reactor has the same properties as the fluid within the reactor. A CSTR can be described by its material - balance according to

$$\frac{d}{dt}n_i = \overset{*}{n}_{i,us} - \overset{*}{n}_{i,ds} + \overset{*}{n}_{i,R} \tag{3.4}$$

For purpose of illustration, figure 3.2 shows schematically all three types of the ideal chemical reactors [29].

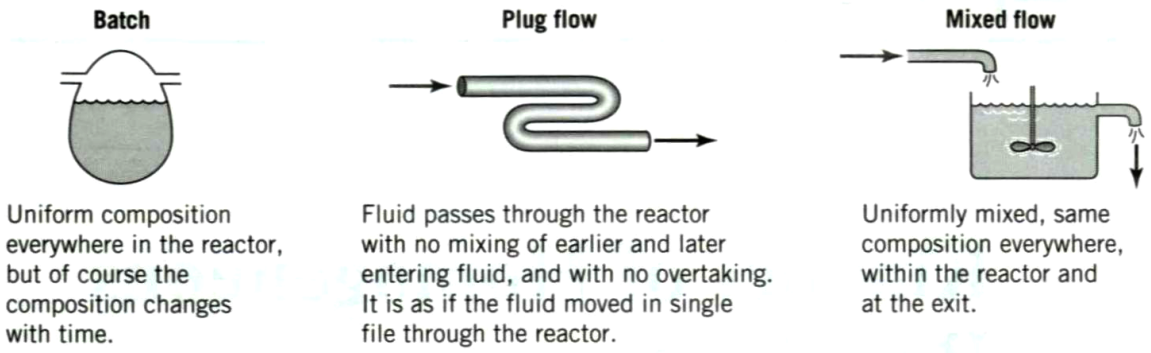

Figure 3.2: Ideal reactor types

Of course, these are simplified and idealised models of real reactors. To adapt these basic types more closely to real reactors, also combinations of the ideal reactors are possible. For example, in order to obtain a residence time behaviour of a real flow reactor, several CSTR can be plugged together to an CSTR cascade. Therefore, the volume of the real flow reactor will be theoretically divided in equal sized CSTR. The behaviour of the resultant CSTR cascade represents a mixture of a ideal CSTR and PFR, because with increasing number of CSTR, the cascade tends to an ideal PFR [16]. Also other combinations and extensions are possible in order to achieve a better correlation to real reactors (for more information refer to [29]).

[1] Material - balance of the PFR represents a system of partial differential equations (PDE) of first order from hyperbolic type in concentrations of each considered gas species.

3.2 Modelling of the Catalytic Converter Model

To describe the SCR catalyst as dynamical model in order to use it in the defined control concept, a so - called control oriented model (COM) of the SCR is needed. Detailed catalyst models for off - line simulations are often very complex and mostly they cannot be used in model - based control approaches computed on an embedded system like an ECU or DCU because of needed resources. Furthermore, these complex models are very stiff due to the fact that the time constants of most chemical reactions are much smaller than those of the heat and mass flow phenomena. However, COM usually are much simpler. Often temperature dynamics and most reactions are lumped into two or three most relevant ones[2]. This simplifies the model significantly and allows them for the use in model - based control approaches as observers [7].

Investigations have shown that the concentrations of the reactants in the SCR catalyst are changing significantly in flow direction of the exhaust gas [19], [23], [24]. Therefore this dependency has to be considered in the SCR catalyst model. Generally, the corresponding ideal reactor model for a catalyst like an SCR is a PFR. As in section 3.1.1 mentioned, PFR are expressed by coupled partial differential equations (PDE). With respect to easier computer implementation (e.g. in a modelling tool like MATLAB - SIMULINK®) and for later use in the model - based control concept, the mathematical description of an ideal PFR cannot be used. Therefore, the PFR behaviour of the SCR catalyst is approximated in flow direction using a CSTR cascade in order to obtain a one - dimensional catalyst model. Using this approach, the catalyst will be partitioned into a number of idealised CSTR cells along the flow axis. Thus the SCR catalyst can be described by ordinary differential equations (ODE) where all variables are assumed to be spatially homogeneous in each cell.

Figure 3.3 shows schematically the approximation of the flow reactor behaviour of the SCR catalyst by using the CSTR cascade approach. The number n of needed CSTR cells or volume elements in flow direction in order to approximate the real flow reactor can be derived experimental by measuring the residence time behaviour of the real catalyst [16]. It has to be mentioned that with increasing discretisation number n also the computational effort increases in order to calculate the output of the reactor. Therefore, with respect to real - time capability of the derived COM of the SCR catalyst a tradeoff between accuracy and needed resources on the embedded system has to be found.

3.2.1 Assumptions and Simplifications

To derive a suitable *lumped - parameter model* of the SCR catalyst following assumptions and simplifications are made:

- Homogeneous distribution over cross section and flow of ideal gas.
- No dynamic mass flow is considered. This means, it is assumed that the exhaust mass flow is large compared to the mass flow of the reactants and therefore the

[2]COM are typically so - called *lumped - parameter models*. This means that they have no spatially varying variables and therefore they are expressed by ODE.

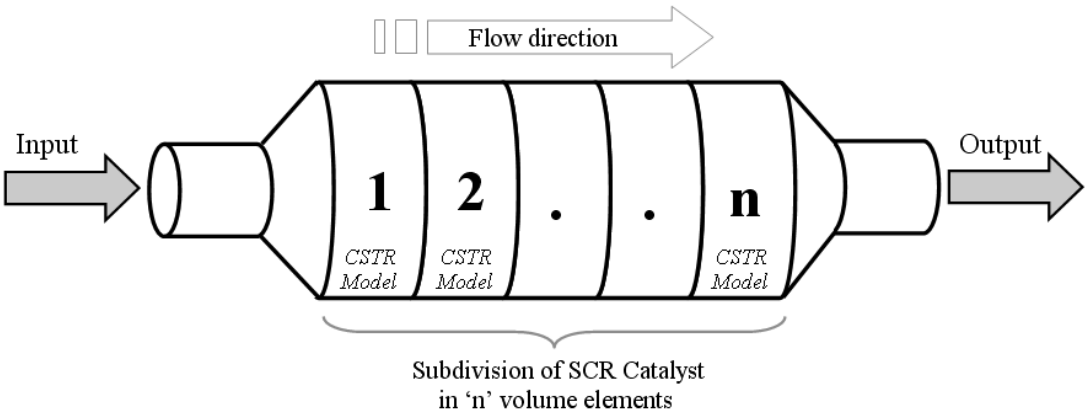

Figure 3.3: Schematic of the one - dimensional SCR catalyst model using the CSTR cascade

change of the mass flow due to the chemical reactions is neglected. Thus the mass flow through the SCR catalyst is assumed to be constant.

- Well mixing of each volume element (ideal CSTR). Therefore the exit stream conditions from each CSTR are the same as the conditions within the corresponding CSTR.
- Only gas species of NO, NO_2, NH_3 and O_2 are considered in the material balance.
- The decomposition of urea to ammonia (refer to equation 1.3) is fast and therefore calculated statically from the desired AdBlue^{TM} dosing quantity upstream the SCR catalyst [19].
- Only adsorption and desorption of NH_3 on the catalyst surface is modelled. Therefore an Eley - Rideal reaction mechanism[3] is used for the SCR kinetics (refer to equations 1.4, 1.5, 1.6).
- Any diffusion of the adsorbed NH_3 on the surface is neglected.
- No adsorption of reaction products is considered.
- Pressure losses along the catalyst are neglected.
- Each CSTR cell behaves as a perfect heat exchanger. Therefore, the exhaust gas temperature at the outlet of each cell is assumed to be equal to the corresponding cell temperature.
- Reaction enthalpies in the energy balance are small compared to the thermal inertia of the SCR catalyst and are therefore neglected [24].

[3]Eley - Rideal reaction mechanism assumes that at least one reactant is adsorbed at the catalyst surface and reacts directly with another reactant from the gas phase [30].

Using these assumptions and simplifications, the needed control - oriented catalytic converter model of the SCR catalyst is in the following derived as mathematical physiochemical lumped - parameter model using inhomogeneous non - linear coupled ordinary differential equations.

3.2.2 Derivation of the Catalytic Converter Equations

Based on the assumptions from section 3.2.1 the needed CSTR equations for one cell are derived especially for the SCR catalyst. Figure 3.4 shows schematically the characteristic quantities of such an CSTR cell.

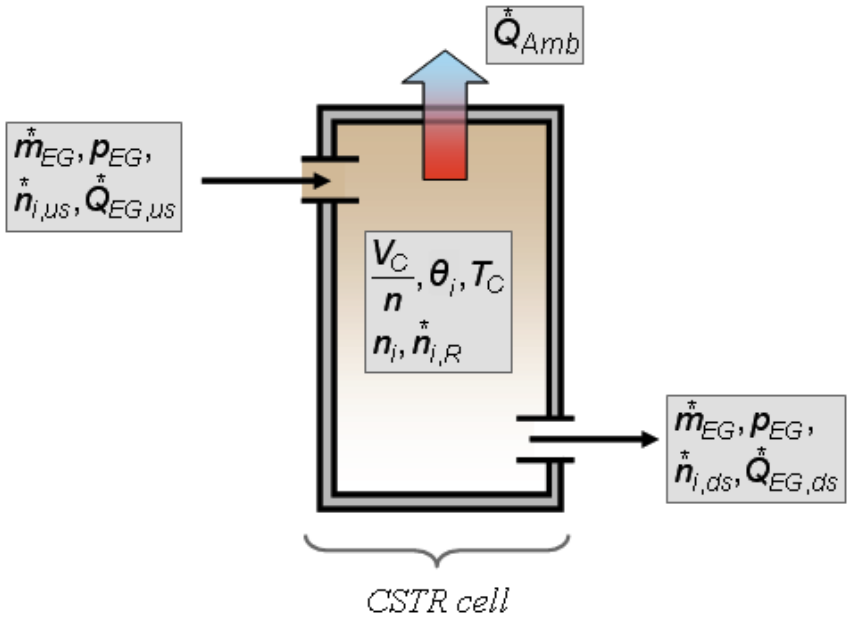

Figure 3.4: Scheme of one CSTR cell

According to the figure, the material - balance for one cell can be written with respect to an arbitrary species i in the gas phase according to

$$\frac{d}{dt}n_i = \dot{n}_{i,us} - \dot{n}_{i,ds} + \dot{n}_{i,R}. \tag{3.5}$$

Further, the quantity of material n_i within the reactor can be calculated using

$$n_i = \frac{V_c}{n} \cdot \epsilon_g \cdot c_i. \tag{3.6}$$

Where ϵ_g is the so - called open frontal area (OFA) of the monolith and corresponds to the fluid volume fraction. OFA can be calculated for a specific catalyst according to [31] by

$$\epsilon_g = \frac{(s-\delta)^2}{s^2}. \tag{3.7}$$

Where s and δ are determined by

$$s = \frac{0.0254}{\sqrt{CPSI}},$$

$$\delta = \delta_{Wall} + 2\delta_{Wc}.$$

Further, the molar flux at inlet and outlet can be calculated with

$$\overset{*}{n}_{i,us} = \overset{*}{V}_{us} \cdot c_{i,us}, \tag{3.8}$$

$$\overset{*}{n}_{i,ds} = \overset{*}{V}_{ds} \cdot c_{i,ds}. \tag{3.9}$$

Finally, the material production due to reaction $\overset{*}{n}_{i,R}$ of an arbitrary gas species i can be calculated according to

$$\overset{*}{n}_{i,R} = \frac{V_c}{n} \cdot \epsilon_g \cdot a_R \sum_j \nu_{ij} \cdot r_j. \tag{3.10}$$

Where a_R is the so - called geometric surface area (GSA) of the monolith and relates to the channel wetted perimeter. GSA can be calculated for a specific catalyst according to [31] by

$$a_R = \frac{4(s-\delta)}{s^2} \tag{3.11}$$

Combining equations 3.6, 3.8, 3.9 and 3.10 together, the material - balance from 3.5 can be rewritten as

$$\frac{d}{dt}c_i = \frac{n}{V_c \cdot \epsilon_g}\left(\overset{*}{V}_{us} \cdot c_{i,us} - \overset{*}{V}_{ds} \cdot c_{i,ds}\right) + a_R \sum_j \upsilon_{ij} \cdot r_j. \tag{3.12}$$

Since it is assumed in section 3.2.1 that the exhaust gas is ideal (ideal gas law), well mixing of each volume element ($c_{i,ds} = c_i$) and each cell behaves as a perfect heat exchanger ($T_{EG,ds} = T_c$), equation 3.12 can be further simplified to

$$\frac{d}{dt}c_i = \frac{n}{V_c \cdot \epsilon_g} \cdot \frac{\overset{*}{m}_{EG} \cdot R}{p_{EG} \cdot M_{EG}} \left(T_{EG,us} \cdot c_{i,us} - T_c \cdot c_i\right) + a_R \sum_j \upsilon_{ij} \cdot r_j. \tag{3.13}$$

The derived equation describes the material balance for one CSTR cell of the SCR catalyst. Note that the reciprocal value of $\frac{n}{V_c \cdot \epsilon_g} \cdot \frac{\overset{*}{m}_{EG} \cdot R \cdot T_c}{p_{EG} \cdot M_{EG}}$ indicates the mean residence time of the exhaust gas in the CSTR cell.

Since the change of an arbitrary concentration i in the gas phase is now known by equation 3.13, the material balance on the catalyst surface is further derived. According to the assumptions in section 3.2.1 the material balance on the surface can be written as

$$\frac{d}{dt}\theta_i = \frac{1}{\Theta_i} \sum_j \upsilon_{ij} \cdot r_j. \tag{3.14}$$

As it can be seen from the equation, the surface coverage of a arbitrary species i is normalised to its maximal surface coverage Θ_i on the catalyst surface.
Finally, according to figure 3.4, the heat balance for one cell can be derived beginning from

$$\frac{d}{dt}Q_c = \frac{1}{n} \cdot m_c \cdot c_{p,c} \cdot \frac{d}{dt}T_c = \overset{*}{Q}_{EG,us} - \overset{*}{Q}_{EG,ds} + \overset{*}{Q}_{Amb} + \overset{*}{Q}_{R}. \tag{3.15}$$

The heat flow of the exhaust gas entering the CSTR cell $\overset{*}{Q}_{EG,us}$ can be written as

$$\overset{*}{Q}_{EG,us} = \overset{*}{m}_{EG} \cdot c_{p,EG} \cdot T_{EG,us}. \tag{3.16}$$

On the other hand, using the assumption that $T_{EG,ds} = T_c$, the heat flow out of the CSTR cell $\overset{*}{Q}_{EG,ds}$ is calculated similar to equation 3.16 according to

$$\overset{*}{Q}_{EG,ds} = \overset{*}{m}_{EG} \cdot c_{p,EG} \cdot T_c. \tag{3.17}$$

Further, the heat losses of the catalyst to the ambient $\overset{*}{Q}_{Amb}$ are calculated using

$$\overset{*}{Q}_{Amb} = \alpha_c \cdot a_c \cdot (T_{Amb} - T_c). \tag{3.18}$$

Since it is assumed in section 3.2.1 that the reactions enthalpies $\overset{*}{Q}_{R}$ are neglected, they have no contribute to the heat balance, thus

$$\overset{*}{Q}_{R} = 0. \tag{3.19}$$

Finally, combining equations 3.15 to 3.19 together, the heat balance for one CSTR cell can be written as

$$\frac{d}{dt}T_c = \frac{n}{m_c \cdot c_{p,c}} \left(\overset{*}{m}_{EG} \cdot c_{p,EG} \cdot (T_{EG,us} - T_c) + \alpha_c \cdot a_c \cdot (T_{Amb} - T_c) \right). \tag{3.20}$$

Where a_c and m_c are calculated using

$$a_c = \frac{1}{n} \cdot d_c \cdot \pi \cdot l_c, \tag{3.21}$$

and

$$m_c = V_c \cdot \rho_c \cdot (1 - \epsilon_g). \tag{3.22}$$

3.2.2.1 Considered Reaction Kinetics

Since the material - and heat - balance is derived for a CSTR cell, the SCR reaction kinetics is in the following considered. Due to complexity of the reaction kinetics of an SCR, the important reaction schemes of it are taken over from *BOOST Aftertreatment*. *BOOST Aftertreatment* is an advanced and fully integrated "Virtual Engine Simulation Tool" from AVL - List GmbH with sophisticated models for exhaust gas aftertreatment devices. It is mainly intended for emission cycle simulation at concept stage of a development process and for tracking and predicting of performance of a designed EAS [31].

Following reaction schemes of an SCR catalyst are taken over from *BOOST Aftertreatment*:

- Adsorption and desorption of NH_3 on the catalyst surface.
- Standard, fast and slow SCR reaction.
- Oxidation of NH_3 on the catalyst surface and in the gas phase.
- Oxidation of NO in the gas phase.

The adsorption of NH_3 on the catalyst surface is considered by

$$NH_3 + S \rightarrow NH_3(S). \tag{3.23}$$

For understanding, the equation describes that the educts ammonia (NH_3) and one free surface site of the catalyst (S) produce one stored ammonia ($NH_3(S)$) molecule on the catalyst surface. The corresponding reaction rate r_{ad} applied for reaction equation 3.23 is defined as

$$r_{ad} = K_{ad} \cdot e^{-\frac{E_{ad}}{T_c}} \cdot c_{NH_3} \left(1 - \theta_{NH_3}\right). \tag{3.24}$$

As it can be seen, r_{ad} is of first order with respect to ammonia in the gas phase and also proportional to the free surface fraction θ_{NH_3}. The temperature dependency of this rate equation is considered by using the standard approach of Arrhenius' law[4].

On the other hand, the desorption of NH_3 from the catalyst surface is considered by

$$NH_3(S) \rightarrow NH_3 + S. \tag{3.25}$$

The corresponding rate equation is defined as

$$r_{de} = K_{de} \cdot e^{-\frac{E_{de}\left(1 - \varepsilon \cdot \theta_{NH_3}\right)}{T_c}} \cdot \theta_{NH_3}. \tag{3.26}$$

As it can be seen, the desorption rate is proportional to the amount of ammonia stored on the surface. Furthermore, for desorption a surface coverage dependency ϵ is additionally taken into account. Also r_{de} contains Arrhenius' law as temperature - dependent term.

[4] Arrhenius' law has been proofed in the past to fit well over wide temperature ranges and is strongly suggested from various standpoints as being a very good approximation to the true temperature dependency [29].

As already mentioned, the SCR kinetics, which is introduced in section 1.2.2, is described in the reaction scheme by using the Eley - Rideal reaction mechanism. Therefore, the "standard SCR" (refer to equation 1.4) is considered by

$$4NH_3(S) + 4NO + O_2 \rightarrow 4N_2 + 6H_2O. \tag{3.27}$$

For the "standard SCR" a rate equation according

$$r_{std} = K_{std} \cdot e^{-\frac{E_{std}}{T_c}} \cdot c_{NO} \cdot \theta_{crit} \left(1 - e^{-\frac{\theta_{NH_3}}{\theta_{crit}}}\right) \tag{3.28}$$

is applied. As it can be seen, r_{Std} is of first order with respect to nitric oxide in the gas phase and it depends on the stored amount of ammonia θ_{NH_3} at the surface. Due to the saturation behaviour of NO_x reduction with increasing θ_{NH_3} (discussed in section 2.2.2), the reaction rate is additionally limited by a critical surface fraction of ammonia θ_{crit}. Further, r_{Std} contains also Arrhenius' law as temperature - dependent term.
The "fast SCR" (refer to equation 1.5) is considered by

$$4NH_3(S) + 2NO + 2NO_2 \rightarrow 4N_2 + 6H_2O. \tag{3.29}$$

For this reaction equation a similar reaction rate as for the "standard SCR" is defined according to

$$r_{fst} = K_{fst} \cdot e^{-\frac{E_{fst}}{T_c}} \cdot c_{NO} \cdot c_{NO_2} \cdot \theta_{crit} \left(1 - e^{-\frac{\theta_{NH_3}}{\theta_{crit}}}\right). \tag{3.30}$$

The reaction rate is now of second order with respect to nitric oxide and nitrogen dioxide in the gas phase. It also depends on θ_{NH_3}, θ_{crit} and uses Arrhenius' law as temperature - dependent term.
Finally, the last of the SCR kinetics, the "slow SCR" (refer to equation 1.6) is considered by

$$8NH_3(S) + 6NO_2 \rightarrow 7N_2 + 6H_2O. \tag{3.31}$$

The corresponding rate equation is given below with

$$r_{slw} = K_{slw} \cdot e^{-\frac{E_{slw}}{T_c}} \cdot c_{NO_2} \cdot \theta_{crit} \left(1 - e^{-\frac{\theta_{NH_3}}{\theta_{crit}}}\right). \tag{3.32}$$

As it can be seen, r_{slw} is again of first order with respect to nitrogen dioxide in the gas phase. According to 3.28 and 3.30, r_{slw} also depends on θ_{NH_3}, θ_{crit} and uses Arrhenius' law as temperature - dependent term.

A undesired side reaction in the SCR catalyst is the oxidation of ammonia [13], [24]. This effect causes AdBlue^{TM} consumption penalty towards higher operating temperatures of the catalyst especially for Cu - ZSM5 catalysts. In order to apply the COM of the SCR catalyst on different SCR hardware configuration the oxidation of ammonia is also considered.

Generally two approaches for ammonia oxidation are defined in *BOOST Aftertreatment*. Both approaches are taken over in the reaction scheme for the COM of the SCR. The first approach describes the oxidation of ammonia on the catalyst surface according to

$$4NH_3(S) + 3O_2 \rightarrow 2N_2 + 6H_2O. \tag{3.33}$$

A rate equation as given below is applied

$$r_{ox} = K_{ox} \cdot e^{-\frac{E_{ox}}{T_c}} \cdot \theta_{NH_3}. \tag{3.34}$$

As it can be seen, the reaction rate is of first order with respect to stored ammonia and of zero order with respect to oxygen. Again, Arrhenius' law is applied as temperature - dependent term.

The second approach describes the oxidation of ammonia directly in the gas phase according to

$$4NH_3 + 3O_2 \rightarrow 2N_2 + 6H_2O. \tag{3.35}$$

The corresponding rate equation is given below with

$$r_{ox,g} = K_{ox,g} \cdot e^{-\frac{E_{ox,g}}{T_c}} \cdot c_{NH_3}. \tag{3.36}$$

Finally, also the nitric oxide oxidation of the SCR catalyst is considered by a reversible rate mechanism. Investigations showed that especially for metal - exchanged zeolites, like Fe - ZSM5, the NO oxidation activity is very high. According to [13] the oxidation of NO to NO_2 is a prerequisite for SCR kinetics, especially for the "fast SCR". Thus NO oxidation mechanism limits the SCR reaction rate and therefore also the NO_x conversion efficiency. Several experiments using different NO_2/NO_x ratios in the feed gas showed that the stationary NO_x reduction capability of the SCR for $NO_2/NO_x > 50\,\%$ decreases slower as for ratios $< 50\,\%$. Therefore, this asymetric behaviour is considered by appliying two different approaches for the SCR reaction rate determining step, the NO oxidation, depending on the equilibrium of NO and NO_2 [31].

The forward reaction of NO is considered by

$$NO + 0.5O_2 \rightarrow NO_2. \tag{3.37}$$

The corresponding rate equation is given below with

$$r_{NO,I} = K_{NO,I} \cdot T_c^{A_{NO,I}} \cdot e^{-\frac{E_{NO,I}}{T_c}} \cdot \left(c_{NO} \cdot c_{O_2}^{0.5} - \frac{c_{NO_2}}{K_{equ}\left(T_c\right)} \right) \cdot \left(1 - \theta_{NH_3}\right). \tag{3.38}$$

If the term $\left(c_{NO} \cdot c_{O_2}^{0.5} - \frac{c_{NO_2}}{K_{equ}(T_c)} \right)$ is positive, then the forward reaction 3.38 is active. On the other hand, if the term becomes negative the back reaction becomes active according to

$$NO_2 \rightarrow NO + 0.5O_2. \tag{3.39}$$

For that case, the rate equation as given below is applied

$$r_{NO,II} = -K_{NO,II} \cdot T_c^{A_{NO,II}} \cdot e^{-\frac{E_{NO,II}}{T_c}} \cdot \left(c_{NO_2} - K_{equ}\left(T_c\right) \cdot c_{NO} \cdot c_{O_2}^{0.5}\right) \cdot \left(1 - \theta_{NH_3}\right). \quad (3.40)$$

Therefore, the resultant reaction scheme for the NO oxidation can be summarised according to

$$r_{NO,g} = \begin{cases} r_{NO,I} & \text{for} \quad \left(c_{NO} \cdot c_{O_2}^{0.5} - \frac{c_{NO_2}}{K_{equ}(T_c)}\right) \geq 0 \\ r_{NO,II} & \text{for} \quad \left(c_{NO} \cdot c_{O_2}^{0.5} - \frac{c_{NO_2}}{K_{equ}(T_c)}\right) < 0 \end{cases} \quad (3.41)$$

For both reaction rates 3.38 and 3.40 the temperature dependent equilibrium constant K_{equ} is calculated according to [31] as

$$K_{equ} = \sqrt{\left(\frac{p_{EG}}{R \cdot T_c}\right)^{-1}} \cdot e^{\left(-9.259 + \frac{6848}{T_c} + 0.2791 \cdot \frac{T_c}{1000} - 0.02245 \cdot \left(\frac{T_c}{1000}\right)^2 - 0.4139 \cdot \ln\left(\frac{T_c}{1000}\right)\right)}. \quad (3.42)$$

3.2.2.2 Entire Catalytic Converter Model

Based on the derived description (equations 3.13, 3.14, 3.20) for a specific CSTR cell of the SCR catalyst and the considered reaction kinetics from section 3.2.2.1, the entire catalytic converter model is further written in a general from. The resultant equations for the k^{th} cell of the catalyst are:

$$\begin{aligned}
\frac{d}{dt}c_{NO,k} &= \frac{n}{V_c \cdot \varepsilon_g} \cdot \frac{\overset{*}{m}_{EG} \cdot R}{p_{EG} \cdot M_{EG}} \left(T_{EG,k-1} \cdot c_{NO,k-1} - T_{c,k} \cdot c_{NO,k}\right) + \\
&\quad + a_R \left(-4 \cdot r_{std,k} - 2 \cdot r_{fst,k} - r_{NO,g,k}\right) \\
\frac{d}{dt}c_{NO_2,k} &= \frac{n}{V_c \cdot \varepsilon_g} \cdot \frac{\overset{*}{m}_{EG} \cdot R}{p_{EG} \cdot M_{EG}} \left(T_{EG,k-1} \cdot c_{NO_2,k-1} - T_{c,k} \cdot c_{NO_2,k}\right) + \\
&\quad + a_R \left(-2 \cdot r_{fst,k} - 6 \cdot r_{slw,k} + r_{NO,g,k}\right) \\
\frac{d}{dt}c_{NH_3,k} &= \frac{n}{V_c \cdot \varepsilon_g} \cdot \frac{\overset{*}{m}_{EG} \cdot R}{p_{EG} \cdot M_{EG}} \left(T_{EG,k-1} \cdot c_{NH_3,k-1} - T_{c,k} \cdot c_{NH_3,k}\right) + \\
&\quad + a_R \left(-r_{ad,k} + r_{de,k} - 4 \cdot r_{ox,g,k}\right) \\
\frac{d}{dt}c_{O_2,k} &= \frac{n}{V_c \cdot \varepsilon_g} \cdot \frac{\overset{*}{m}_{EG} \cdot R}{p_{EG} \cdot M_{EG}} \left(T_{EG,k-1} \cdot c_{O_2,k-1} - T_{c,k} \cdot c_{O_2,k}\right) + \\
&\quad + a_R \left(-0.5 \cdot r_{NO,g,k}\right) \\
\frac{d}{dt}\theta_{NH_3,k} &= \frac{1}{\Theta_{NH_3}} \left(r_{ad,k} - r_{de,k} - 4 \cdot r_{std,k} - 4 \cdot r_{fst,k} - 8 \cdot r_{slw,k} - 4 \cdot r_{ox,k}\right) \\
\frac{d}{dt}T_{c,k} &= \frac{n}{m_c \cdot c_{p,c}} \left(\overset{*}{m}_{EG} \cdot c_{p,EG} \cdot \left(T_{EG,k-1} - T_{c,k}\right) + \alpha_c \cdot a_c \cdot \left(T_{Amb} - T_{c,k}\right)\right)
\end{aligned} \quad (3.43)$$

Note, for the special case of the first CSTR cell ($k = 1$) in the cascade, the input values from the $(k-1)^{th}$ cell refer to the upstream quantities of the SCR (e.g. $c_{NO,us}$). As it

can be seen from the equations, the derived control - oriented catalytic converter model of the SCR catalyst for one cell is a lumped - parameter model using inhomogeneous non - linear coupled ordinary differential equations. The COM consists for each cell k of 6 state variables ($c_{NO,k}$, $c_{NO_2,k}$, $c_{NH_3,k}$, $c_{O_2,k}$, $\theta_{NH_{3,k}}$, $T_{c,k}$). Thus the entire model order for n cells is given by

$$N = n \cdot 6 \tag{3.44}$$

For example, if a zero - dimensional SCR catalyst model should be obtained, then $n = 1$ and thus $N = 6$.

3.3 Useful Implementation of the Converter Model in a Modelling Tool

Since the one - dimensional COM of the SCR catalyst is derived (refer to section 3.2), it is further implemented in a modelling tool in order to investigate its performance and validity in representative experiments by simulation. Often in simulations which are using a one - dimensional model approach, different discretisation or cell numbers n in flow direction are needed. In the specific case of the control - oriented SCR model such simulations for example can deal with investigations on the real - time capability of the COM, where the tradeoff between accuracy and needed resources has to be considered. Because of this, in order to allow a fast and easy change of the cell number n, a variable implementation of the COM in the modelling tool MATLAB - SIMULINK®[5] is investigated within this thesis. Therefore, in the following a brief description of the "cell number variable" COM is given.

In order to illustrate how the COM is implemented "cell number variable", the entire catalytic converter model (refer to ODE system 3.43) is firstly notional separated in two parts. These are: Changing of state variables of one cell due to

- Mass and heat flow phenomena,
- Chemical reaction kinetics.

Note, no simplifications of the derived COM from equation 3.43 are made. Just the two different parts of the model are in the following derived independent from each other "cell number variable". Since the two parts are cell variable, they are connected again to the entire catalytic converter model.

3.3.1 Cell Number Variable Mass and Heat Flow Phenomena

For simplicity, in the following explanations the used gas species (NO, NO_2, NH_3, O_2) in the COM are substituted using i instead of writing explicit all four gas components.

[5] MATLAB® is a numerical computing environment developed by *The MathWorks*. The additional package SIMULINK® bases on MATLAB® and allows graphical simulation and model - based design of dynamic and embedded systems.

Therefore, the first part, change of state variables due to mass and heat flow phenomena, can be derived from equation 3.43 for the first cell as

$$\begin{aligned} \frac{d}{dt}c_{i,1} &= \frac{n}{V_c \cdot \varepsilon_g} \cdot \frac{\overset{*}{m}_{EG} \cdot R}{p_{EG} \cdot M_{EG}} \left(T_{EG,us} \cdot c_{i,us} - T_{c,1} \cdot c_{i,1}\right) \\ \frac{d}{dt}\theta_{NH_3,1} &= 0 \\ \frac{d}{dt}T_{c,1} &= \frac{n}{m_c \cdot c_{p,c}} \left(\overset{*}{m}_{EG} \cdot c_{p,EG} \cdot (T_{EG,us} - T_{c,1}) + \alpha_c \cdot a_c \cdot (T_{Amb} - T_{c,1})\right) \end{aligned} \tag{3.45}$$

and for the k^{th} cell according to

$$\begin{aligned} \frac{d}{dt}c_{i,k} &= \frac{n}{V_c \cdot \varepsilon_g} \cdot \frac{\overset{*}{m}_{EG} \cdot R}{p_{EG} \cdot M_{EG}} \left(T_{EG,k-1} \cdot c_{i,k-1} - T_{c,k} \cdot c_{i,k}\right) \\ \frac{d}{dt}\theta_{NH_3,k} &= 0 \\ \frac{d}{dt}T_{c,k} &= \frac{n}{m_c \cdot c_{p,c}} \left(\overset{*}{m}_{EG} \cdot c_{p,EG} \cdot (T_{EG,k-1} - T_{c,k}) + \alpha_c \cdot a_c \cdot (T_{Amb} - T_{c,k})\right) \end{aligned} \tag{3.46}$$

These two equations are combined together to one general CSTR cell in SIMULINK®. This is accomplished by combination of the catalyst input signals ($c_{i,us}$, $T_{EG,us}$) and the feedback of the "$(k-1)$ states" ($c_{i,k-1}$, $T_{c,k-1}$) of each cell to the inputs of the general CSTR cell. Furthermore, the ammonia loading θ_{NH_3} needs not to be considered in the feedback, due to the fact that the loading of the $(k-1)^{th}$ cell has no direct influence on the loading in the k^{th} cell. Figure 3.5 shows the implementation of the general CSTR cell in SIMULINK® with the feedback of the "$(k-1)$ states" and the characteristic in - and outputs.

When considering n cells in the COM, the different ammonia loadings $\theta_{NH_3,k}$, concentrations $c_{i,k}$ and temperatures $T_{c,k}$ in all CSTR cells can be summarised to vectors according to

$$\theta_{\mathbf{NH_3}} = \begin{bmatrix} \theta_{NH_3,1} \\ \vdots \\ \theta_{NH_3,n} \end{bmatrix}, \mathbf{c_i} = \begin{bmatrix} c_{i,1} \\ \vdots \\ c_{i,n} \end{bmatrix}, \mathbf{T_c} = \begin{bmatrix} T_{c,1} \\ \vdots \\ T_{c,n} \end{bmatrix}. \tag{3.47}$$

Because of the fact that for the calculation of the state variables of the last cell ($k = n$), only the outputs of the $(n-1)^{th}$ cell are need, the combined input vectors (SCR catalyst inputs and internal feedback of the "$(k-1)$ states") are defined as

$$\tilde{\mathbf{c}}_\mathbf{i} = \begin{bmatrix} c_{i,us} \\ c_{i,1} \\ \vdots \\ c_{i,n-1} \end{bmatrix}, \tilde{\mathbf{T}}_\mathbf{c} = \begin{bmatrix} T_{EG,us} \\ T_{c,1} \\ \vdots \\ T_{c,n-1} \end{bmatrix}. \tag{3.48}$$

Based on this approach (refer to figure 3.5) and using the relationship 3.46, the mass and heat flow phenomena inside the CSTR cascade is implemented cell number n variable in

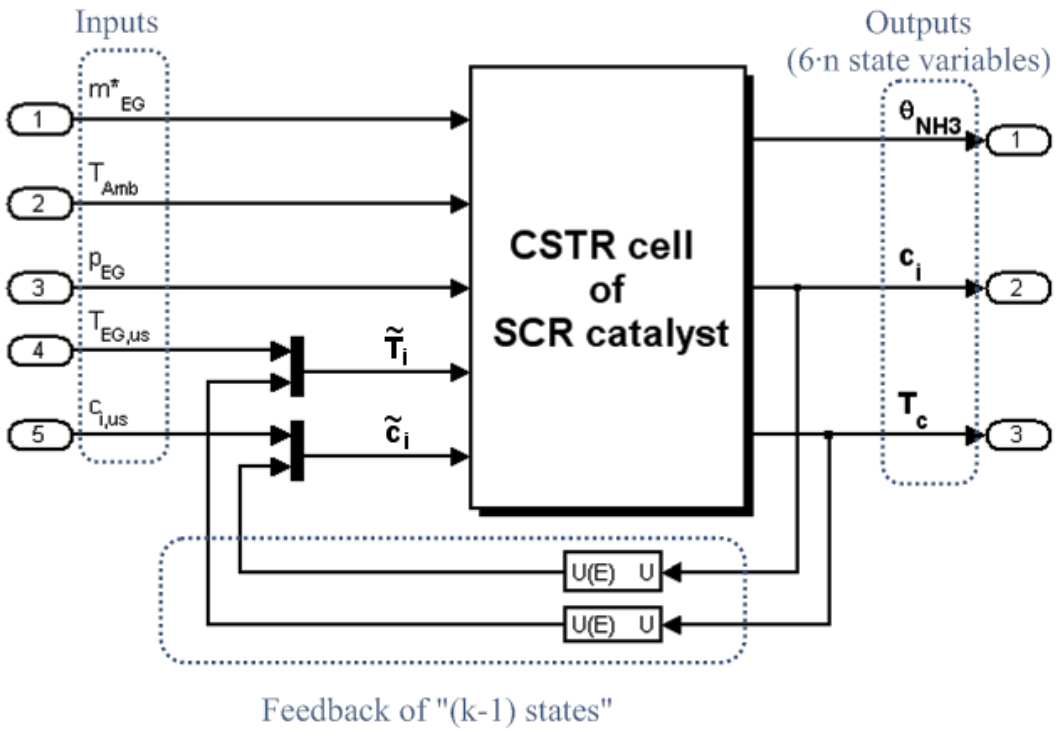

Figure 3.5: Feedback of state variables of CSTR cell in SIMULINK model

SIMULINK®. Therefore, the size of the input and output vectors $\tilde{\mathbf{c}}_\mathbf{i}$, $\tilde{\mathbf{T}}_\mathbf{c}$, $\mathbf{c_i}$, $\mathbf{T_c}$ and $\theta_{\mathbf{NH_3}}$ are changed according to the wanted discretisation. For illustration, the heat balance from equation 3.46 can be written in "n variable" implementation according to

$$\frac{d}{dt}\mathbf{T_c} = \frac{n}{m_c \cdot c_{p,c}} \left(\overset{*}{m}_{EG} \cdot c_{p,EG} \cdot \left(\tilde{\mathbf{T}}_\mathbf{c} - \mathbf{T_c} \right) + \alpha_c \cdot a_c \cdot \left(T_{Amb} \cdot \begin{bmatrix} 1 \\ \vdots \\ 1 \end{bmatrix} - \mathbf{T_c} \right) \right). \quad (3.49)$$

Where T_{Amb} is multiplied with an $n \times 1$ vector in order to achieve the same dimension as $\mathbf{T_c}$.

3.3.2 Cell Number Variable Chemical Reaction Kinetics

The second part, change of state variables due to chemical reaction kinetics, can be written according to ODE system 3.43 for the k^{th} cell in matrix notation as

$$\frac{d}{dt} \begin{bmatrix} c_{NO,k} \\ c_{NO_2,k} \\ c_{NH_3,k} \\ c_{O_2,k} \\ \theta_{NH_3,k} \\ T_{c,k} \end{bmatrix} = \Lambda_k \cdot \Gamma_k \cdot \mathbf{r_k}. \quad (3.50)$$

Where, Λ_k and Γ_k are 6×6 and 6×8 coefficient matrices and $\mathbf{r_k}$ is an 8×1 vector of occurring reaction rates ($r_{j,k}$) in the k^{th} cell. The coefficient matrix Λ_k can be written as

$$\Lambda_k = \begin{bmatrix} a_R & 0 & 0 & 0 & 0 & 0 \\ 0 & a_R & 0 & 0 & 0 & 0 \\ 0 & 0 & a_R & 0 & 0 & 0 \\ 0 & 0 & 0 & a_R & 0 & 0 \\ 0 & 0 & 0 & 0 & \frac{1}{\Theta_{NH_3}} & 0 \\ 0 & 0 & 0 & 0 & 0 & 0 \end{bmatrix}.$$

Further, the coefficient matrix Γ_k represents the stoichiometric factors from the reaction equations (refer to section 3.2.2.1) and can be written according to

$$\Gamma_k = \begin{bmatrix} 0 & 0 & -4 & -2 & 0 & 0 & 0 & -1 \\ 0 & 0 & 0 & -2 & -6 & 0 & 0 & 1 \\ -1 & 1 & 0 & 0 & 0 & 0 & -4 & 0 \\ 0 & 0 & 0 & 0 & 0 & 0 & 0 & -0.5 \\ 1 & -1 & -4 & -4 & -8 & -4 & 0 & 0 \\ 0 & 0 & 0 & 0 & 0 & 0 & 0 & 0 \end{bmatrix}.$$

Finally, the vector of reaction rates $\mathbf{r_k}$ for the k^{th} cell can be written as

$$\mathbf{r_k} = \begin{bmatrix} r_{ad,k} \\ r_{de,k} \\ r_{std,k} \\ r_{fst,k} \\ r_{slw,k} \\ r_{ox,k} \\ r_{ox,g,k} \\ r_{NO,g,k} \end{bmatrix}.$$

Where the reaction rates $r_{j,k}$ are defined by the equations 3.24, 3.26, 3.28, 3.30, 3.32, 3.34, 3.36 and 3.41.

Since the matrix notation for one cell is known, the relationship 3.50 is further extended for variable cell numbers n according to

$$\frac{d}{dt} \begin{bmatrix} \mathbf{c_{NO}} \\ \mathbf{c_{NO_2}} \\ \mathbf{c_{NH_3}} \\ \mathbf{c_{O_2}} \\ \theta_{\mathbf{NH_3}} \\ \mathbf{T_c} \end{bmatrix} = \Lambda \cdot \Gamma \cdot \mathbf{r}. \tag{3.51}$$

Where $\mathbf{c_i}$ ($\mathbf{c_{NO}}$, $\mathbf{c_{NO_2}}$, $\mathbf{c_{NH_3}}$, $\mathbf{c_{O_2}}$), $\theta_{\mathbf{NH_3}}$ and $\mathbf{T_c}$ are the same vectors as defined in equation 3.47. The dimension of the matrices Λ and Γ for n cells are $6n \times 6n$ and $6n \times 8n$ and $\mathbf{r}$ is an $8n \times 1$ vector. The coefficient matrix Λ can be written for n cells according to

$$\Lambda = \begin{bmatrix} \mathbf{a_R} & 0 & 0 \\ 0 & \frac{1}{\Theta_{NH_3}} \cdot \mathrm{I} & 0 \\ 0 & 0 & 0 \cdot \mathrm{I} \end{bmatrix}.$$

Where $\mathbf{a_R}$ is a $4n \times 4n$ diagonal matrix and I is a $n \times n$ unit matrix according to

$$\mathbf{a_R} = \begin{bmatrix} a_R & 0 & 0 \\ 0 & \ddots & 0 \\ 0 & 0 & a_R \end{bmatrix}, \mathrm{I} = \begin{bmatrix} 1_1 & 0 & 0 \\ 0 & \ddots & 0 \\ 0 & 0 & 1_n \end{bmatrix}.$$

Further, the stoichiometric matrix Γ_k can be written can be written for n cells according to

$$\Gamma = \begin{bmatrix} 0 & 0 & -4 \cdot \mathrm{I} & -2 \cdot \mathrm{I} & 0 & 0 & 0 & -1 \cdot \mathrm{I} \\ 0 & 0 & 0 & -2 \cdot \mathrm{I} & -6 \cdot \mathrm{I} & 0 & 0 & 1 \cdot \mathrm{I} \\ -1 \cdot \mathrm{I} & 1 \cdot \mathrm{I} & 0 & 0 & 0 & 0 & -4 \cdot \mathrm{I} & 0 \\ 0 & 0 & 0 & 0 & 0 & 0 & 0 & -0.5 \cdot \mathrm{I} \\ 1 \cdot \mathrm{I} & -1 \cdot \mathrm{I} & -4 \cdot \mathrm{I} & -4 \cdot \mathrm{I} & -8 \cdot \mathrm{I} & -4 \cdot \mathrm{I} & 0 & 0 \\ 0 & 0 & 0 & 0 & 0 & 0 & 0 & 0 \cdot \mathrm{I} \end{bmatrix}.$$

Where I is again an $n \times n$ unit matrix. Finally, the vector of reaction rates $\mathbf{r}$ for n cells can be written as an $8n \times 1$ vector according to

$$\mathbf{r} = \begin{bmatrix} r_{ad,1} \\ \vdots \\ r_{ad,n} \\ r_{de,1} \\ \vdots \\ r_{de,n} \\ \vdots \\ \vdots \\ r_{NO,1} \\ \vdots \\ r_{NO,n} \end{bmatrix}.$$

Applying the matrix notation from equation 3.51 in SIMULINK®, also the chemical reaction kinetics of the SCR model is implemented cell number variable. As a result, combining together the two parts, cell variable mass and heat flow phenomena and cell variable chemical reaction kinetics, the entire SCR model is derived cell number variable.

3.4 Verification of the Catalytic Converter Model

Since a cell variable COM of the SCR catalyst is derived (refer to sections 3.2 and 3.3), it is in the following verified in illustrating experiments. In order to proof the validity of the COM, it is verified primarily in simulation by using a sophisticated SCR catalyst model from *BOOST Aftertreatment* and further by using measurement data from an engine test bed. It has to be mentioned for the compactness of the thesis, only summarised verification results of the control - oriented SCR model are documented in the following. Therefore, the verification of the COM is separated in two parts:

- Verification using the sophisticated *BOOST* SCR model.
- Verification using engine test bed measurements.

For both parts, a transient engine test cycle called FTP - 75 (Federal Test Procedure)[6] is used in order to verify the COM of the SCR catalyst. The FTP - 75 itself consists of 3 segments, the *cold start phase*, the *transient phase* and the *hot start phase*. Since the *cold start phase* is not very interesting for the verification of the COM due to the low EAS device temperatures ($T_c << 200\,°C$), this phase is skipped in the here shown FTP cycles. Therefore, the here shown "modified" FTP - 75 is starting with a preconditioned SCR catalyst ($T_c \approx 450\,°C$) in the *hot start phase* and after that, the *transient phase* is applied. Figure 3.6 shows the for the SCR process important inputs to the SCR catalyst in this "modified" FTP - 75.

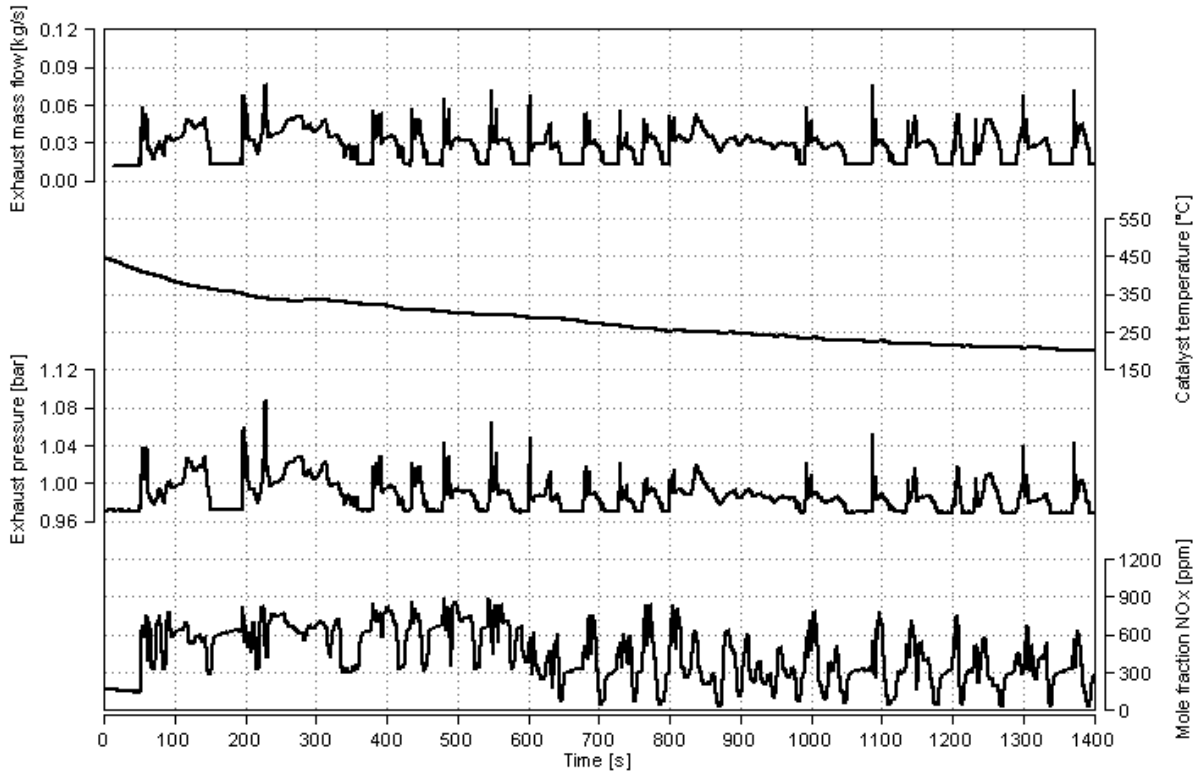

Figure 3.6: Modified FTP - 75 for the verification of the COM

As it can be seen, the duration of the test is 1400 s (*hot start phase* plus *transient phase*). All shown quantities in the figure refer to the upstream position of the SCR catalyst. Further, at $t = 0\,s$ the SCR catalyst temperature starts at $T_c \approx 450\,°C$ and decreases to $T_c \approx 200\,°C$ at $t = 1400\,s$. Since the SCR catalyst temperature is high enough over the entire FTP - 75, the ammonia dosing is switched on in the whole test cycle without of risks with respect to foul or to deactivate the SCR catalyst as discussed in [11].

[6] FTP - 75 is a transient test cycle used for emission certification of light duty vehicles in the USA. For more detailed information refer to [32].

The needed parametrisation of the COM (physical and chemical model parameters) for the different verifications, is taken over from the results of an AVL's in - house R & D project. Within this project a Fe - ZSM5 based SCR catalyst was characterised. Therefore, the used entire parameter set is documented in appendix **??**. For all here shown verification results a cell number of $n = 5$ is used, thus the model order of the COM is $N = 30$.

3.4.1 Verification using the sophisticated BOOST SCR Model

Since *BOOST Aftertreatment* contains a sophisticated SCR catalyst model for offline simulations, it is used for the verification of the COM (for detailed information on BOOST's SCR model refer to [31]). The verification of the COM is carried out by using the same parameter sets for the two SCR models as documented in appendix **??**. Furthermore, the two models are simulated offline in the FTP - 75 test cycle, by applying transient measurement data from the test bed to their inputs. The specific simulated test cycle uses a constant feedratio of $\alpha = 1.6$. Figure 3.7 shows the comparison between COM and BOOST in this transient test cycle. For simplicity, only the SCR catalyst important quantities, cumulative NO_x and NH_3 mass up - and downstream the catalyst are shown in two figures.

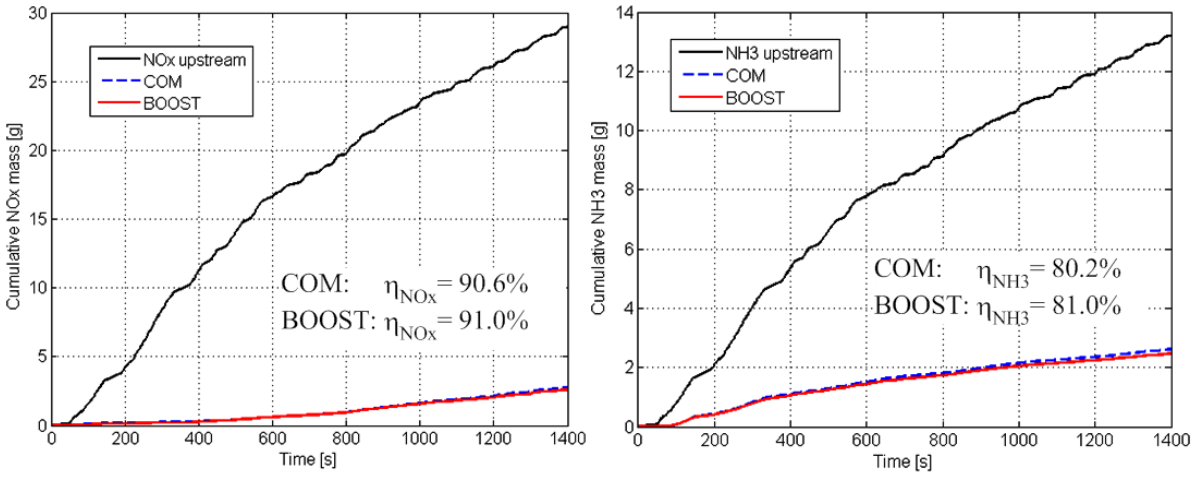

Figure 3.7: Comparison of the two SCR models (COM, BOOST)

In the left part of the figure it can be seen that BOOST and COM are calculating nearly the same cumulative NO_x mass downstream the SCR catalyst and therefore also nearly the same NO_x conversion (η_{NO_x}). Additionally, also the calculated NH_3 mass downstream the catalyst (right part) is nearly the same for both models and accordingly to that also the NH_3 conversion (η_{NH_3}).

On the whole, the simulation results of the transient test cycle between BOOST and COM are showing very good correlations. The small occurring deviations between the two models are mainly caused by the made simplifications for the COM as discussed in section 3.2.1. Especially the disregard of dynamic mass transfer, pressure loss and reaction enthalpies causes the main differences. Nevertheless, the control - oriented SCR

model has acceptable accuracy compared to BOOST and is therefore further verified using a real SCR catalyst.

3.4.2 Verification using Test Bed Measurements

Since the validity of the control - oriented SCR model is proofed by using *BOOST Aftertreatment*, the model can be further compared with measurements of the SCR catalyst from the engine test bed. In order to investigate different performances of the real SCR catalyst in comparison with the COM, several FTP - 75 test cycles are performed. For each test cycle different feedratios are applied according to:

- FTP with $\alpha = 1.0$
- FTP with $\alpha = 1.2$
- FTP with $\alpha = 1.4$
- FTP with $\alpha = 1.6$

For every FTP the gas composition downstream the SCR catalyst is measured in order to compare it with the simulation result of the COM in the same test cycle. According to previous shown verification, again the SCR catalyst important quantities, cumulative NO_x and NH_3 mass up - and downstream the catalyst are evaluated for both, real catalyst and COM. Beginning with the cumulative NO_x mass, figure 3.8 shows the cycle results for the FTPs $\alpha = 1.0$ and $\alpha = 1.2$.

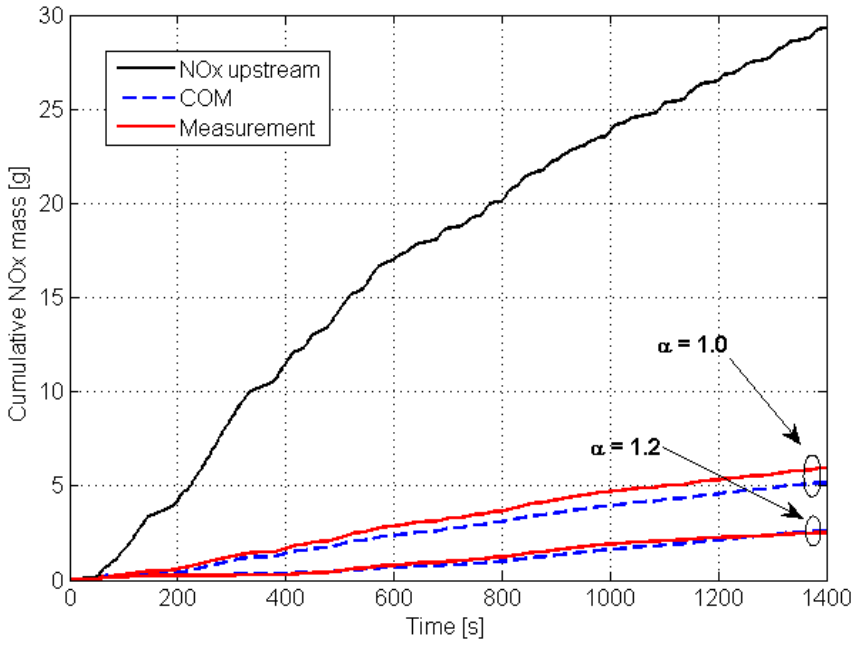

Figure 3.8: Comparison of the cumulative NO_x mass in different FTPs

Since for the feedratios $\alpha = 1.4$ and $\alpha = 1.6$, the cumulative NO_x mass downstream catalyst is not significant lower due to the NO_x reduction saturation effect (discussed in section 2.2.3), these two test cycles are not illustrated in the figure. As expected, with increasing feedratio, the NO_x mass of both, measurement and COM decreases. The correlation between test bed measurement and COM for $\alpha = 1.0$ is acceptable. The COM estimates for this case a higher NO_x reduction as the measurement. For $\alpha = 1.2$ the correlation between COM and measurement is very good. This is mainly due to the saturation effect of NO_x reduction for high feedratios.

In addition, figure 3.9 shows the cumulative NH_3 mass up - and downstream the catalyst for measurement and COM. For this case, all of the four FTPs are shown, since the cumulative NH_3 mass changes significantly with increasing feedratio.

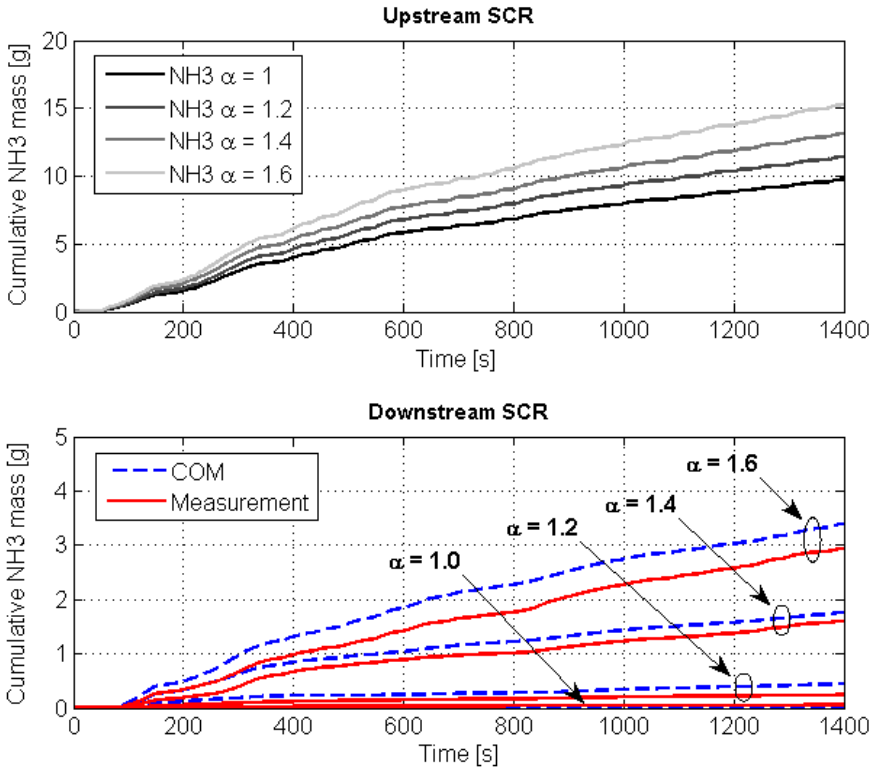

Figure 3.9: Comparison of the cumulative NH_3 mass in different FTPs

As it can be seen in the upper part of figure, with increasing feedratio also the cumulative NH_3 mass upstream the catalyst increases linearly. Accordingly in the lower part of figure also the NH_3 mass downstream the catalyst increases. While for $\alpha = 1$ and $\alpha = 1.2$ the NH_3 slip is more or less negligible, for $\alpha = 1.4$ and $\alpha = 1.6$ a significant NH_3 mass is cumulated. Apart from that, also in the case of NH_3 slip, the COM correlates good to the measurement in the FTP test cycles.

As summary of all four FTPs, in table 3.1 an overview of the important results of the COM verification using test bed measurements is given. The shown values are calculated for each FTP as overall cycle results for the whole test procedure.

Feedratio [-]	NO_x conversion, η_{NOx} [%]		NH_3 conversion, η_{NH3} [%]		Mean NH_3 slip, $\bar{x}_{NH3}$ [ppm]	
	COM	Measurement	COM	Measurement	COM	Measurement
1.0	82.0	80.0	100.0	99.4	0.0	2.0
1.2	91.0	91.4	96.2	97.8	17.0	11.0
1.4	90.8	89.8	87.8	85.6	73.0	67.0
1.6	90.5	92.3	77.7	80.7	139.0	126.0

Table 3.1: Summary of test cycles with constant feedratio

For illustration, more detailed results of the $\alpha = 1.6$ FTP is enclosed in appendix A.2. Several cutout from this FTP containing NO_x and NH_3 fractions up - and downstream the SCR catalyst from measurement and COM are shown.

Furthermore, for completeness figure 3.10 shows the verification of the implemented temperature model according to equation 3.20 in the COM.

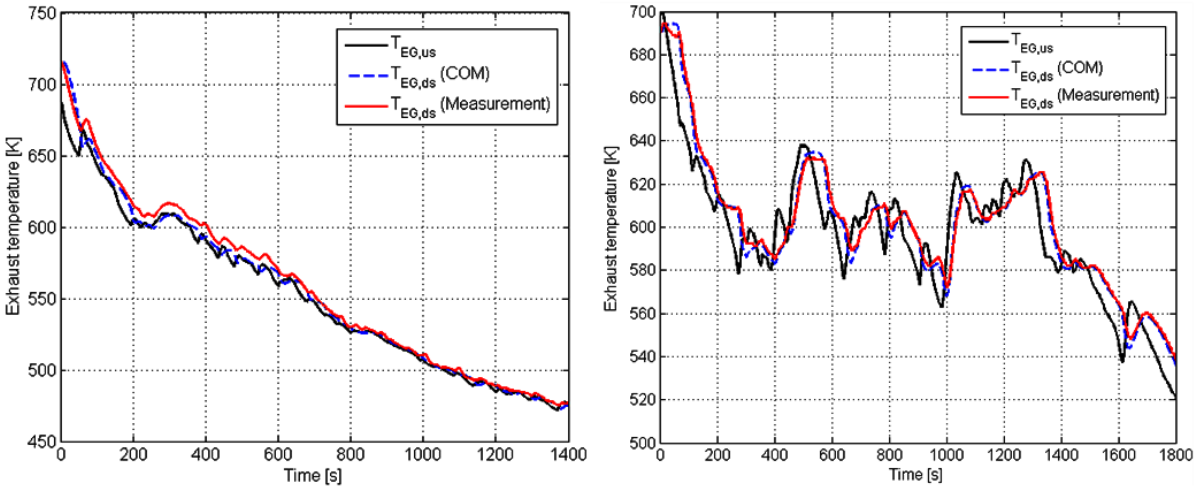

Figure 3.10: Performance of the temperature model in FTP and ETC

The left part of the figure shows the comparison of the temperature profile up - and downstream the SCR catalyst in the modified FTP test cycle between measurement and COM. In order to verify the temperature model also in more dynamic operating conditions, additionally an ETC (European Transient Cycle)[7] is simulated and compared to test bed measurements. The result is shown in the right part of the figure. As it can be seen, for both, FTP and ETC test cycle the temperature model of the COM corresponds very well to the measurement.

[7]ETC cycle bases on real road cycle measurements of commercial vehicles and is used for emission certification of heavy duty vehicles in Europe. For more detailed information refer to [33].

3.5 Discussion

Inside this chapter, a one - dimensional control - oriented SCR catalyst model for the usage in the defined control concept from section 2.4 is presented. In order to allow the computation of the SCR model on an embedded system like an ECU, the PFR behaviour of the real SCR catalyst is approximated in flow direction by using a CSTR cascade. Therefore, the SCR catalyst is discretised by n ideal CSTR cells and thus represented by an ODE system of $n \cdot 6$ order. Due to the complexity of the reaction kinetics of an SCR, the important reaction schemes are taken over from AVL's *BOOST Aftertreatment*. An advantage of this approach is that the kinetic parameters used in the COM are identically compared to the used parameters in the sophisticated SCR Model in BOOST and are therefore easy exchangeable.

In order to allow fast and flexible simulations, a CSTR cell variable structure of the COM is investigated and implemented in the modelling tool MATLAB - SIMULINK®. Simulations using different numbers of CSTR cells along the flow direction show that it is usually sufficient to use two up to five cells to achieve a acceptable tradeoff between model accuracy and needed computational effort [7]. Thus the model verification is performed using a model discretisation of 5.

The derived control - oriented SCR catalyst model is verified against a sophisticated BOOST SCR model and test bed measurements. For the verification an existing parametrisation of a today common applied Fe - ZSM5 based SCR catalyst is used. The comparison between BOOST model and the COM shows more or less the same result in the simulated FTP test cycle. The deviations between the calculated outputs of the two models are small. Furthermore, the verification of the COM using test bed measurements shows good correlations to the real catalyst. Only for lower temperatures of the catalyst ($T_c < 250\,^{\circ}\mathrm{C}$), like in the last third of the modified FTP, the deviations between real catalyst and COM increase (refer to appendix A.2). This behaviour could be improved by an further adaptation of the used kinetic parameters. Due to the fact that the characterisation of an SCR catalyst is not focus of this thesis, this is not performed.

Finally, based on the verification results presented within this chapter it can be said that the control - oriented SCR model has sufficient accuracy compared to BOOST and test bed measurements and is therefore used in the defined control concept and for further investigations in simulation regarding ammonia loading control.

Chapter 4

Realisation of the Model - Based Control Concept

The intention of this chapter is to show how the defined control concept from chapter 2 is conducted and furthermore how the control algorithm is parametrised for the application on the real system. At the beginning, basic experiments with the derived SCR catalyst model are shown. The outcomes of these experiments are discussed and used as input for the controller design. Afterwards, the controller design is performed using the so - called *inward approach*. Based on this, the determination of the optimal reference values for the loading control is shown. Finally, the outcomes of the chapter are summarised and discussed.

4.1 General Remarks

Since in chapter 3 a valid control - oriented model of the SCR catalyst is derived, this model is in the following used for further investigations on the control concept. As in section 2.4 discussed, the defined control variable of the SCR catalyst is its ammonia loading θ_{NH_3}. Because of the fact that the COM is a one - dimensional model, several ammonia loading information $\theta_{NH_3,k}$ are available. Since only the ammonia fraction upstream the SCR $x_{NH_3,us}$ is controlled by a loading controller to influence the different ammonia loadings in the cells, as first approach a mean ammonia loading $\bar{\theta}_{NH_3}$ of all loading information will be used as control variable. Therefore, a controller has to be designed which allows fast and adequate control of the estimated mean ammonia loading of the COM according to a desired setpoint $\bar{\theta}_{ref}$. Furthermore, also the determination of the setpoint $\bar{\theta}_{ref}$ has to be considered, since a major requirement for the control algorithm is the achievement of an adequate SCR catalyst performance for stationary and transient operating conditions. Therefore, a integrated and systematic calibration procedure has to be found for $\bar{\theta}_{ref}$ in order to determine optimal the setpoint according to the desired tradeoff between achievable NO_x conversion and resultant NH_3 slip.

Figure 4.1 shows corresponding to the defined control concept (refer to figure 2.8) the nominal closed - loop system for the $\bar{\theta}_{NH_3}$ control based on the control - oriented SCR model. As it can be seen, the chosen closed - loop system is in unity - feedback configuration and

is a classical single - variable[1] control problem.

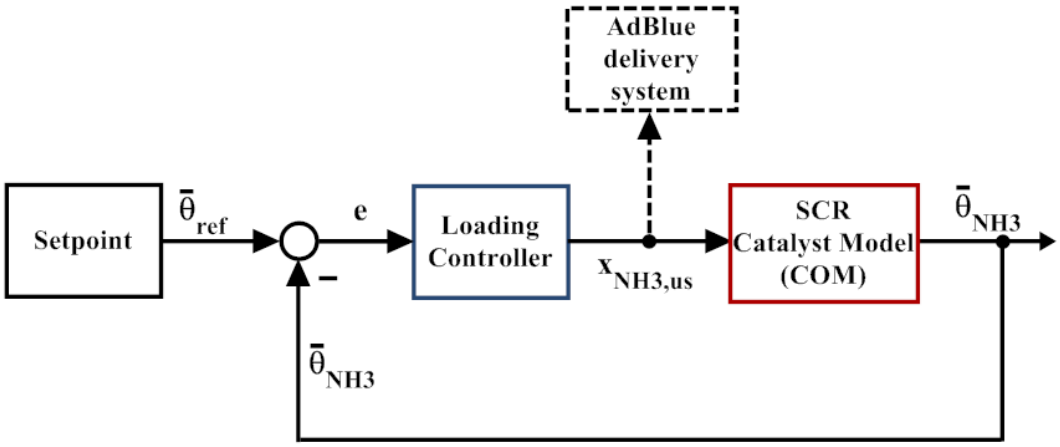

Figure 4.1: Closed - loop system for $\bar{\theta}_{NH_3}$ control

It can be said that the *SCR Catalyst Model* is used as a "virtual sensor" which delivers the ammonia loading $\bar{\theta}_{NH_3}$ information for the closed - loop system. The *Loading controller* uses this "virtual sensor" information in order to calculate based on the control error the ammonia gas fraction $x_{NH_3,us}$. As already mentioned in section 2.4, the ammonia gas fraction $x_{NH_3,us}$ is therefore the actuating signal in the entire control system. Further, the calculated actuating signal $x_{NH_3,us}$ is directly used in the AdBlue^{TM} delivery system in order to dose upstream the real SCR catalyst the corresponding AdBlue^{TM} quantity (symbolised by the dashed lines).

Note, for the following shown investigations on loading control of the COM within this chapter, the verified parameter set of the Fe - ZSM5 based SCR catalyst is used (refer to appendix **??**).

4.2 Basic Experiments on the Catalytic Converter Model

In order to design an adequate *Loading Controller* the important dynamic properties of the control plant (*SCR Catalyst Model*) are firstly investigated. To asses the stationary and dynamic behaviour of the plant, step responses are applied on the SCR model. Since the determined actuating signal $x_{NH_3,us}$ is not intuitive when applying step responses, again the feedratio α is used as same as in section 2.2.2. The relationship between α and $x_{NH_3,us}$ can be easily derived according to

$$\alpha = \frac{\overset{*}{n}_{NH_3,us}}{\overset{*}{n}_{NO_x,us}} = \frac{x_{NH_3,us}}{x_{NO_x,us}}, \tag{4.1}$$

[1]Single - variable systems have only one input and only one output. Often also called "single - input / single - output (SISO) systems [34].

since $\overset{*}{n}_i = x_i \cdot \overset{*}{n}_{EG}$. Therefore it can be written from the relation 4.1,

$$x_{NH_3,us} = \alpha \cdot x_{NO_x,us}. \tag{4.2}$$

For illustration, figure 4.2 shows in principle the setup for the basic experiments on the COM in order to investigate to control plant behaviour of $\alpha \rightarrow \bar{\theta}_{NH_3}$.

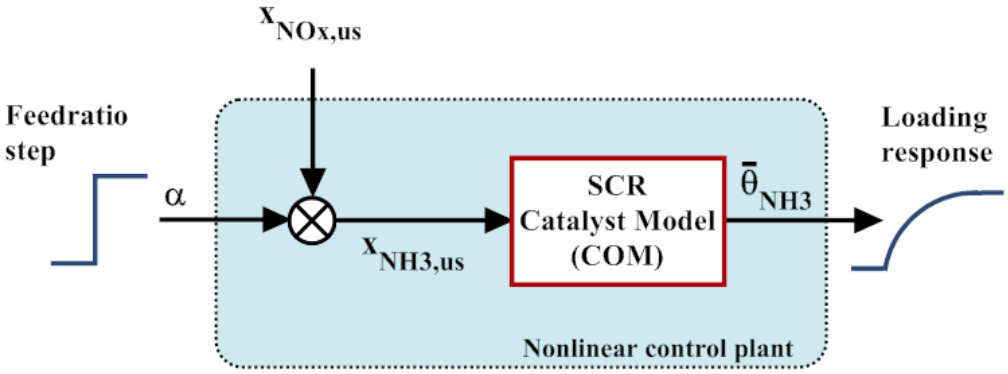

Figure 4.2: Open - loop excitation of the control plant (COM)

For sure, for the control design itself a linear plant model is desired. But to derive a linear plant for $\alpha \rightarrow \bar{\theta}_{NH_3}$, at the beginning open - loop excitations are performed on the nonlinear control plant.

4.2.1 Investigations using Feedratio Step Responses

For the step response investigations on the nonlinear control plant, again the six stationary operating points (OP 1 to OP 6) of the SCR catalyst from the engine test bed are used (refer to section 2.2.2). The characteristic quantities for each operating point from table 2.1 are applied in simulation to the inputs of the COM. After a stabilisation phase for the catalyst model, the α step responses are performed. At the beginning feedratio steps from $\alpha = 0 \rightarrow 1$ are applied.

Figure 4.3 shows summarised all obtained step responses from the operating points. For a better visualisation the step responses are split up in two diagrams (OP 1 - OP 3 and OP 4 - OP 6), since the dynamic behaviour of the control plant varies in a high range. As it can be seen, when the feedratio step is applied at $t = 100\,\mathrm{s}$ the mean ammonia loading $\bar{\theta}_{NH_3}$ increases immediately in the COM without any time delay. This behaviour is explainable, since no mass transport or time delays in the dosing actuator are considered in the COM. In the left part of the figure, the dynamic behaviour of the plant is very slow. For example in OP 1 the ammonia loading $\bar{\theta}_{NH_3}$ is stable at $t \approx 900\,\mathrm{s}$. This is due to the fact that at OP 1 - OP 3 the catalyst temperatures T_c and exhaust mass flows $\overset{*}{m}_{EG}$ is low. On the opposite, with increasing T_c and $\overset{*}{m}_{EG}$ the dynamic behaviour becomes faster (right part of the figure). This behaviour is according to the observations on the real SCR from section 2.2.2, where the $NO_x\,/\,NH_3$ conversion becomes faster. Further,

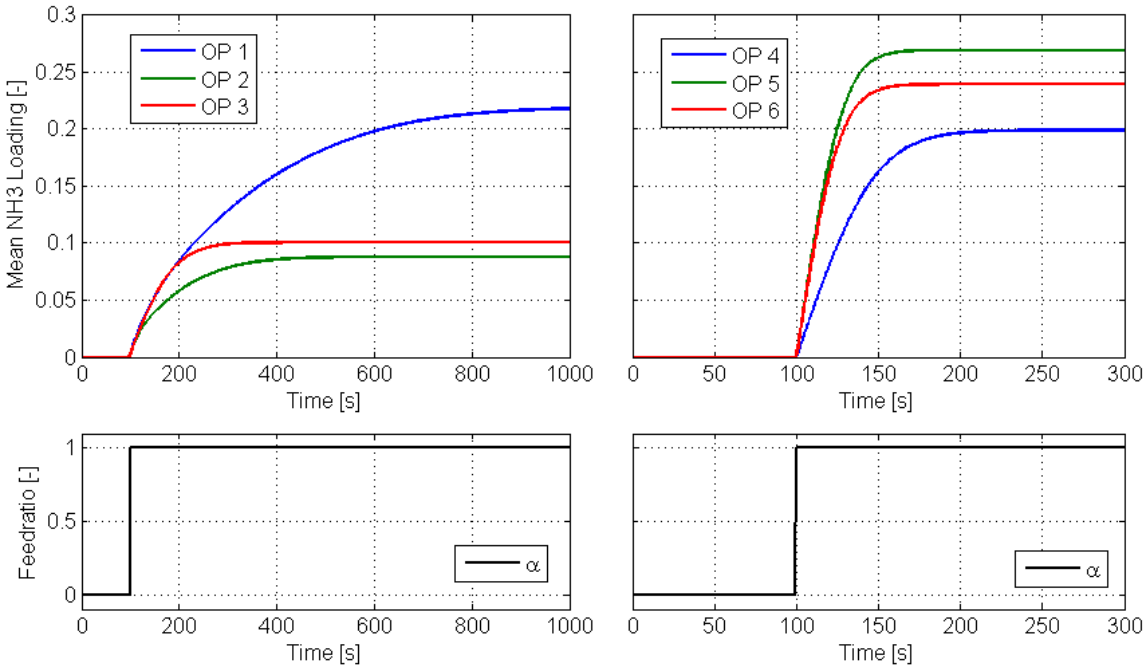

Figure 4.3: Performed step responses on the control plant (COM)

also a dependency of the stationary achieved ammonia loading on the operating point can be seen when applying a $\alpha = 0 \rightarrow 1$ step. This behaviour corresponds again to the observations on the real catalyst where the NO_x / NH_3 reduction capability changes significant in the different operating points.

Apart from that, the step responses in all operating points are further approximated by a plant behaviour of first order systems (PT1), represented by a transfer function according to

$$G(s) = k_\alpha \cdot \frac{1}{\tau \cdot s + 1}. \tag{4.3}$$

Therefore, Table 4.1 gives a quantitative summary of all step responses with the important values of the operating point (T_c, $\overset{*}{m}_{EG}$) and the characteristic values of the PT1 plant.

			OP 1	OP 2	OP 3	OP 4	OP 5	OP 6
Excitation	Feedratio, α	[-]	0 → 1.0	0 → 1.0	0 → 1.0	0 → 1.0	0 → 1.0	0 → 1.0
Operating Point	Exhaust mass flow, $m_{EG,us}$	[kg/h]	200.26	222.00	255.05	327.88	356.91	470.62
	Catalyst temperature, T_c	[°C]	224	299	348	398	453	438
Plant Parameter	Gain, k_α	[-]	0.220	0.088	0.101	0.199	0.269	0.239
	Time constant, T	[s]	226.00	93.00	64.20	33.50	19.62	18.50

Table 4.1: Summary of identified plant parameter

Furthermore, comparing the identified time constants of the mean loading $\bar{\theta}_{NH_3}$ with the measured time constants of NO_x / NH_3 conversion from the real catalyst (refer to table

2.2) it can be seen that they are in the same range as the "NH_3 plant" time constants. This outcome is explainable, since the NH_3 fraction downstream the SCR can only be stable, when the ammonia loading $\bar{\theta}_{NH_3}$ inside the catalyst is stable.

Since the *Loading Controller* applies arbitrary feedratios when controlling the ammonia loading $\bar{\theta}_{NH_3}$ of the COM, also step responses are performed using different feedratios in order to investigate the nonlinear control plant behaviour. Figure 4.4 shows exemplarily for OP 3 the step responses of the feedratio steps $\alpha = 0 \rightarrow 0.6,\ 0.7,\ 0.8,\ 0.9,\ 1.0$.

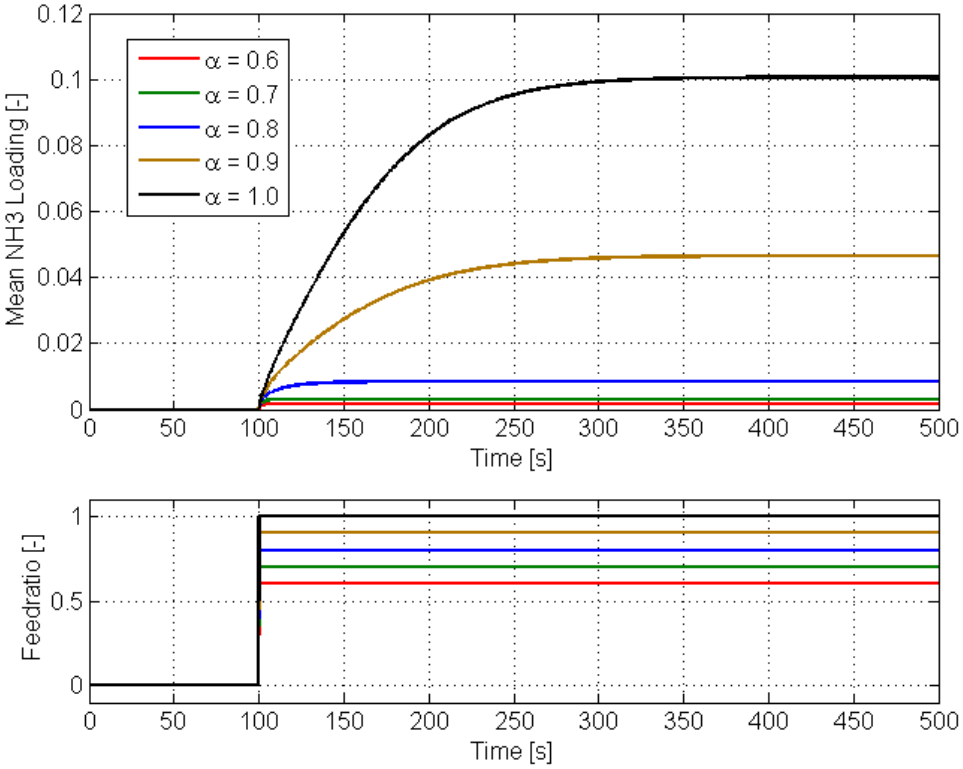

Figure 4.4: Different step responses in OP 3

As it can be seen in the figure, the plant behaviour of the *SCR Catalyst Model* is highly nonlinear regarding to the gain. While for feedratio steps $\alpha = 0 \rightarrow 0.6,\ 0.7,\ 0.8$ the resultant stationary ammonia loading is relatively low ($< 1\,\%$), for feedratio steps $\alpha = 0 \rightarrow 0.9, 1.0$ the resultant stationary loading increases up to $10\,\%$ surface coverage fraction.

4.2.2 Summary and Discussion of the Basic Experiments

Based on the investigations on the control - oriented SCR model using feedratio step responses, following important observations are summarised:

- As expected, the step responses of mean ammonia loading $\bar{\theta}_{NH_3}$ in the different operating points are showing similar behaviour as the open - loop investigations on the real catalyst (refer to section 2.2.2).

- The dynamic behaviour of the control plant ($\alpha \rightarrow \bar{\theta}_{NH_3}$) can be characterised by using linear first order systems (PT1) without time delay. This fact allows the appliance of a relatively simple *Loading Controller*, like e.g. a linear PI - controller.
- The plant parameters (k_α, τ) are strongly changing with the operating point of the SCR catalyst (T_c, $\overset{*}{m}_{EG}$). Since the catalyst has to be controlled adequate in each operating point, this has to be considered in the *Loading Controller*.
- Step responses using different feedratios in an operating point are showing that the plant behaviour is highly nonlinear regarding the gain k_α. Due to the fact that for the closed - loop system, shown in figure 4.1, a linear control law is desired, this nonlinear behaviour of the control plant regarding k_α has to be considered. Therefore, in the following further investigations on linearisation of the control plant are made.

4.3 Static Linearisation of the Nonlinear Control Plant

Since the control plant is highly nonlinear regarding its gain k_α, this behaviour has to be compensated. This is done in order to allow the appliance of a preferred linear *Loading Controller* in the closed - loop system according to figure 4.1.

4.3.1 Input Linearisation

In order to investigate the nonlinear plant behaviour of the catalyst model regarding the gain k_α, several step responses, as performed in the experiment documented in figure 4.4, are performed in each operating point. For these investigations, the feedratio steps are increased by $\Delta\alpha = 0.1$ beginning from $\alpha = 0$ up to $\alpha = 2$. After the steady state conditions for each feedratio step are reached, the resultant stationary ammonia loading $\bar{\theta}_{NH_3}$ is listed. Therefore, using this approach, a static relationship between feedratio and mean ammonia loading according to

$$\bar{\theta}_{NH_3} = f(\alpha) \tag{4.4}$$

is obtained.

Figure 4.5 shows graphically this derived relationship exemplarily for OP 3. As it can be seen, there is a monotonically increasing behaviour of the obtained relationship. With increasing feedratio, the ammonia loading also increases. According to figure 4.4, for feedratios $\alpha \leq 0.8$ the resultant ammonia loading is small ($< 1\,\%$) and for higher feedratios the ammonia loading increases up to $\approx 46\,\%$ of the possible surface coverage of the catalyst. Furthermore, the nonlinear behaviour of the contol plant regarding the stationary gain can be clearly seen in the figure.

Due to the fact that the relationship $\bar{\theta}_{NH_3} = f(\alpha)$ is monotonic and therefore unique, the nonlinear static behaviour of the control plant regarding k_α can be compensated by using the inverted characteristic at the input of the control plant in order to linearise it [35].

Therefore, in order to obtain this inverted characteristic, primarily for all operating points the static relationship between feedratio and resultant ammonia loading is investigated.

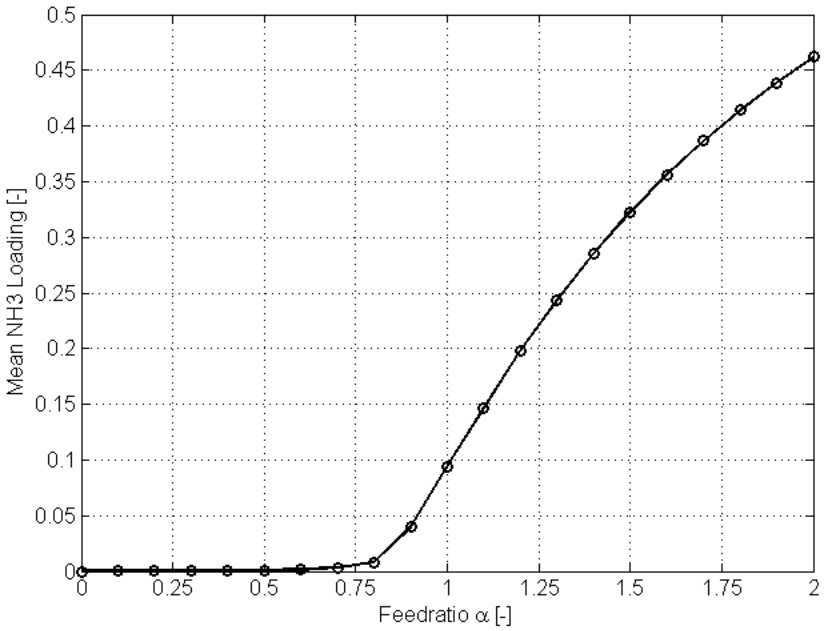

Figure 4.5: Stationary correlation between α and $\bar{\theta}_{NH_3}$ in OP 3

Figure 4.6 shows the characteristic curves for the different operating points (OP 1 - OP 6). In order to compare the curves to each other, all mean ammonia loadings are normalised for every operating point by using their maximal values at $\alpha = 2.0$.

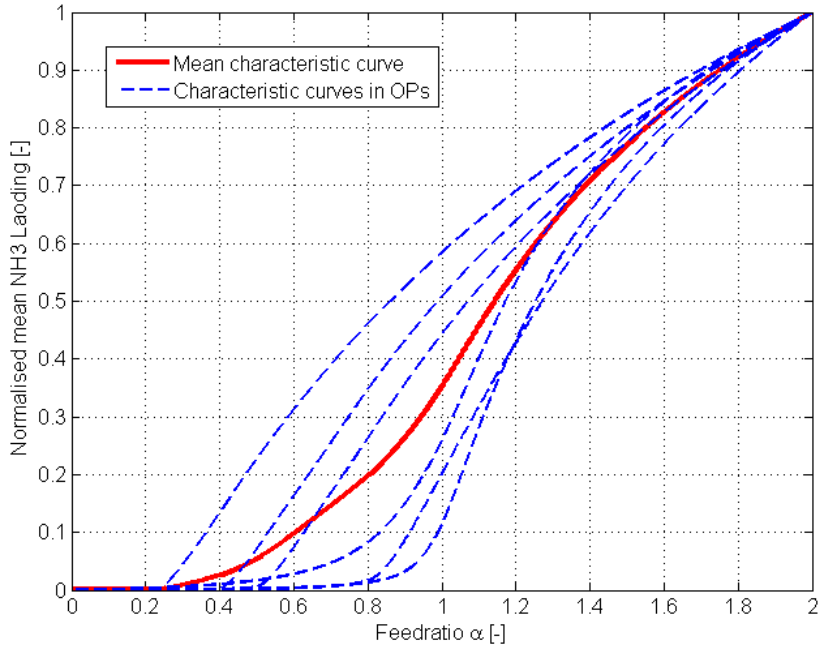

Figure 4.6: Normalised characteristic $\bar{\theta}_{NH_3}$ curves

As it can be seen, the characteristic curves differ slightly for each operating point. Since for the linearisation of the control plant only one static relationship can be considered, a

mean normalised characteristic curve $\bar{\theta}_{NH_3,norm}$ of all operating points is calculated (red line in the figure). This curve should approximate the nonlinear plant behaviour regarding k_α in the entire operating range of the SCR catalyst.

Since the mean static relationship between $\bar{\theta}_{NH_3,norm}$ and α is known, the inverted characteristic curve can be derived according to

$$\alpha = f^{-1}\left(\bar{\theta}_{NH_3,norm}\right). \tag{4.5}$$

Defining a new variable α_{lin} (linearised feedratio) as input for the control plant which is normalised to the range of α (in the here shown case $\alpha \in [0, 2]$), relation 4.5 can be further written as

$$\alpha = f^{-1}\left(\bar{\theta}_{NH_3,norm}\right) = g\left(\alpha_{lin}\right) \cdot \alpha_{max}. \tag{4.6}$$

Where $\alpha_{max} = 2$. Using this approach, the inverted characteristic curve is obtained, which is normalised to the input range of the feedratio α to the nonlinear control plant.

Figure 4.7 shows the inverted characteristic curve which linearises the nonlinear control plant at the input.

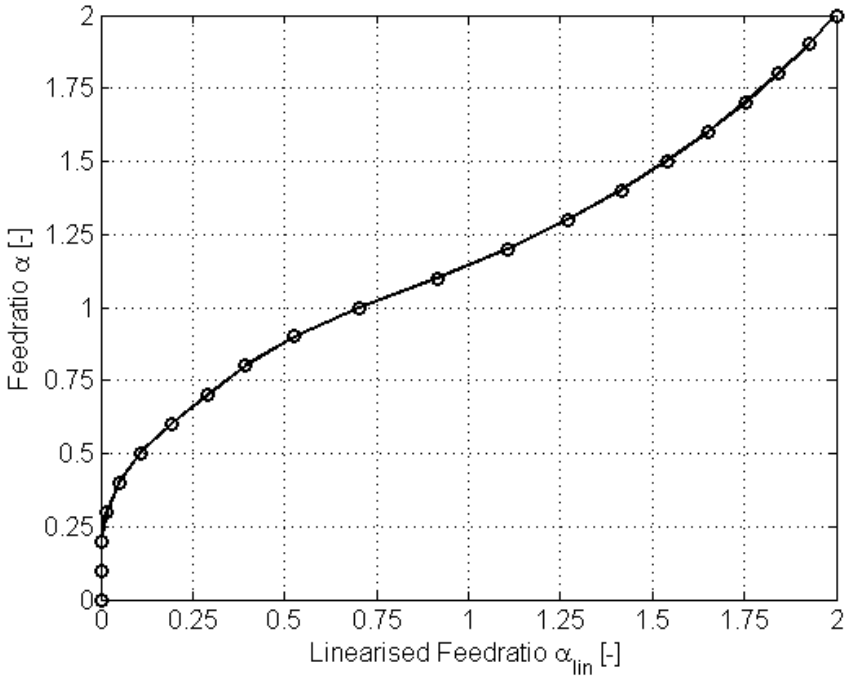

Figure 4.7: Characteristic curve between α_{lin} and α

As it can be seen, the inverted curve compensates the nonlinear plant behaviour especially for feedratios $\alpha \leq 1.25$. For higher feedratios, the static behaviour of the plant becomes more and more linear between α_{lin} and α.

Because of the fact that the control plant is now linearised using α_{lin}, the plant behaviour of the new "linearised control plant" is in the following investigated. Therefore, the step responses in the different operating points (OP 1 - OP 6) are performed again using α_{lin}.

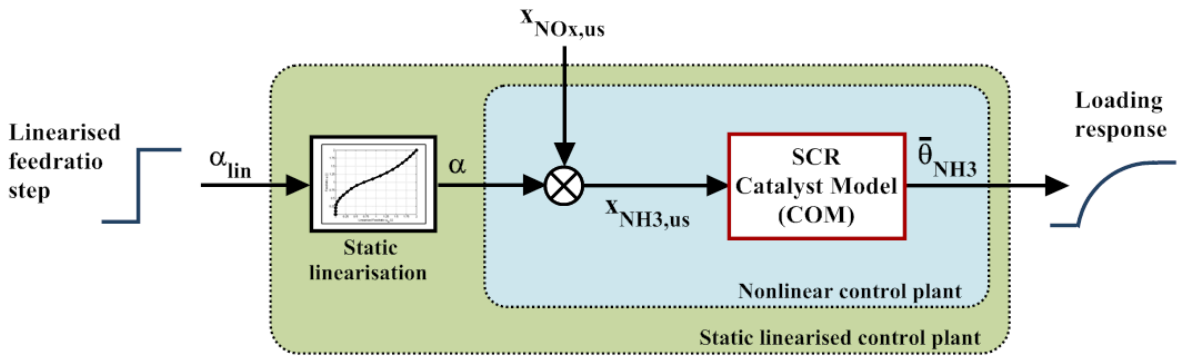

Figure 4.8: Linearised control plant $\alpha_{lin} \rightarrow \bar{\theta}_{NH_3}$

For illustration, figure 4.8 shows the derived linearised control plant ($\alpha_{lin} \rightarrow \bar{\theta}_{NH_3}$) with the static linearisation at the input.

Table 4.2 gives a summary of all step responses using the linearised feedratio α_{lin}. Again, in order to characterise the dynamic behaviour, a PT1 behaviour of the control plant according to

$$G(s) = k_{\alpha,lin} \cdot \frac{1}{\tau \cdot s + 1} \tag{4.7}$$

is assumed.

			OP 1	OP 2	OP 3	OP 4	OP 5	OP 6
Excitation	Linearised feedratio, α_{lin}	[-]	0 → 1.0	0 → 1.0	0 → 1.0	0 → 1.0	0 → 1.0	0 → 1.0
Operating Point	Exhaust mass flow, $m_{EG,us}$	[kg/h]	200.26	222.00	255.05	327.88	356.91	470.62
	Catalyst temperature, T_c	[°C]	224	299	348	398	453	438
Plant Parameter	Gain, $k_{\alpha lin}$	[-]	0.370	0.293	0.223	0.199	0.194	0.202
	Time constant, T	[s]	243.50	112.10	67.00	39.00	25.00	22.80

Table 4.2: Summary of plant parameter of the linearised plant

As it can be seen, the obtained values for $k_{\alpha,lin}$ and τ differ slightly from the values in table 4.1. While the time constants are nearly the same, the gains have different values, since they are linearised by α_{lin}.

4.3.2 Verification of the Input Linearisation

Because of the fact that the actuating signal of control - oriented SCR model is linearised in section 4.3.1, the static behaviour of the linearised plant is further evaluated for the different operating points. In order to investigate the behaviour of the static linearised plant over the entire range of the actuating signal, a slow ramp instead of step responses is applied at the input of the plant. Additionally, also the identified first order models from table 4.2 are compared to the linearised plant model.

Figure 4.9 shows exemplarily the result of the applied ramp for OP 3. Additionally to the linearised control plant with its identified PT1 model, also the non - linearised plant with its identified PT1 model from table 4.1 are visualised in the figure.

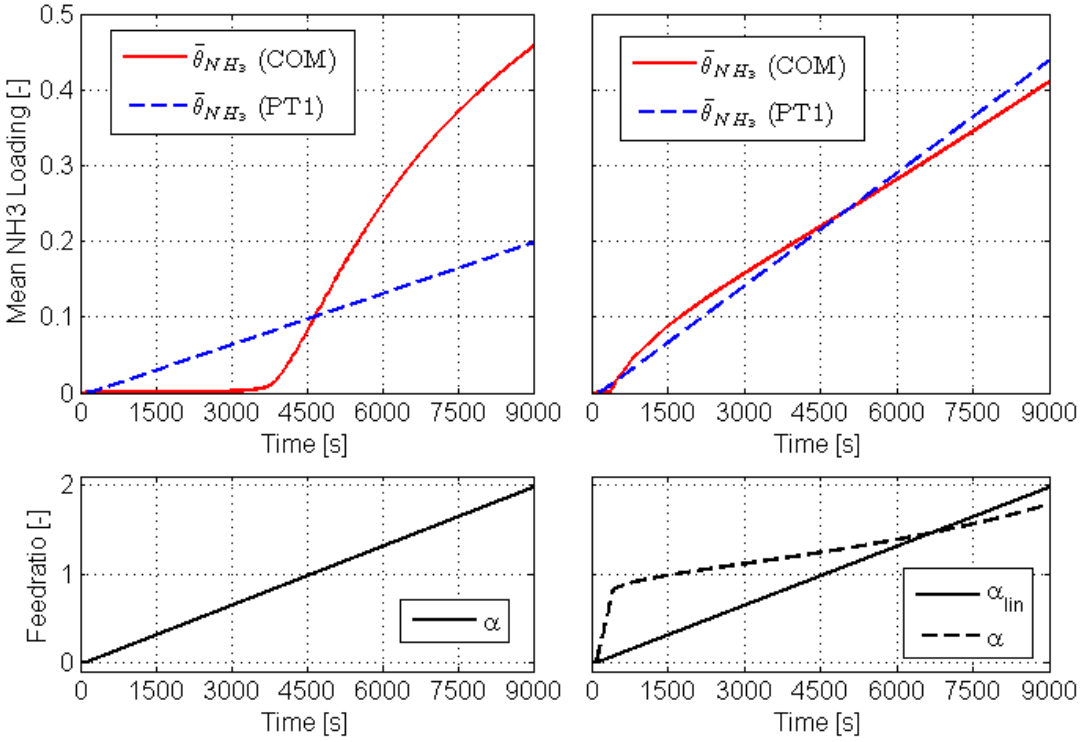

Figure 4.9: Ramp responses of the non - linearised and linearised control plant

As it can be seen in the left part of the figure for the non - linearised plant, the correlation between the PT1 model and the nonlinear plant is poor over the entire feedratio range. Only for $\alpha = 1$ at $t \approx 4500\,\mathrm{s}$, the mean loading of the COM and the idealised PT1 model correspond to each other. This is due to the fact that the PT1 model is identified for the feedratio step $\alpha = 0 \rightarrow 1$ (refer to table 4.1).

On the other hand, using the linearised feedratio as input for the control plant (right part of the figure), the correlation between the identified PT1 model and the COM is much better over the entire feedratio range. The small deviations between the COM and the PT1 model are mainly caused by the usage of the mean linearisation curve achieved from all operating points (refer to figure 4.7).

Due to the good results of the verification of the input linearisation it can be said that the plant behaviour of the COM ($\alpha_{lin} \rightarrow \bar{\theta}_{NH_3}$) in an operating point can be simplified characterised with sufficient accuracy using the linear PT1 model. Therefore, according to the shown closed - loop system (refer to figure 4.1) for each operating point of the catalyst a linear *Loading Controller* can be used. Since the plant parameters are strongly dependent on the operating point, also the control parameters have to be adapted according to the changing control plant. This approach of varying control parameters depending on the operating point of a system is commonly known as *gain scheduling* in the literature. For more detailed information on *gain scheduling* refer to [36], [37].

4.4 Controller Design

Based on the results of section 4.2 and 4.3 a linear *Loading Controller* is in the following designed, which achieves a desired steady - state and transient performance for controlling the mean ammonia loading $\bar{\theta}_{NH_3}$ of the COM. As already mentioned, in order to consider the changing dynamic behaviour of the control plant depending on the operating point of the catalyst, the principal of *gain scheduling* is used. The basic idea of this technique is, to design linear controllers for several operating points of the nonlinear plant and implement the resulting family of linear controllers as a single controller, the so - called *gain - scheduled controller*. The parameters of this *gain - scheduled controller* are changed by monitoring of the actual operating point. The variables which define the actual operating point are the so - called *scheduling variables* [37]. For the concrete case of controlling the linearised control - oriented SCR model, from the basic experiments is known that the performance of the control plant is strongly dependent on the catalyst temperature and exhaust mass flow. Thus, these quantities are defined as *scheduling variables* for the *gain - scheduled controller* according to the relation

$$Controller\,parameters = f(T_c, \overset{*}{m}_{EG}). \tag{4.8}$$

Therefore, for the identified linear control plants from table 4.2, a design method for the needed controller structure and its parameters has to be chosen. Due to the fact that the control plant can be approximated by the linear, time invariant system $G(s)$ (refer to equation 4.7), several methods from linear control engineering are available for the current problem. Basically, the properties of stability and steady - state performance of the closed - loop system are important for the selection of the controller.

Instead of using classical linear control design approaches like empirical methods (e.g. Ziegler / Nichols [34]), root - locus method or frequency - domain method, a quite different design method is used in order to achieve an adequate *Loading Controller* within this work. The here used method is the so - called *inward approach*. Classical control design approaches typically try to derive the control structure with its parametrisation from open - loop investigations. Therefore, often the needed controllers are searched step - by - step until the overall system meets the design specifications. Such approaches are often also called *outward approach*, since the design process starts from internal compensators and then designs an overall system to meet the required design specifications [34].

The *inward approach* is compared to the classical design approaches completely different. This method starts with the choice of a desired overall system behaviour by defining a transfer function $T_d(s)$. The chosen $T_d(s)$ has to meet the design specifications for the closed - loop system. Based on this choice, the needed controller is calculated directly by a set of linear algebraic equations in consideration of the given control plant $G(s)$. The resulting transfer function $T(s)$ follows from the interconnection of the calculated controller and the plant. Figure 4.10 illustrates the basic configuration of the *inward approach* adapted for the loading control of the SCR model.

Where T(s) and G(s) from the figure can be written as rational function of the two polynomials according to

$$G(s) = \frac{\mu(s)}{\upsilon(s)},\ T(s) = \frac{\mu_T(s)}{\upsilon_T(s)}. \tag{4.9}$$

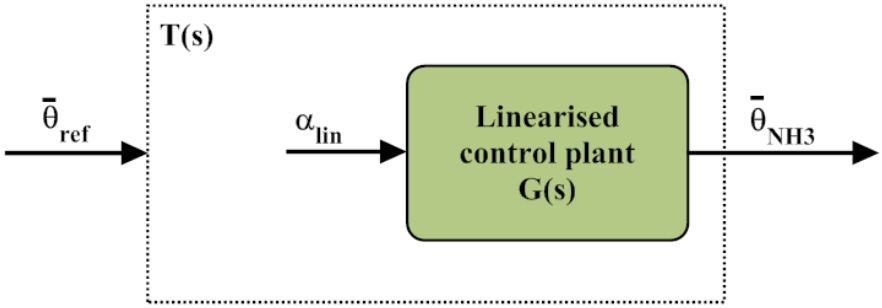

Figure 4.10: Control design method using the Inward Approach

In order to realise the appropriate controller, different requirements for the implementation of the overall transfer function must be given. The choice of the desired overall system behaviour is not arbitrary. Some constraints in the definitions of $T_d(s)$ have to be considered, in order to prevent the occurrence of several problems like loss of total stability or realisability. Therefore, the overall desired transfer function $T_d(s)$ must fulfil some specific requirements. This means, for a practical realisation of the overall transfer function it has to be clarified, if for the given plant $G(s)$ and the chosen $T_d(s)$ the problem is even solvable.

Basically $T_d(s)$ is implementable if and only if following conditions are fulfilled [38]:

- The denominator polynomial $\nu_T(s)$ from $T_d(s)$ is a *Hurwitz* - polynomial[2].
- All unstable roots of $\mu(s)$ from $G(s)$ are also numerator roots of $\mu_T(s)$ from $T_d(s)$.
- The degree difference between numerator and denominator of $T_d(s)$ may not be smaller than from $G(s)$. Thus, $\deg(\nu_T(s)) - \deg(\mu_T(s)) \geq \deg(\nu(s)) - \deg(\nu(s))$.

Note, in the three above stated criteria no explicit constraints regarding the controller structure and parametrisation is made. The entire controller itself follows directly from the implementable chosen $T_d(s)$ regarding $G(s)$.

4.4.1 Controller Design using the Inward Approach

Since the design method for the *Loading Controller* is chosen (*inward approach*), the needed control algorithm with its parametrisation is now calculated exemplary for one operating point (OP 3).

Basically, there are no restrictions for the choice of the controller configuration in order to fulfil the desired overall transfer function $T_d(s)$. Therefore, different approaches can be used (e.g. unity - feedback, two - parameter or plant input / output feedback configuration [34]). As chosen approach within this thesis, the closed - loop system for $\bar{\theta}_{NH_3}$ control

[2] A *Hurwitz* - polynomial is a polynomial whose coefficients are positive real numbers and whose zeros are located in the left half - plane of the complex plane [38]. A transfer function containing a *Hurwitz* - polynomial as denominator is called BIBO - stable.

(refer to figure 4.1) is defined in unity - feedback configuration. Because of this definition, the *inward approach* can be used for a arbitrary pole placement of the resultant overall transfer function $T(s)$ [34], [38]. For illustration, figure 4.11 shows exemplary the specific closed - loop system for OP 3.

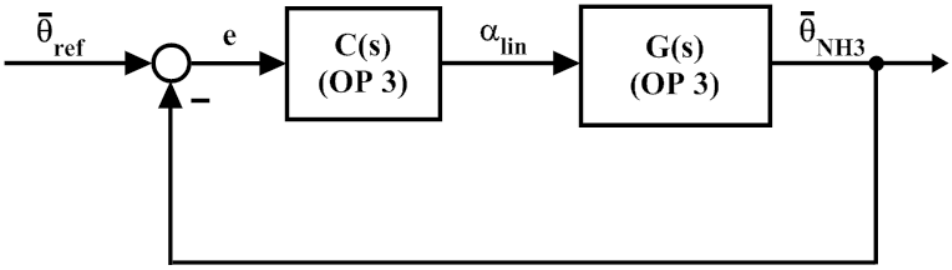

Figure 4.11: Closed - loop system for the control design (example for OP 3)

Where the controller $C(s)$ can be written also as rational function of the two polynomials according to

$$C(s) = \frac{b(s)}{a(s)}, \tag{4.10}$$

and the control plant $G(s)$ according to

$$G(s) = \frac{\mu(s)}{\upsilon(s)} = \frac{0.223}{67\ s + 1} \tag{4.11}$$

for OP 3. Therefore, the resultant overall transfer function $T(s)$ can be written in general form according to

$$T(s) = \frac{C(s) \cdot G(s)}{1 + C(s) \cdot G(s)} = \frac{b(s) \cdot \mu(s)}{a(s) \cdot \upsilon(s) + b(s) \cdot \mu(s)}. \tag{4.12}$$

Since the resultant transfer function $T(s)$ should be the desired overall transfer function $T_d(s)$ it must be

$$T(s) = \frac{b(s) \cdot \mu(s)}{a(s) \cdot \upsilon(s) + b(s) \cdot \mu(s)} \stackrel{!}{=} T_d(s). \tag{4.13}$$

Thus,

$$\frac{b(s) \cdot \mu(s)}{a(s) \cdot \upsilon(s) + b(s) \cdot \mu(s)} \stackrel{!}{=} \frac{\mu_{T,d}(s)}{\upsilon_{T,d}(s)}. \tag{4.14}$$

As it can be seen from relation 4.14, using a unity - feedback controller configuration, the denominator polynomial of $T(s)$ can be calculated according to the desired poles defined in $\upsilon_{T,d}(s)$ using

$$a(s) \cdot \upsilon(s) + b(s) \cdot \mu(s) \stackrel{!}{=} \upsilon_{T,d}(s). \tag{4.15}$$

The numerator polynomial of $T(s)$ is determined by the resultant $b(s)$ which fulfils relation 4.15. Because of this, in unity - feedback configuration of a closed - loop system, the numerator polynomial of $T(s)$ cannot be defined arbitrary.

The relationship 4.15 is of the type $1 = \mu b + \upsilon a$, which refers in the literature to the *Diophantine equation* [38]. In the equation 4.15, $\nu(s)$ and $\upsilon(s)$ are given by the control plant $G(s)$, the roots of $\upsilon_{T,d}(s)$ are the poles of the overall system $T_d(s)$ which has to be defined. Thus, $a(s)$ and $b(s)$ are the unknown polynomials of the controller $C(s)$ which are obtained by solving the *Diophantine equation* 4.15.

4.4.1.1 Choice of the Desired Overall Transfer Function

Since the controller polynomials $a(s)$ and $b(s)$ can be calculated by solving of the *Diophantine equation*, at first the desired overall transfer function $T_d(s)$ is defined. A common practically approach is to assign $T_d(s)$ the dynamic behaviour of a second order system with a dominant pole pair. Therefore, the desired overall transfer function is chosen according to

$$T_d(s) = \frac{\omega_0^2}{s^2 + 2\,d\,\omega_0\,s + \omega_0^2}. \tag{4.16}$$

Where, the damping factor d and the eigenfrequency ω_0 determines the dynamic behaviour of the system. The required system performance is specified by means of the step response in time - domain. The values of d and ω_0 are chosen in a way that a desired overshoot M_p and a desired rising - time t_r of the second order system are achieved. The relationship between M_p, t_r and d, ω_0 is illustrated in appendix B.1.

For the dynamic behaviour of the closed - loop system for ammonia loading control, following performance of the desired overall transfer function $T_d(s)$ is chosen:

- No overshoot of the controlled system is allowed, since too high $\bar{\theta}_{NH_3}$ could cause NH_3 slip. Thus, $M_p = 1$.
- The rising - time t_r of the controlled system should be approximately the half of the time constant τ of the control plant, in order to achieve fast the desired ammonia loading. Thus, $t_r \approx \frac{\tau}{2} = 33.5\,\mathrm{s}$

Using this specification, the desired second order system can be written according to

$$T_d(s) = \frac{0.009025}{s^2 + 0.19\,s + 0.009025}. \tag{4.17}$$

Where,

$d = 1$,

$\omega_0 = 0.0950\,rad/s$.

Note, according to the three stated criteria regarding implementability of the desired overall transfer function it can be said that the chosen $T_d(s)$ from equation 4.17 is implementable.

4.4.1.2 Calculation of the *Loading Controller*

Since a implementable desired overall transfer function is derived, the needed loading controller $C(s)$ is further calculated using the *Diophantine equation* stated in equation 4.15. Because of the fact that $T_d(s)$ is chosen of second order, an additional degree of freedom is available for calculating the controller $C(s)$ by the *Diophantine equation*[3]. Therefore, using this additionally degree of freedom it makes sense, to ensure a certain steady - state performance of the closed - loop system. In the case of ammonia loading control, the stationary accuracy of $\bar{\theta}_{NH_3}$ regarding $\bar{\theta}_{ref}$ is fundamental in order to achieve the desired tradeoff between NO_x reduction and NH_3 slip. Thus, to ensure stationary accuracy of resultant overall transfer function, it has to fulfil the relation

$$T(0) = \frac{b(0)\,\mu(0)}{a(0)\,\upsilon(0) + b(0)\,\mu(0)} = 1. \tag{4.18}$$

Obviously, this can only be achieved if $a(0)\,\upsilon(0) = 0$. In order to fulfil this relation, either the controller or the plant must have a pole at $s = 0$. Since the control plant $G(s)$ does not have this behaviour (PT1 model), the integrating property must be achieved in the controller $C(s)$. Basically, the integrating behaviour is fulfilled, if the denominator polynomial $a(s)$ of the controller fulfils the condition $a_0 = 0$ [38].
Since the additionally degree of freedom is reasonable used, the *Diophantine equation* for the closed - loop system can be written in matrix notation in general form according to

$$\begin{bmatrix} \upsilon_0 & 0 & \mu_0 & 0 \\ \upsilon_1 & \upsilon_0 & \mu_1 & \mu_0 \\ 0 & \upsilon_1 & 0 & \mu_1 \\ 1 & 0 & 0 & 0 \end{bmatrix} \begin{bmatrix} a_0 \\ a_1 \\ b_0 \\ b_1 \end{bmatrix} = \begin{bmatrix} \upsilon_{0\,T,d} \\ \upsilon_{1\,T,d} \\ \upsilon_{2\,T,d} \\ 0 \end{bmatrix}. \tag{4.19}$$

Further, for the specific case of OP 3, the set of linear algebraic equations can be written as

$$\begin{bmatrix} 1 & 0 & 0.223 & 0 \\ 67 & 1 & 0 & 0.223 \\ 0 & 67 & 0 & 0 \\ 1 & 0 & 0 & 0 \end{bmatrix} \begin{bmatrix} a_0 \\ a_1 \\ b_0 \\ b_1 \end{bmatrix} = \begin{bmatrix} 0.009025 \\ 0.19 \\ 1 \\ 0 \end{bmatrix}. \tag{4.20}$$

Solving the set of equations regarding to unknown controller coefficients, a *Loading Controller* according to

$$C(s) = \frac{b_1\,s + b_0}{a_1\,s + a_0} = \frac{52.51\,s + 2.71}{s} \tag{4.21}$$

is derived for OP 3. As it can be seen, the achieved linear controller is of first order and has the integrating property as defined, since $a_0 = 0$. Furthermore, the derived transfer function of the controller is commonly known as *PI - Controller*, which is a typically used

[3]Note, to obtain a unique solution of the *Diophantine equation*, the order of the wanted controller $C(s)$ has to be lower by 1 as the order of the control plant $G(s)$ [38].

controller approach in industrial processes. Therefore, according to the notation of a typical *PI - Controller*, the coefficients of $C(s)$ are in the following represented by the controller gain k_p and the integral time constant T_i. Thus the *PI - Controller* can be written in general form as

$$C(s) = k_p \, \frac{T_i \, s + 1}{T_i \, s} \tag{4.22}$$

With the specific parameters for OP 3

$$k_p = 52.51,$$

$$T_i = 19.40 \, s.$$

Since the needed controller structure with its parametrisation is derived, the *Loading Controller* is in the following verified by using the linearised control - oriented SCR model. Figure 4.12 shows the closed - loop behaviour of the designed *Loading Controller* for a step response of $\bar{\theta}_{ref} = 0 \rightarrow 0.1$ in OP 3.

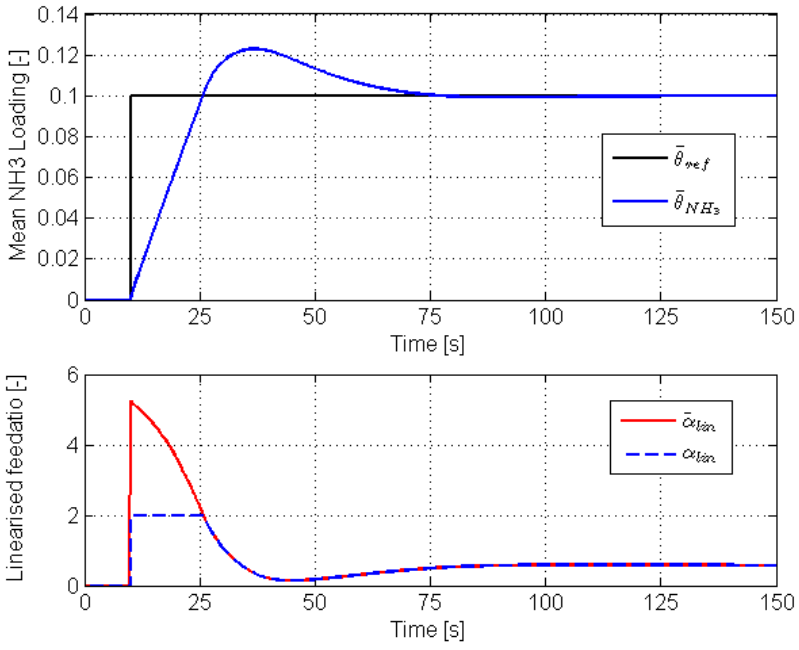

Figure 4.12: Step response of desired loading on linearised plant (COM)

As it can be clearly seen in the upper part of the figure, the actual loading $\bar{\theta}_{NH_3}$ has a huge overshoot of $\geq 20\,\%$ during the control of $\bar{\theta}_{NH_3}$ to $\bar{\theta}_{ref} = 0.1$. Since in section 4.4.1.1 the desired overall transfer function $T_d(s)$ is defined in order to avoid overshots, this unwanted behaviour is deeper investigated. Therefore, in the lower part of the figure the actuating signal α_{lin} and the unlimited controller output $\tilde{\alpha}_{lin}$ is shown. Note, in section 4.3.1 the linearised feedratio α_{lin} is defined for $\alpha_{lin} \in [0, 2]$, thus it is limited. As it can be seen from the actuating signals $\tilde{\alpha}_{lin}$ and α_{lin}, when the step is applied at $t = 10\,\mathrm{s}$ it comes to a windup - effect of the integral part of the controller. Altough the reference

value of $\bar{\theta}_{ref} = 0.1$ is reached at $t \approx 25\,\mathrm{s}$, the actuating signal is still high at $\alpha_{lin} = 2$. Until $\tilde{\alpha}_{lin}$ reaches to upper limitation boundary, α_{lin} is reduced again. Nevertheless, this reduction is much to late in order to avoid the overshoot in $\bar{\theta}_{NH_3}$. Because of the fact that such a behaviour of the closed - loop system could cause high NH_3 slip, it is therefore not acceptable and has to be eliminated. Thus, a so - called anti - windup measure is in the following implemented in the *Loading Controller*.

4.4.1.3 Anti - Windup Measure for the *Loading Controller*

As in the previous section shown, the *Loading Controller* has to be extended with an anti - windup measure in order to avoid overshooting of the control variable $\bar{\theta}_{NH_3}$ caused by windup of the integral part of the controller. Therefore, a daily common used anti - windup measure is implemented in the controller. Figure 4.13 shows the realised anti - windup concept according to [38].

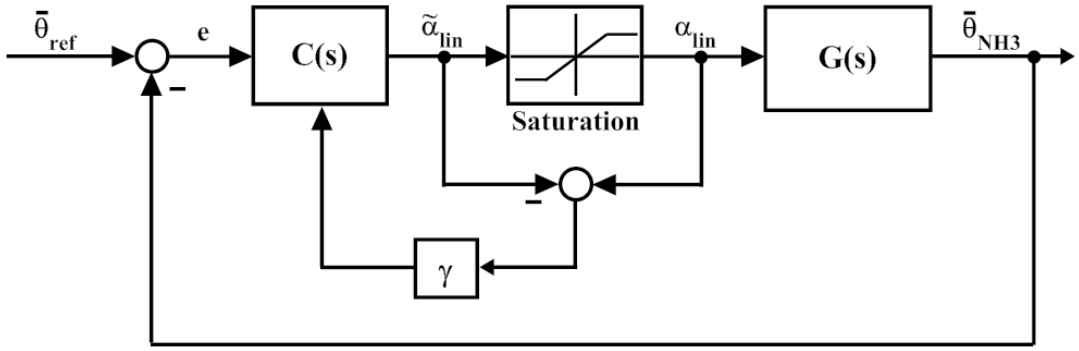

Figure 4.13: Anti - windup measure for the *Loading Controller*

As it can be seen, the difference between $\tilde{\alpha}_{lin}$ and α_{lin} is weighted with an adequate chosen factor γ and fed back to the *Loading Controller*. More precisely, the fed back information is applied additive at the input of the integrator in $C(s)$ and works against the windup effect of it, if the controller is in the limitation.

For simplicity, the weighting factor γ is determined by simulation on the linearised control - oriented SCR model. A good anti - windup behaviour is achieved using $\gamma = 0.9$. Figure 4.14 shows again the closed - loop behaviour of the designed *Loading Controller* with and without anti - windup measure for the step response of $\bar{\theta}_{ref} = 0 \rightarrow 0.1$ in OP 3.

As it can be seen, the appliance of the anti - windup measure improves the closed - loop behaviour of the designed *Loading Controller* significant. The step response of $\bar{\theta}_{NH_3}$ using anti - windup measure contains no unwanted overshot, according to the desired overall transfer function $T_d(s)$. Furthermore, the actual loading for this case, reaches the reference value after the appliance of the reference variable step within $\Delta t \approx 35\,\mathrm{s}$. This is according to the desired transient performance of the closed - loop system defined in section 4.4.1.1. Finally, also the stationary accuracy of the closed - loop system can be seen, since $\bar{\theta}_{NH_3}$ reaches exact $\bar{\theta}_{ref} = 0.1$.

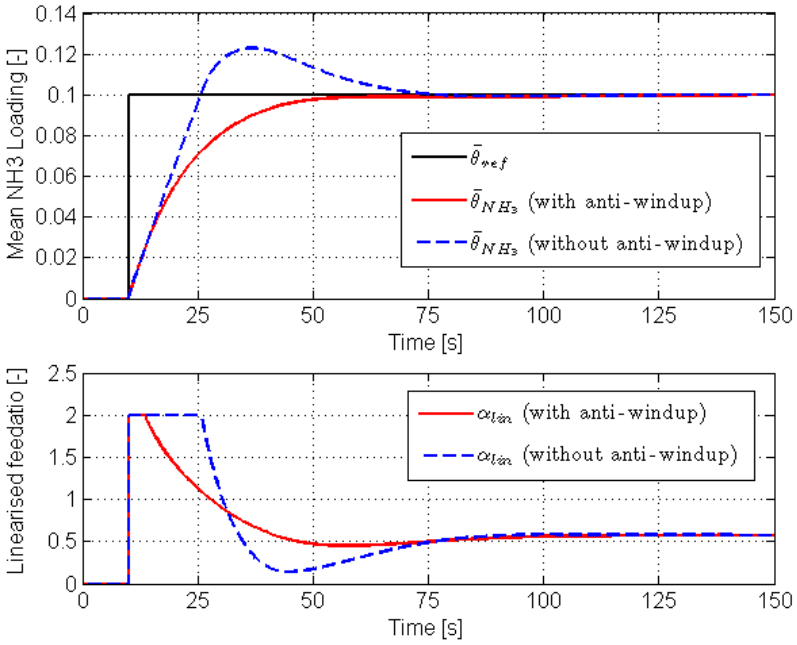

Figure 4.14: Step responses with / without anti - windup measure for *Loading Controller*

4.4.2 Gain - Scheduled *Loading Controller*

Since exemplary for OP 3 a linear *Loading Controller* is designed using the *inward approach* (refer to section 4.4.1), also for the remaining operating points (OP 1, OP 2, OP 4, OP 5 and OP 6) the same approach is used to derive the linear controllers. Table 4.3 summaries the calculated *Loading Controller* parameters with their corresponding operating point.

			OP 1	OP 2	OP 3	OP 4	OP 5	OP 6
Operating Point	Exhaust mass flow, $m_{EG,us}$	[kg/h]	200.26	222.00	255.05	327.88	356.91	470.62
	Catalyst temperature, T_c	[°C]	224	299	348	398	453	438
Controller Parameter	Controller gain, k_p	[-]	31.54	39.44	52.51	58.92	60.50	58.26
	Integral time constant, T_i	[s]	70.85	32.87	19.40	11.30	7.23	6.58

Table 4.3: Summary of *Loading Controller* parameters for all operating points

In order to achieve the *gain - scheduled controller*, the controller parameters k_p and T_i are changed by the defined *scheduling variables* T_c and $\overset{*}{m}_{EG}$ (refer to relation 4.8) by using a practical map - based approach. The two derived controller parameter maps containing the six operating points are visualised in appendix B.2.

4.5 Determination of the Optimal Setpoints according the NO_x / NH_3 Tradeoff

In the previous section (refer to 4.4) a *gain - scheduled Loading Controller* is derived, which allows the control of the actual mean ammonia loading $\bar{\theta}_{NH_3}$ of the COM to any reasonable chosen loading setpoint $\bar{\theta}_{ref}$ in the entire operating range of the SCR catalyst. Since in every operating point of the SCR catalyst plenty of $\bar{\theta}_{ref}$ can be chosen, a method has to be investigated, which determines optimally the loading setpoint depending on an "overall control objective". For understanding, an "overall control objective" in case of the SCR catalyst control is not the control of $\bar{\theta}_{NH_3}$ to a specific $\bar{\theta}_{ref}$, but rather to achieve a desired performance of the catalyst, e.g. a specific tradeoff between achievable NO_x conversion and resultant NH_3 slip. The ammonia loading control is only a means to the end in order to achieve the desired "overall control objective".

Therefore, at the beginning an "overall control objective" for the SCR catalyst is defined. According to the stated requirements in section 2.3 the "overall control objective" for the SCR catalyst is formulated as:

"Easy to adjust optimal tradeoff control between achievable NO_x conversion and resultant NH_3 slip of the SCR catalyst"

In order to derive from this formulated control objective the needed quantitative values for the loading setpoints $\bar{\theta}_{ref}$, a connection between them has to be found. A way to solve this problem is to formulate the "overall control objective" mathematically as a quality criterion or cost function. Such a quality criterion can be further quantitative evaluated and the optimal setpoints $\bar{\theta}_{ref}$ for the closed - loop loading control for each operating point of the SCR catalyst can be derived from it.

According to the stated "overall control objective" the quality criterion is derived according to

$$J = \beta \cdot p \cdot x_{NO_x,ds} + (1 - \beta) \cdot q \cdot x_{NH_3,ds}. \tag{4.23}$$

Where the NO_x conversion and NH_3 slip are connected to each other in the quality criterion by adding of the gas fractions $x_{NO_x,ds}$ and $x_{NH_3,ds}$. Further, a linear weighting factor β, in the following referred to as *tradeoff index*, is introduced. The *tradeoff index* is defined for $\beta \in [0, 1]$, and as it can be seen from the equation, using low β's, high $x_{NH_3,ds}$ are penalised in the resultant cost function and on the opposite using high β's, high $x_{NO_x,ds}$ are penalised. Therefore, using the *tradeoff index*, the contribution of the occurring gas fractions downstream the SCR to the cost function J can be linearly weighted between them. Thus β allows a easy and intuitive adjustment of the desired tradeoff between NO_x conversion and NH_3 slip. Additionally, two constant a priori weighting factors p and q are used the weight $x_{NO_x,ds}$ and $x_{NH_3,ds}$.

4.5.1 Steady - State Optimisation using the Quality Criterion

The above stated quality criterion (refer to equation 4.23) is evaluated for the six operating points (OP 1 - OP 6) by simulation on the control - oriented SCR Model. For simplicity, the following examinations explain the evaluation only for one operating point, OP 3.

In order to evaluate the cost function, the NO_x / NH_3 fractions downstream the SCR catalyst and the *tradeoff index* β are varied in the operating point. Therefore, a step - wise variation of the dosing quantity by using again the feedratio ($\alpha \in [0, 1.5]$) is performed in order to vary the NO_x / NH_3 fractions downstream the COM. For each feedratio step, the *tradeoff index* β is varied in its defined range ($\beta \in [0, 1]$) in order to weight linearly the resultant NO_x / NH_3 fractions different. Additionally, in order to penalise NH_3 slip higher than NO_x fractions apart from the weighting via the *tradeoff index*, the two constant weighting factors are determined with $p = 1$ and $q = 2$. Figure 4.15 shows the resultant evaluated cost function J as function of the varied variables, feedratio α and *tradeoff index* β for OP 3.

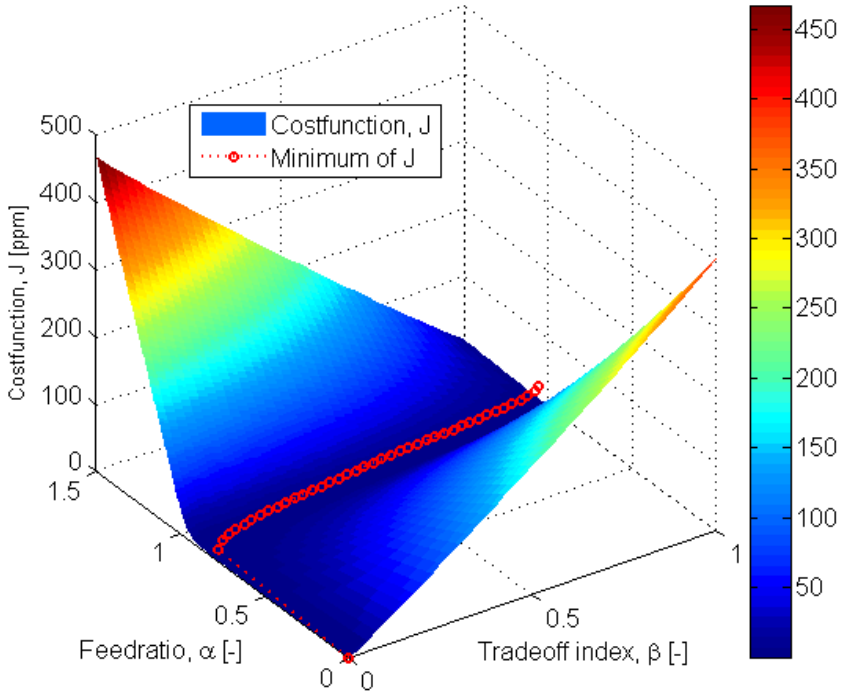

Figure 4.15: Evaluated cost function J for OP 3

As it can be seen, the optimal values for the stationary needed dosing quantity, represented by the feedratio α, depending on the *tradeoff index* β can be derived from the cost function J where it is minimal (symbolised with dashed red line in the figure). The resultant line shows the expected behaviour, which with increasing *tradeoff index* β, also the feedratio needs to be increased in order to reduce the NO_x fractions downstream the catalyst. This is because of the fact that with higher β's the NO_x fractions downstream the catalyst are more penalised by the cost function than the NH_3 fractions (refer to equation 4.23).

Since the needed feedratio α depending on the *tradeoff index* β is optimally determined by using the cost function, also automatically the optimal mean ammonia loading $\bar{\theta}_{NH_3}$ is determined. This can be said, because in the stationary case, if α is optimal also the resultant $\bar{\theta}_{NH_3}$ is optimal (refer to section 2.4). Therefore, using this correlation in steady - state conditions, directly the optimal loading setpoint $\bar{\theta}_{ref}$ by applying the optimal feedratio α can be derived on the COM. For illustration, figure 4.16 shows the

correlation between optimal α, derived from the cost function J, and resultant optimal $\bar{\theta}_{ref}$ depending on *tradeoff index* β for OP 3.

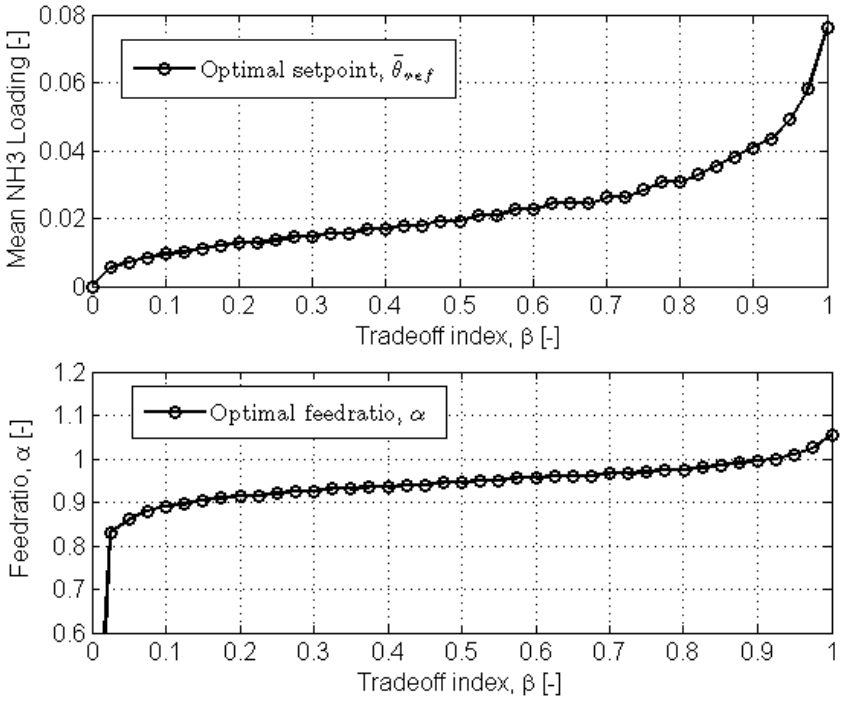

Figure 4.16: Relation between optimal α and $\bar{\theta}_{ref}$ (steady - state)

As it can be seen, with increasing β, the feedratio α and according to that also the desired ammonia loading $\bar{\theta}_{ref}$ increases. Therefore, for a chosen *tradeoff index* β, directly the corresponding optimal needed loading setpoint $\bar{\theta}_{ref}$ for the closed - loop control is determined.

4.5.2 Choice of the *Tradeoff Index*

For sure, using the *tradeoff index* makes a change of the performance of the catalyst towards higher NO_x reductions or lower NH_3 slip more intuitive, than tuning directly the setpoint $\bar{\theta}_{ref}$. But at the moment, still an open point is how to choose an adequate value for the *tradeoff index* β.

Because of the fact that for any operating point the optimal feedratio and thus also the dosing quantity is known from the cost function J depending on β, also the interesting quantities regarding the "overall control objective" can be derived. Therefore, NO_x conversion and NH_3 slip of the SCR catalyst are calculated in order to obtain characteristic curves which allow a reasonable determination of the *tradeoff index*. Figure 4.17 shows the derived characteristic curves.

Because of the fact that for every operating point such characteristic curves of the catalyst can be derived, for simplicity the shown curves in figure 4.17 represent a mean characteristic behaviour of the catalyst in all six operating points regarding NO_x conversion and

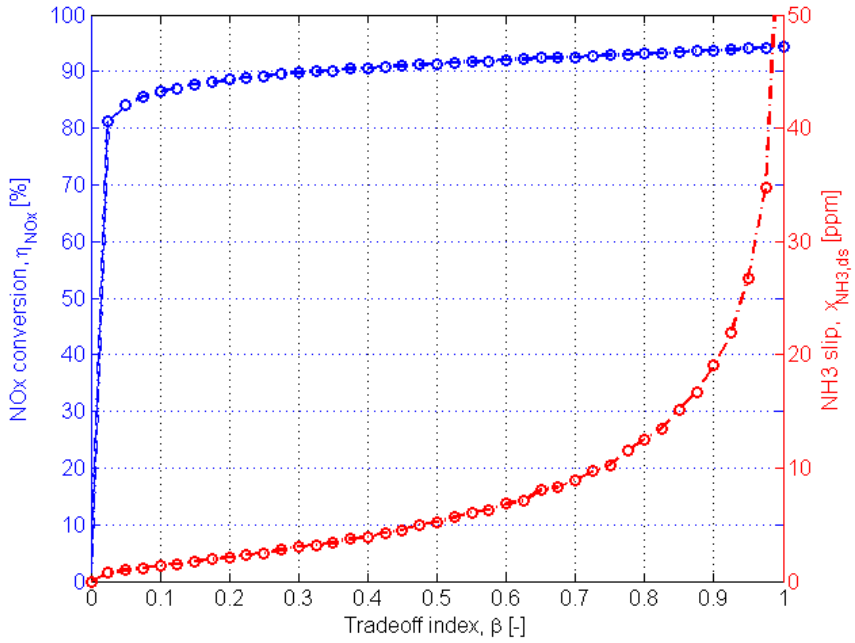

Figure 4.17: Characteristic curves according to the "overall control objective"

NH_3 slip. Nevertheless, from these curves interesting performance properties of the investigated SCR catalyst can be seen. The two curves are showing the maximal and optimal achievable steady - state performance of the used SCR catalyst regarding NO_x conversion (left blue axis) and resultant NH_3 slip (right red axis) depending on the tradeoff index β. This representation is in terms of the stated "overall control objective" at the beginning of this section. Using these characteristic curves, a desired performance of the catalyst can be graphically chosen, and thus the corresponding optimal setpoints for the *Loading Controller* are automatically determined.

Therefore, according to the requirements (refer to section 2.3) a integrated calibration methodology is available, which allows an easy adjustment of the desired NO_x conversion and NH_3 slip only by using the *tradeoff index* β.

Furthermore, in order to consider different optimal loading setpoints $\bar{\theta}_{ref}$ depending on the catalyst operating point, again a map - based approach is used according to the parameter maps of the *gain - scheduled controller* (refer to section 4.4.2). Thus regarding the different loading setpoints it can be written,

$$\bar{\theta}_{ref} = f(T_c, \overset{*}{m}_{EG}). \tag{4.24}$$

For illustration, figure 4.18 shows such a resultant map of optimal setpoints $\bar{\theta}_{ref}$ for the entire operating range of the SCR catalyst. The shown map represents the optimal loading setpoints for a chosen *tradeoff index* of $\beta = 0.5$.

As it can be seen, the desired optimal ammonia loading is high for low catalyst temperatures and low exhaust mass flows. With increasing operating point variables, also the optimal ammonia loading decreases significantly. Generally it can be said that the desired ammonia loading in the whole operating range of the catalyst is low. In the here shown

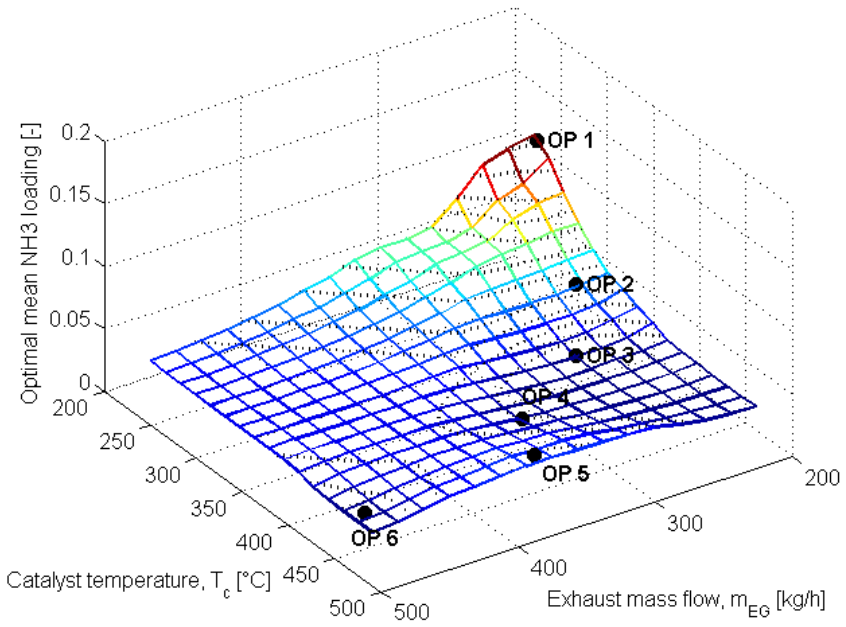

Figure 4.18: Derived setpoint map of $\bar{\theta}_{ref}$ for $\beta = 0.5$

example ($\beta = 0.5$) the maximal desired mean ammonia loading is $\bar{\theta}_{ref} \approx 15\,\%$. This instance of such low desired ammonia loadings is according to the made observations in section 2.2.3, where it is derived from the basic experiments that with increasing feedratio and therefore also increasing ammonia loading, the NO_x reduction capability of the catalyst saturates. Thus, much higher $\bar{\theta}_{NH_3}$ would lead to moderate higher NO_x reduction rates, but to significant higher NH_3 slip.

4.6 Discussion

Within this chapter the realisation of the defined model - based control concept from section 2.4 is presented. The developed and verified control - oriented SCR catalyst model from chapter 3 is used as basis for the investigations regarding ammonia loading control of the SCR catalyst.

At the beginning, the desired closed - loop system for the control of the mean ammonia loading of the COM is defined in unity - feedback configuration. Since the basic experiments on the COM are showing a highly nonlinear behaviour of the control plant regarding feedratio steps at the input, this nonlinearity is static linearised by using a characteristic curve at the input of the nonlinear model. Therefore a new control variable α_{lin} is introduced.

After that, the linearised control plant is tried to be approximated using linear first order models. Since the plant characteristics of the COM changes significantly with its operating point, individual for the six available operating points from the test bed, linear first order models are identified. The achieved results using the input linearised SCR model in comparison with the different linear first order models showed good correlation

between them.

Based on this outcome, the *gain - scheduling* approach is used in order to consider the operating point dependent dynamic behaviour of the catalyst and to allow further the usage of linear control theory methods to design the *Loading Controller*. The chosen design method for the *gain - scheduled controller* is the *inward approach*. Using this methodology, a classical PI - controller is derived from the specifications for the closed - loop system, where its parameters are gain - scheduled depending on catalyst temperature and exhaust mass flow by using a map - based approach. Furthermore, also a anti - windup measure for the *Loading Controller* is implemented in order to avoid undesired overshoots of the controlled ammonia loading due to windup effects.

At the end of this chapter, a methodology is presented, which allows an optimal determination of the needed ammonia setpoint $\bar{\theta}_{ref}$ for the loading control of the COM. A intuitive calibration parameter, the so - called *tradeoff index* β is introduced, in order to allow a optimal adjustment of the tradeoff between achievable NO_x reduction and resultant NH_3 slip. Again, according to *gain - scheduling* approach used for the *Loading Controller*, also the optimal derived loading setpoints are gain - scheduled using the same map - based approach.

Finally, it has to be mentioned that the defined model - based control concept from section 2.4 also comprises to use of the feedback information of the NO_x sensor downstream the SCR catalyst in order to adapt the *SCR Catalyst Model* to the real plant. Unfortunately this last part of the concept, containing *SCR Model Adaptation* and NO_x *Sensor Model*, could not be finished within this thesis. The prioritisation had to be changed during the work on this topic, since limited availability of the SCR system on the engine test bed has forced to prefer the verification of the so far developed open - loop model - based control concept under real conditions. This verification on the test bed was one of the major objectives of this thesis (refer to section 1.3.2).

Nevertheless, for the verification, if the defined model - based control concept with its NO_x / NH_3 tradeoff control in principle works under real conditions on the engine test bed, the adaptation of *SCR Catalyst Model* using the NO_x sensor is not necessarily needed.

Chapter 5

Experimental Results

The intention of this chapter is to illustrate the validity and the performance of the developed control concept for SCR systems within this thesis. Therefore, the main important test bed results of the model - based control strategy are shown. At the beginning, a short overview of the experimental setup itself is given. Finally, the performance of the loading control of the SCR catalyst in transient engine test cycles is shown and the results are discussed.

5.1 Experimental Setup

According to the stated objectives of this thesis, the developed model - based control concept for an SCR catalyst is tested on an engine test bed under real conditions. Therefore, at AVL - List GmbH an adequate equipped engine test bed is used in order to verify the defined control concept.

5.1.1 Configuration of the Engine Test Bed

The used engine test bed at AVL is a state of the art dynamic engine test cell for steady - state and transient testing of IC engines in arbitrary test procedures. The test cell itself is equipped with a dynamometer (*DynoExact APA* series from AVL)[1] and modern measurement devices beginning from simple temperature or pressure sensors up to sophisticated gas composition measurement devices (e.g. *SESAM FTIR*).

The CI engine used for the experimental verification of the SCR control algorithm on this test bench is a Volvo *NED5* engine. The engine itself has five cylinders, arranged in - line, with a total displacement of 2.401 l. Further, the engine is turbocharged, intercooled and contains an EGR system. The maximum power is limited to 120 kW at 4000 rpm. As control device of the engine, a standard ECU (EDC16) from the company BOSCH is used which is calibrated to meet Euro IV legislation limits. Since the engine is only used to generate exhaust gas for the investigations on the EAS, more focus on it is not provided in the following.

[1] For more detailed information on AVL's *DynoExact APA* refer to [39].

The exhaust gas aftertreatment system of the *NED5* engine consists of an DOC catalyst and an SCR catalyst connected in series. As already mentioned in section 1.1.2, DOC catalysts are used in combination with SCR catalysts to increase their NO_x reduction capability by improving the NO_2 / NO_x ratio. The location of the reducing agent injection for the SCR catalyst is between both catalysts. In order to achieve a well conditioning of the injected AdBlue^{TM} to ammonia, a mixing length of approximately 70 cm is installed after the injection location. In order to avoid excessive temperature loss due to the long pipe length, all pipes are thermally insulated using glass - fiber wraps.

To give an impression how the described engine test cell looks like, figure 5.1 shows a picture of it with focus on the EAS used for this verification.

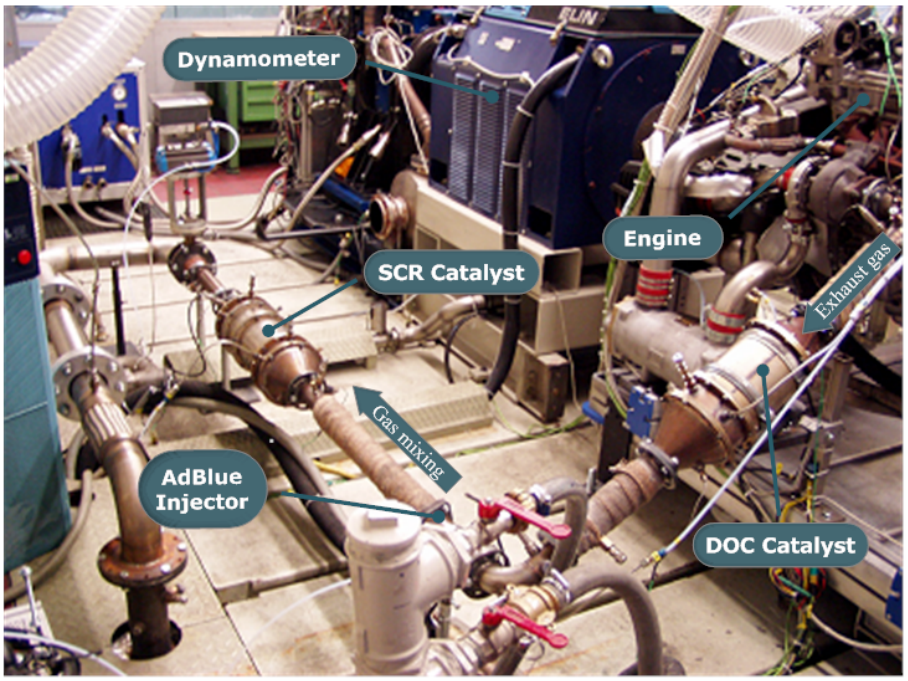

Figure 5.1: Test cell used for the verification of the model - based control concept

Furthermore, figure 5.2 shows a detailed picture of the used zeolite - based SCR catalyst (Fe - ZSM5) from *Johnson Matthey* with a total catalyst volume of 2.47 l. The used parameter set for the COM of this catalyst is attached in appendix **??**.

5.1.2 Rapid Prototyping Environment

In order to verify fast and uncomplicated the SCR control concept on the test bed, a real - time rapid prototyping system (RPS) is applied. The commonly in automotive industry applied *ES1000 - System* from the company ETAS GmbH is used. The *ES1000 - System* is an experimental target hardware which contains a real - time simulation controller board (version *ES 1135.1*) with arbitrary expendable interface boards like CAN communication boards, analog or digital I/O boards, and many more. In combination with INTECRIO®[2],

[2]INTECRIO® is a code generation software also from ETAS GmbH.

Figure 5.2: Zeolite - based SCR catalyst (Fe - ZSM5) from *Johnson Matthey*

code from different behavioural modelling tools like MATLAB - SIMULINK® can be generated, in order to integrate and execute the programmed models on the RPS.

Since all experimental investigations regarding the model - based control of the SCR catalyst are made based on MATLAB - SIMULINK®, the ETAS tool chain, comprising INTECRIO® and *ES1000 - System* is the optimal solution for the testing of the control concept on the engine test bed. Figure 5.3 shows an overview of the RPS with the used sensors and dosing actuator.

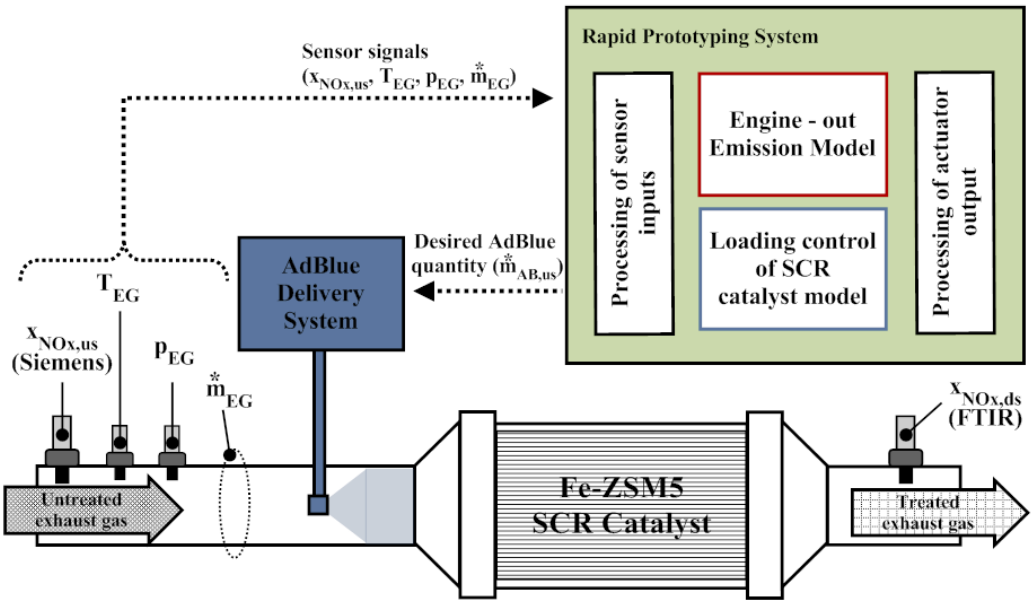

Figure 5.3: Rapid prototyping system with used sensors and dosing actuator

As it can be seen, the developed dosing algorithm is verified in open - loop configuration without the usage of the commercial available Siemens NO_x sensor downstream the SCR catalyst (refer to section 4.6). The needed inputs for the dosing algorithm are therefore $x_{NO_x,us}$, T_{EG}, p_{EG} and $\dot{m}_{EG}$. According to the basic experiments (refer to section 2.2.2), for the verification of the performance of the control concept, a *SESAM FTIR* measurement device is used to analyse the gas composition downstream the real catalyst. As already

mentioned in section 2.1.1.2, for accurate dosage of the desired AdBlue^{TM} quantity in the exhaust, a *Denoxtronic* from BOSCH is used (symbolised with the block *AdBlue^{TM} Delivery system*).

The RPS itself contains the developed ammonia loading control algorithm based on the control - oriented SCR catalyst model. Because of the fact that the SCR model needs as input apart from the NO_x fraction $x_{NO_x,us}$ also the NO_2 / NO_x ratio and the O_2 fraction $x_{O_2,us}$, additionally a simple map - based engine - out emission model is implemented in the RPS. Furthermore, in order to allow a reliable calculation of the SCR model with adequate resources on the RPS target, a discretisation of the COM of $n = 2$ is chosen for the verification of the control concept on the test bed.

5.2 Results of the Model - Based Control Strategy

Since an adequate experimental environment consisting of engine test bed and RPS is available (refer to section 5.1), the developed control concept is tested under real conditions.

5.2.1 Test Procedure for the Verification of the Control Concept

As test procedure for the verification of the model - based control concept, again the "modified" FTP - 75 as defined in section 3.4 is chosen. In order to verify the tradeoff control concept, different *tradeoff indexes* are chosen which represent the desired NO_x/NH_3 tradeoff in the "modified" FTP - 75. Figure 5.4 shows five defined β's using the derived characteristic curve of the steady - state SCR catalyst performance (refer to section 4.5.2).

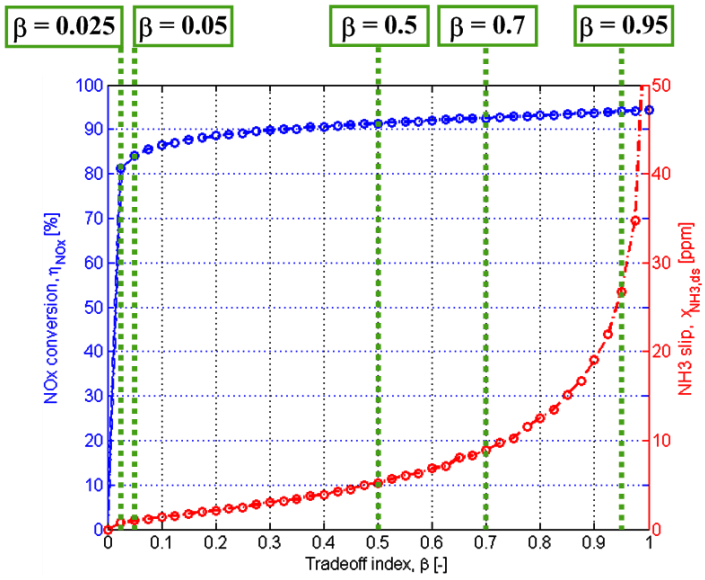

Figure 5.4: Chosen β's for the verification of the control concept

As it can be seen, the chosen values of β vary over its entire range beginning from $\beta = 0.025$ (low desired NH_3 slip and therefore low NO_x conversion), up to $\beta = 0.95$ (high desired NO_x conversion and therefore high resultant NH_3 slip). For all of the five defined *tradeoff indexes* automatically a corresponding setpoint map $\bar{\theta}_{ref}$ is derived according to the shown example of $\beta = 0.5$ in figure 4.18. Since that the five setpoint maps, which are optimally determined with respect to the "overall control objective", are available, the different calibrations are tested in the "modified" FTP - 75 in the following.

5.2.2 Performance of the Tradeoff Control in FTP - 75

At the beginning, for illustration of the control behaviour of the developed gain - scheduled *Loading Controller*, figure 5.5 shows the performance of it in the whole "modified" FTP. The chosen example represents the tradeoff control using the *tradeoff index* of $\beta = 0.95$.

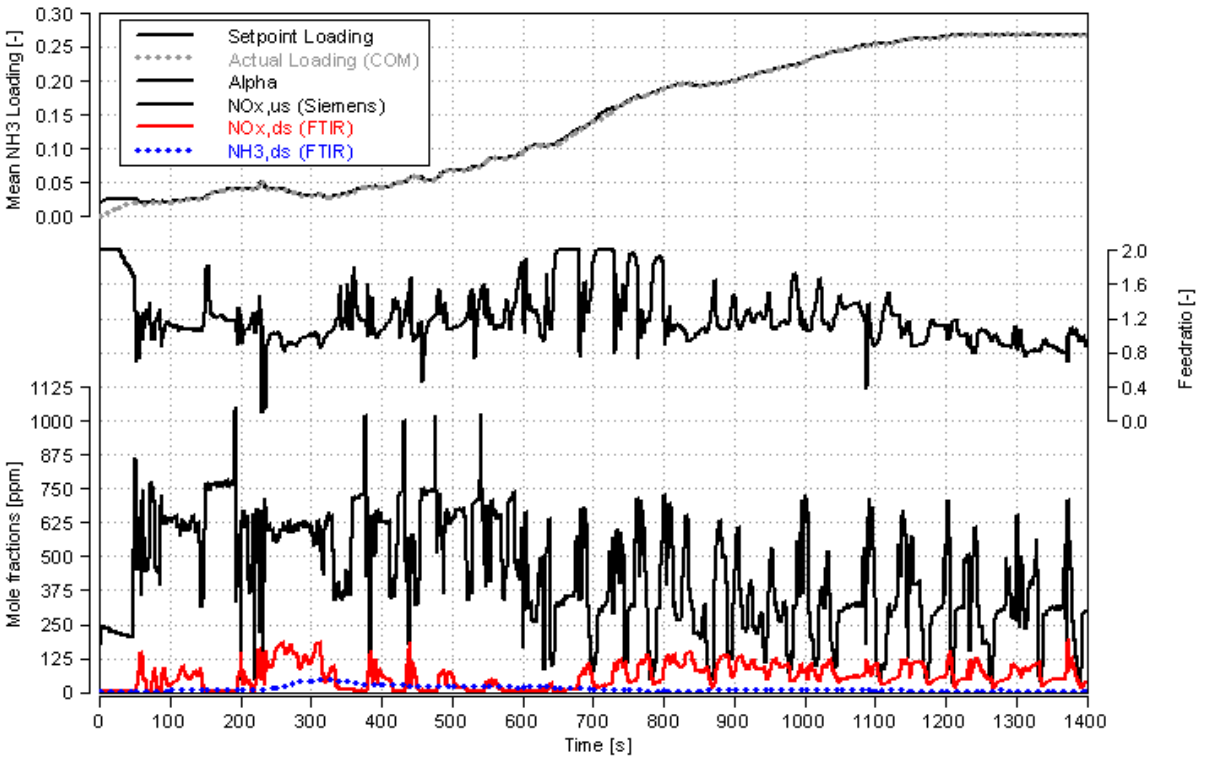

Figure 5.5: Performance of the loading control in FTP ($\beta = 0.95$)

As it can be seen, the actual ammonia loading $\bar{\theta}_{NH_3}$ of the COM follows very good the changing loading setpoint $\bar{\theta}_{ref}$. The desired loading at the beginning of the test cycle ($t \approx 0 \ldots 400\,\mathrm{s}$) is very low ($\bar{\theta}_{ref} < 5\,\%$) due to the high temperatures of the preconditioned SCR catalyst. This low loading setpoint increaseses up to $\bar{\theta}_{ref} \approx 27\,\%$ at $t = 1400\,\mathrm{s}$ because of decreasing operating temperatures of the catalyst (refer to section 3.4). Nevertheless, since the initial ammonia loading of the catalyst is zero, the *Loading Controller* applies immediatley at $t = 0\,\mathrm{s}$ its maximal feedratio $\alpha = 2$ in order to achieve the loading setpoint. As it can be seen, the setpoint is reached at $t \approx 100\,\mathrm{s}$ without

overshooting and therefore no significant NH_3 slip occurs. Furthermore, the *Loading Controller* uses the possible adjusting range of its actuating signal well, in order to follow the loading setpoint. Only between $t \approx 650 \ldots 750\,\mathrm{s}$ the *Loading Controller* reaches its saturation. But as it can be seen, the applied anti - windup measure works well, since the actuating signal stays not too long in the saturation and therefore an overshoot of $\bar{\theta}_{NH_3}$ can not be seen. Apart from that, within this specific FTP using a $\beta = 0.95$, a overall SCR system performance of $\eta_{NO_x} = 85.0\,\%$ and a mean NH_3 slip in the whole cycle of $\bar{x}_{NH_3,ds} = 12.4\,\mathrm{ppm}$ is achieved.

Furthermore, figure 5.6 shows a cutout between $t = 800 \ldots 1000\,\mathrm{s}$ of all FTP test cycles with the different applied *tradeoff indexes* in comparison.

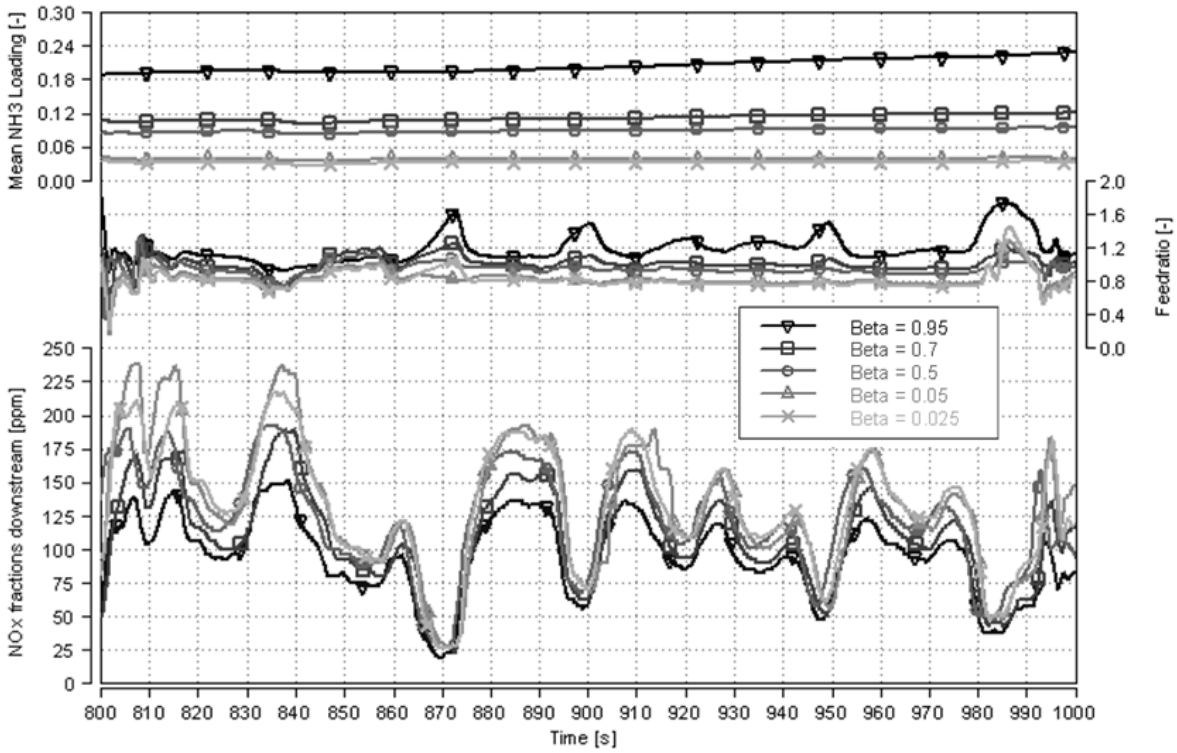

Figure 5.6: Different *tradeoff indexes* in FTPs (cutout)

As it can be seen, the actual loading $\bar{\theta}_{NH_3}$ within these 200 s changes not significantly. As expected, with increasing *tradeoff index*, also the ammonia loading increases. The effect of this increasing loading can be further clearly seen in the resultant applied feedratio from the *Loading Controller*, which is at the highest for $\beta = 0.95$ and at the lowest for $\beta = 0.025$. According to that, also the NO_x fractions downstream the SCR catalyst decrease with increasing β. Only for the values of $\beta = 0.025$ and $\beta = 0.05$ this trend cannot be clearly seen, since the ammonia loadings and therefore the resultant feedratios are nearly the same. Therefore, the seen differences between these two β values in the NO_x fractions is more or less based on measuring inaccuracies and thus negligible. But apart from that, the here shown example visualises clearly that the defined control concept in combination with the tradeoff control using the *tradeoff index* β works well under real conditions.

In order to visualise all SCR process important quantities, figure 5.7 shows the cumulative values of NO_x and NH_3 mass up- and downstream the SCR catalyst. The values are calculated for the whole "modified" FTP test cycles.

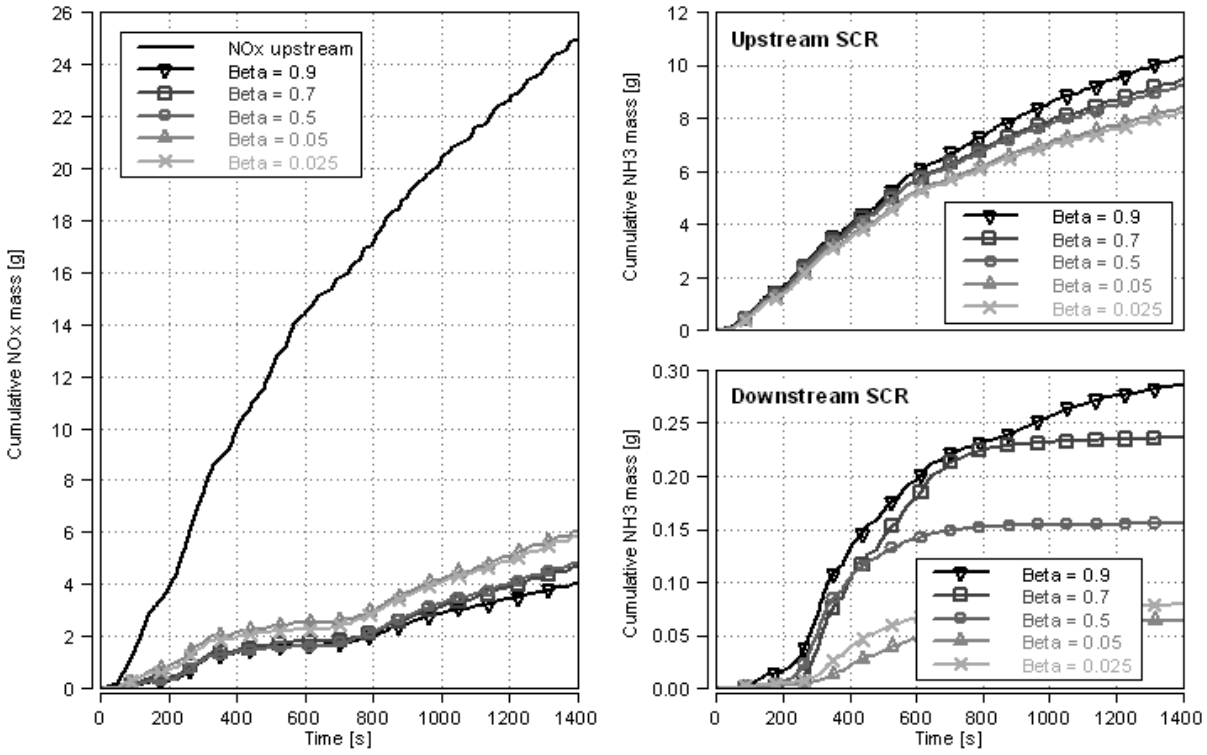

Figure 5.7: Comparison between the cumulative FTP results using different β's

As it can be seen in the left part of the figure, the cumulative NO_x mass downstream the SCR catalyst decreases with increasing *tradeoff index*. This is according to the shown cutout of the FTPs in figure 5.6. Furthermore, in the upper right part of the figure the cumulated NH_3 mass upstream the SCR catalyst is shown. The behaviour is as expected that with increasing *tradeoff index* also the ammonia consumption increases. In the specific case here, the consumption increases from $\beta = 0.025$ to $\beta = 0.95$ at approximately 28 %. In the lower right part of the figure the cumulated NH_3 mass downstream the SCR catalyst is shown. Again, also for this case the behaviour is as expected. As already mentioned, for the *tradeoff indexes* of $\beta = 0.025$ and $\beta = 0.05$ the effect of increasing SCR system performance with higher β cannot be seen. For this case, measuring inaccuracies and system tolerances become siginficant due to more or less same applied feedratios and therefore the measurement results of these two cases are not reliable.

Finally, in order to evaluate the model-based control concept regarding the defined "overall control objective", the achieved results in the "modified" FTPs are compared to the desired SCR system performances which are defined at the beginning of this section (refer to figure 5.4). Figure 5.8 shows the important results of this evaluation.

As it can be seen, the figure comprises the steady-state NO_x / NH_3 tradeoff and the

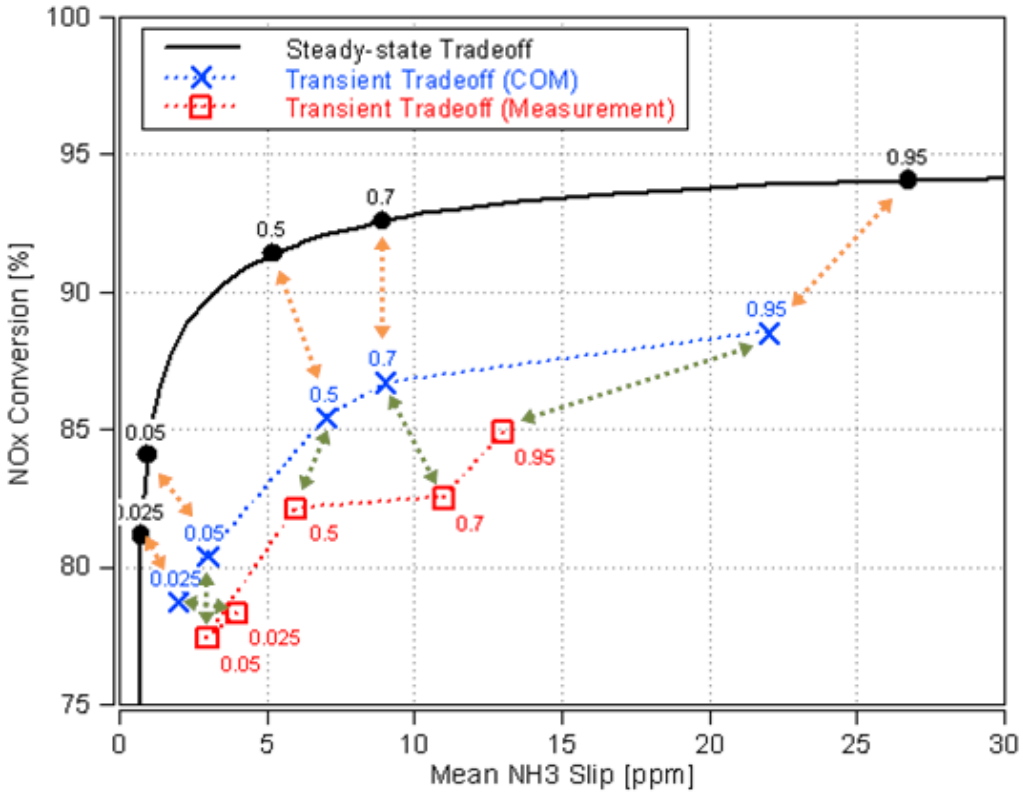

Figure 5.8: Steady - state optimum and FTP test cycle results

achieved transient performance of the SCR model (*COM*) and the real catalyst (*Measurement*) in the "modified" FTPs. Note, the steady - state NO_x / NH_3 tradeoff is obtained by performing the stationary optimisation using the defined quality criterion (refer to section 4.5.1).

Based on the shown results in the figure it can be said that the concept of the model - based control of the SCR catalyst works well. The uncomplicated and fast adjustment of the NO_x / NH_3 tradeoff using the tradeoff index β shows the desired behaviour. In comparison with the simulated steady - state optimum (black line) the transient result of the COM in the "modified" FTP loses performance regarding NO_x conversion and NH_3 slip (symbolised with orange arrows). These losses in the transient test cycle could be reduced for instance by choosing operating point dependent different *tradeoff indexes*, since the here shown results are obtained by using a mean *tradeoff index* of all six operating points. Furthermore, also a higher number of operating points and a better distribution of them in the entire operating range of the SCR catalyst could minimize the transient performance losses of the SCR catalyst.

Apart from that, additionally to the losses in transient operating conditions, there also occurs a difference between the calculated cycle results form the COM and the measured cycle results (symbolised with green arrows). This difference is mainly based on the currently used parametrisation of the COM which could be further improved (refer to section 3.5) and further on the not applied model adaptation using the NO_x sensor downstream the real SCR catalyst (refer to section 4.6). Both measures should improve the seen

difference between COM and real SCR catalyst.

Finally, as overview all obtained results from the five "modified" FTPs with their corresponding steady - state optima are summarised quantitative in table 5.1. As it can be seen, the best performance of the SCR system regarding NO_x reduction in the "modified" FTP is achieved with $\eta_{NO_x} = 85.0\,\%$ in combination with a mean NH_3 slip of $\bar{x}_{NH_3,ds} = 12.4\,\text{ppm}$.

Tradeoff index, β [-]	NOx Conversion, η_{NOx} [%]			Mean NH3 slip, $\bar{x}_{NH3}$ [ppm]		
	Steady-state	FTP test cycle		Steady-state	FTP test cycle	
		COM	Measurement		COM	Measurement
0.025	81.2	78.9	78.3	0.7	2.1	3.9
0.05	84.1	80.5	77.5	1.0	3.1	3.1
0.5	91.4	85.5	82.1	5.2	7.1	6.0
0.7	92.6	86.7	83.1	8.9	8.9	11.1
0.95	94.1	88.5	85.0	26.7	21.9	12.4

Table 5.1: Summary of overall test cylce results using different β

It has to be mentioned that the here shown test cycle results are obtained under real conditions without any additional calibration effort of the control algorithm on the engine test bed itself. The entire model - based control strategy is exclusively calibrated in simulation.

Chapter 6

Summary and Outlook

6.1 Summary of the Developed Control Concept

The aim of this thesis is the development of a state - of - the - art control algorithm for SCR systems for mobile applications.

Initially, general remarks to internal combustion engines, their pollutants and entailed exhaust gas aftertreatment are given. In the course of that, the SCR technology is introduced which allows significant reduction of nitrogen oxides (NO_x) emissions by means of a reducing agent called AdBlue^{TM}. Furthermore, the need of such a sophisticated technology to overcome the problem of environmental pollution and to meet future emission legislations is shown. In the following, the control of SCR systems for mobile applications is discussed in general. For completeness, also a brief description of today's already existing control strategies for SCR catalysts with their advantages and drawbacks is given.

After these general remarks on SCR systems, the main topic of this thesis, the development of a control concept for SCR systems is presented. In order to derive an ideal control concept, firstly basic experiments on an engine test bed using a zeolite - based SCR catalyst from *Johnson Matthey* are performed. Based on the outcome of these experimental investigations, a model - based control concept is derived and its properties are discussed.

Core of the investigated model - based control concept is an one - dimensional control - oriented SCR catalyst model which is developed within this thesis. The model itself is discretised in flow direction of the exhaust gas by ideal CSTR cells and is therefore described by ordinary differential equations. Due to the complexity of the reaction kinetics of an SCR catalyst, the important chemical reaction schemes are taken over from AVL's *BOOST Aftertreatment*.

In order to allow fast and flexible simulations using the developed SCR catalyst model, a CSTR cell number variable structure of the entire model is investigated. The obtained cell number variable SCR catalyst model is implemented in the modelling tool MATLAB - SIMULINK®.

At the end of the modelling investigations, the derived control - oriented SCR catalyst model is verified by an sophisticated SCR model from *BOOST Aftertreatment* and test bed measurements of an real catalyst. Based on the obtained results from this verification

it can be said that the developed control - oriented SCR model is valid and has sufficient accuracy compared to the sophisticated SCR model as well as to the real catalyst on the engine test bed.

The developed and verified control - oriented SCR catalyst model is further used as basis for the investigations regarding ammonia loading control of the real SCR catalyst. Initially, basic experiments with the SCR catalyst model are made, where the outcomes of these experiments are used as input for the controller design. Since the control - oriented SCR catalyst model is showing a highly nonlinear behaviour regarding feedratio steps at the input, the SCR model is statically linearised by using a characteristic curve at the input of the nonlinear model. Therefore, for the controller design itself, a linear design method, the *inward approach* is used. In order to consider the operating point dependent dynamic behaviour of the catalyst, the concept of *gain - scheduling* is applied for the developed *Loading Controller*.

Since a major objective of this thesis is the development of an integrated calibration procedure for fast and optimal adjustment of the NO_x reduction versus NH_3 slip tradeoff, a methodology is investigated, which allows the optimal determination of the setpoint $\bar{\theta}_{ref}$ for the loading control according to the desired tradeoff. An intuitive calibration parameter, the *tradeoff index* β is introduced, which can be used to adjust optimal this tradeoff.

Because of the fact that limited engine test bed availability forced to prefer the verification of the so far developed model - based control concept without the *SCR Model Adaptation* using the downstream NO_x sensor, the work on the topic is not finished within this thesis. Nevertheless, for the verification of the model - based control concept with its NO_x / NH_3 tradeoff control, the adaptation routine of *SCR Catalyst Model* is not necessarily needed.

At the end of this thesis, the important test bed results of the developed model - based control concept are presented. The performance of the loading control of the SCR catalyst is verified in transient engine test cycles by using different desired NO_x / NH_3 slip tradeoffs. Based on the achieved results in the test cycles it can be said that the developed model - based control concept for SCR systems for mobile applications is usable under real conditions and achieves adequate NO_x reduction rates. Moreover, the outcome and documented experiences of this work provide a verified control concept for SCR systems which can be used as a bases for further developments.

6.2 Outlook

Based on the developed control concept within this thesis, the following further developments are reasonable:

- Since the *SCR Model Adaptation* using the downstream NO_x sensor is not finished yet within this work, the research on this topic should be done primarily. Furthermore, this feedback information of the SCR system could be further used for model - based diagnostic purposes of the entire SCR system. The principal integration of the commercial NO_x sensor in the control concept is already derived in section 2.4.

- In order to use more sophisticated control concepts, like optimal control (e.g LQ - regulator [15]), further investigations can be made regarding the linearisation of the control - oriented SCR model. Therefore, deeper research has to be made regarding the important non - linearities of the model and how they can be linearised (e.g. operating point dependent linearisation of the COM using the *Jacobian matrix* [15], [37]).

- Since the parametrisation of the SCR model is taken from an existing parameter set within this thesis, for further developments additional investigations can be made regarding automated parametrisation of the SCR model. This means for example, using parameter optimisation routines which automatically derive the model parameters from measurement data according to a defined quality criteria.

- Finally, additionally to the already performed performance verifications on the engine test bed, the developed control concept could be further verified in comparison to other control strategies (e.g. *Denoxtronic* from BOSCH). Such a benchmark could be done regarding calibration effort, performance, and reliability of the tested control strategies.

Appendix A

Additional Measurement Results

A.1 Feedratio Step Responses

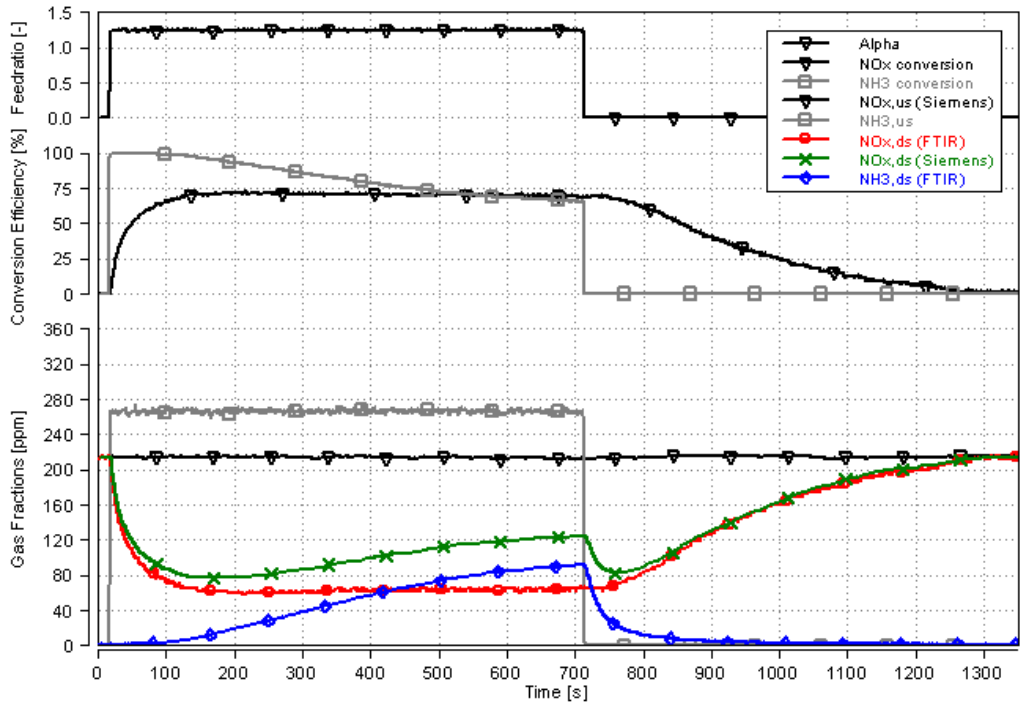

Figure A.1: Step response for $\alpha = 0 \rightarrow 1.2$ in OP 1

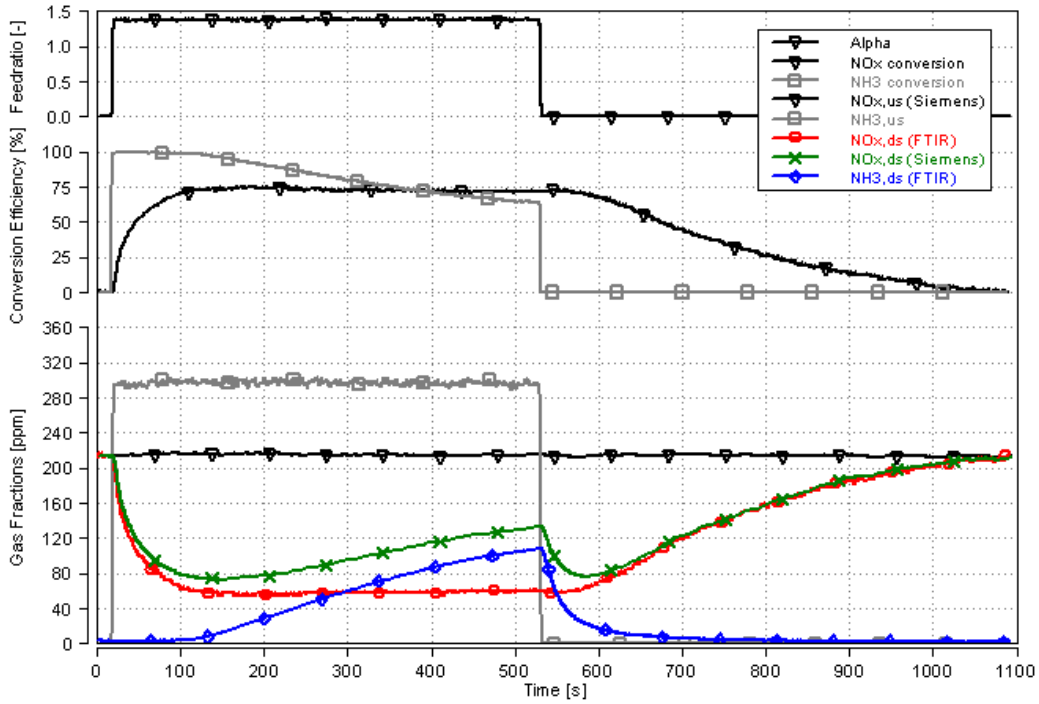

Figure A.2: Step response for $\alpha = 0 \rightarrow 1.4$ in OP 1

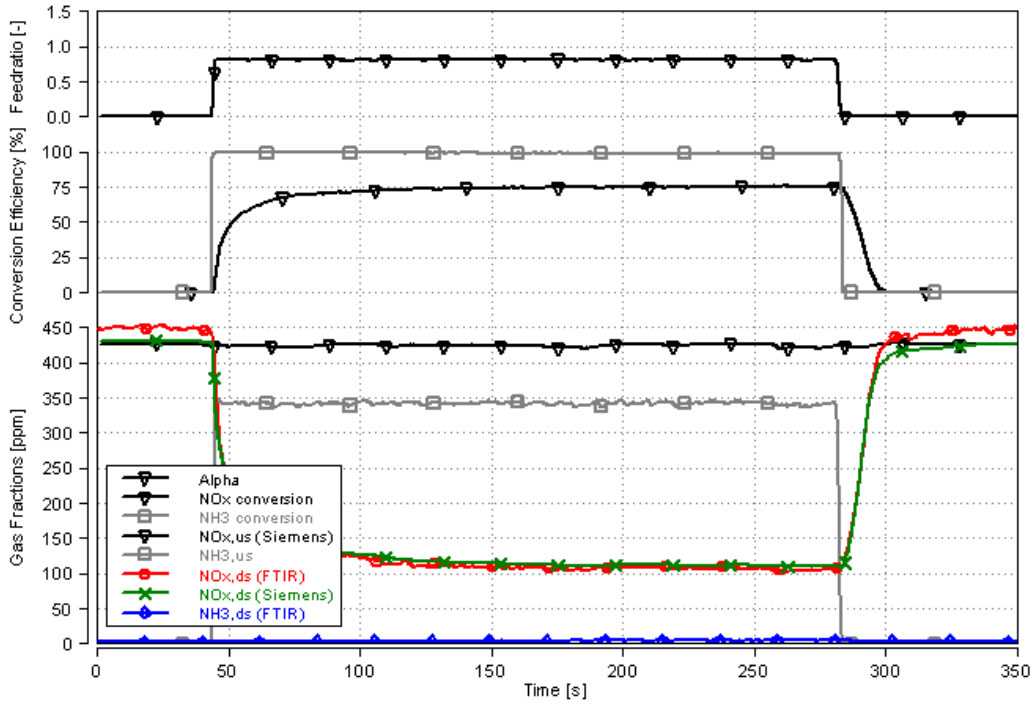

Figure A.3: Step response for $\alpha = 0 \rightarrow 0.8$ in OP 2

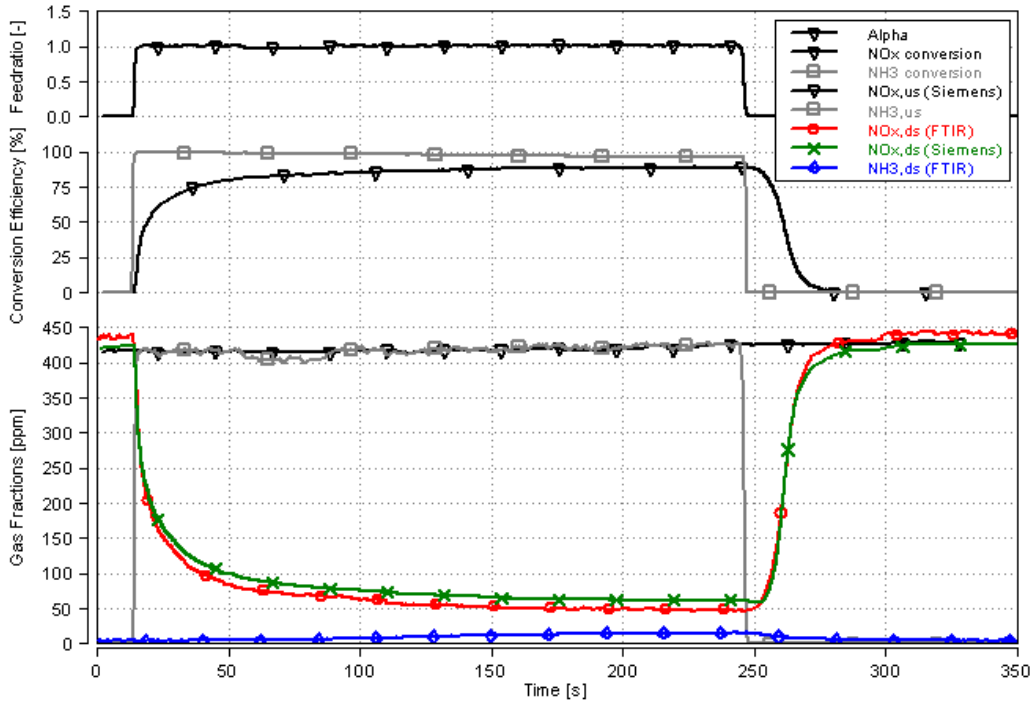

Figure A.4: Step response for $\alpha = 0 \rightarrow 1.0$ in OP 2

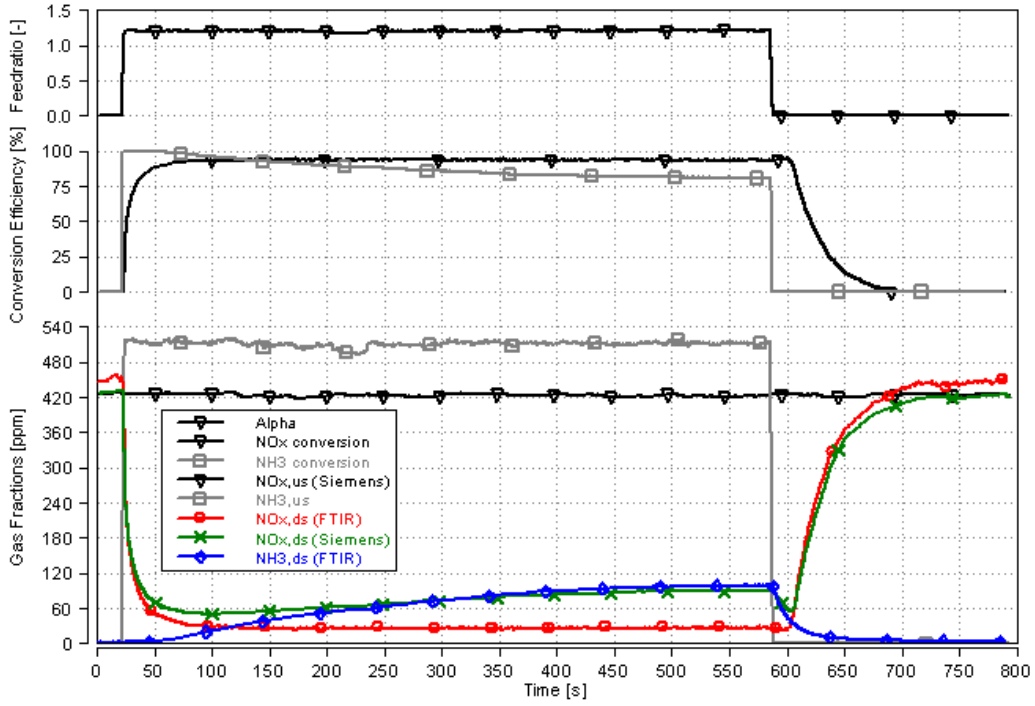

Figure A.5: Step response for $\alpha = 0 \rightarrow 1.2$ in OP 2

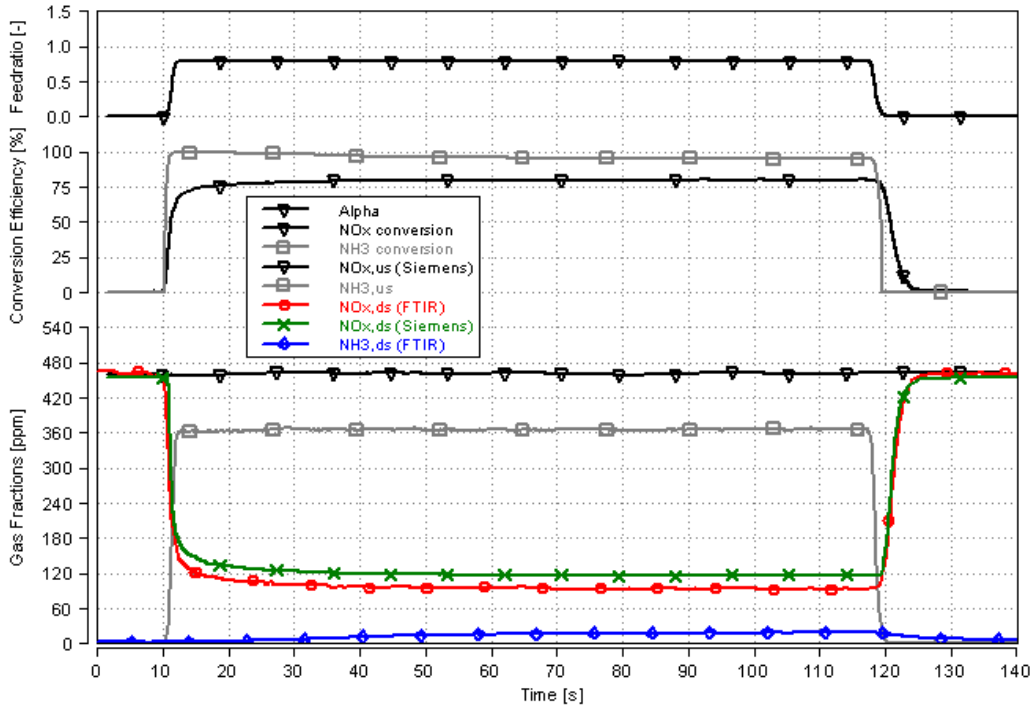

Figure A.6: Step response for $\alpha = 0 \rightarrow 0.8$ in OP 4

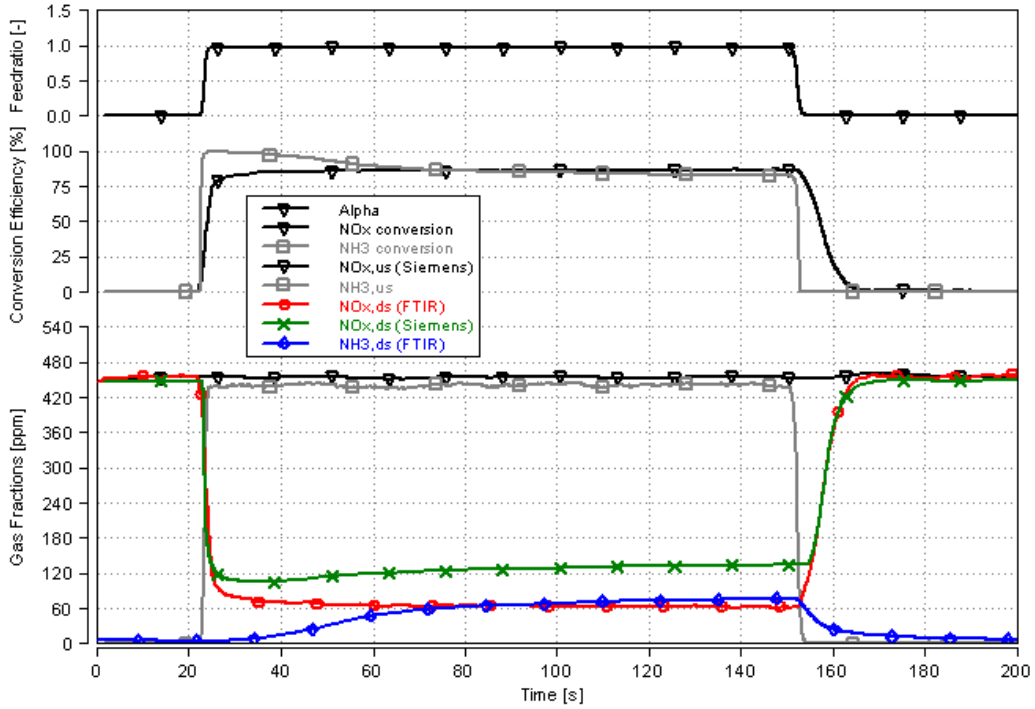

Figure A.7: Step response for $\alpha = 0 \rightarrow 1.0$ in OP 4

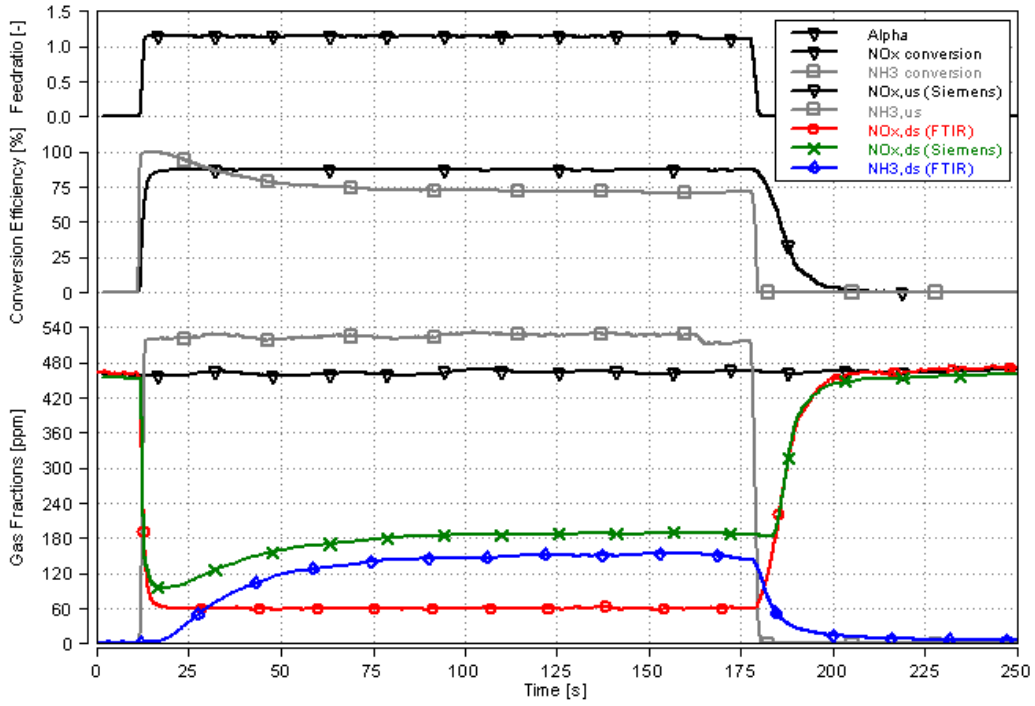

Figure A.8: Step response for $\alpha = 0 \rightarrow 1.2$ in OP 4

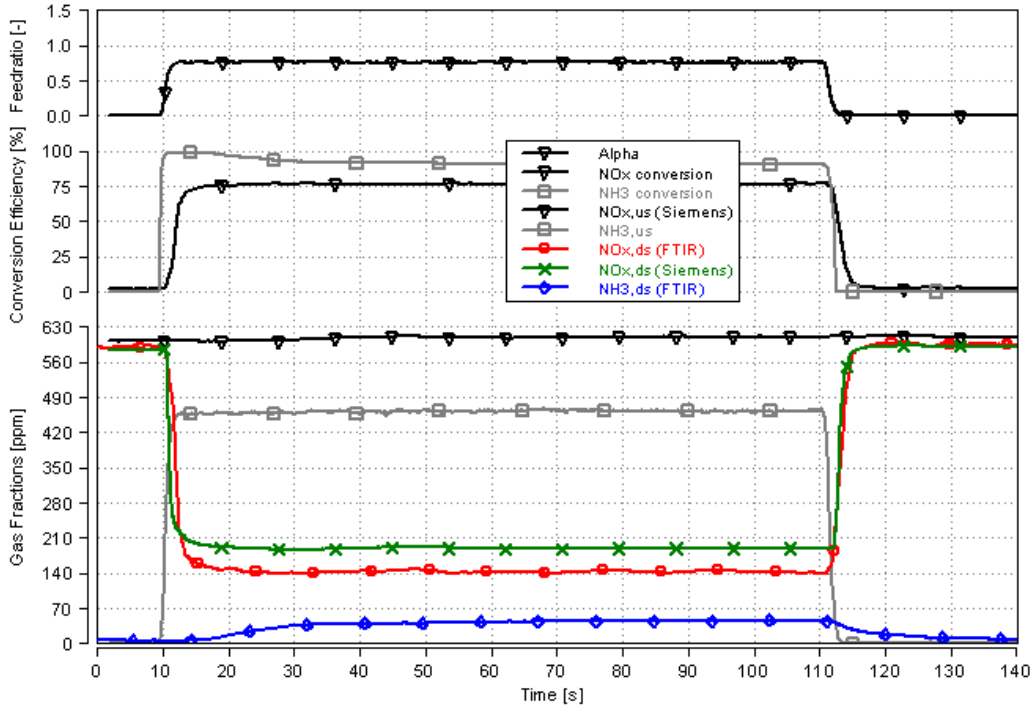

Figure A.9: Step response for $\alpha = 0 \rightarrow 0.8$ in OP 5

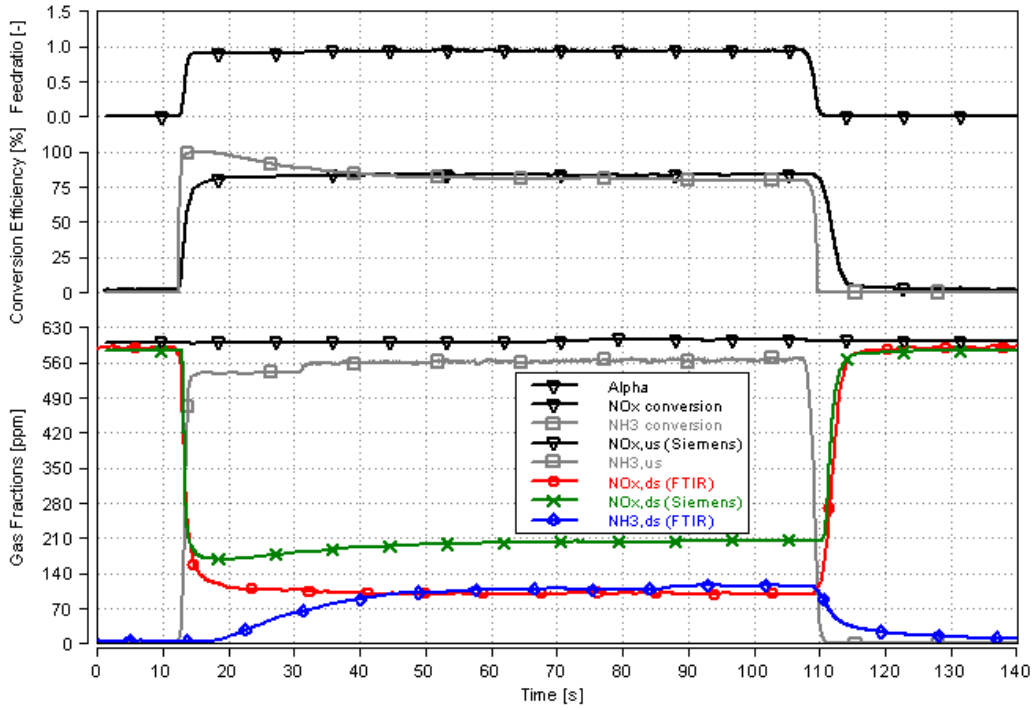

Figure A.10: Step response for $\alpha = 0 \rightarrow 1.0$ in OP 5

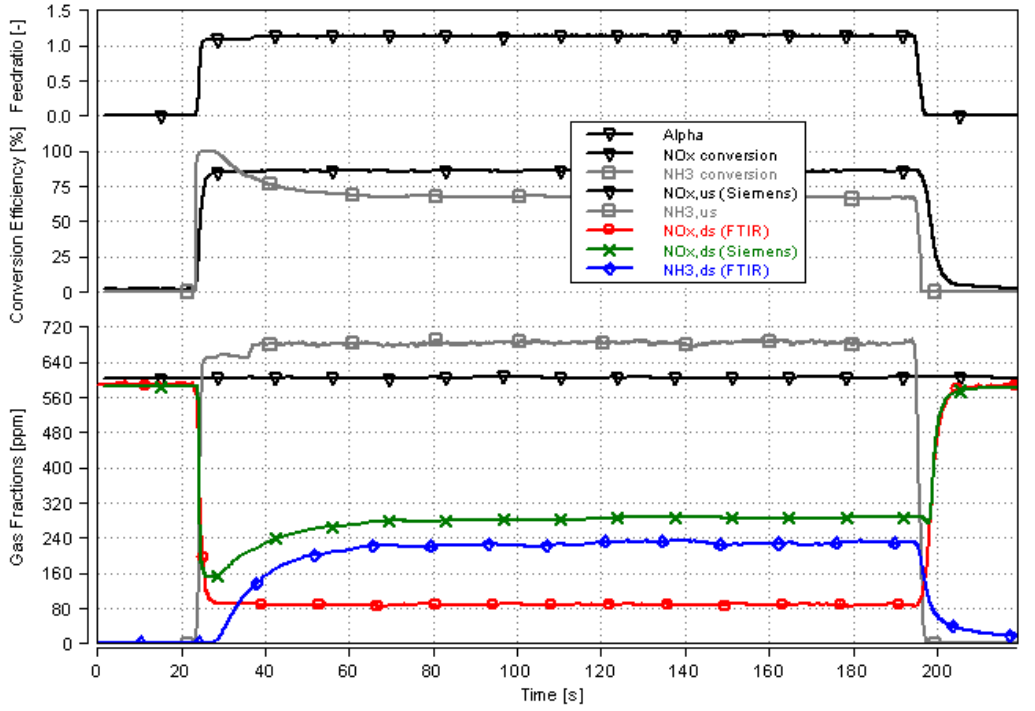

Figure A.11: Step response for $\alpha = 0 \rightarrow 1.2$ in OP 5

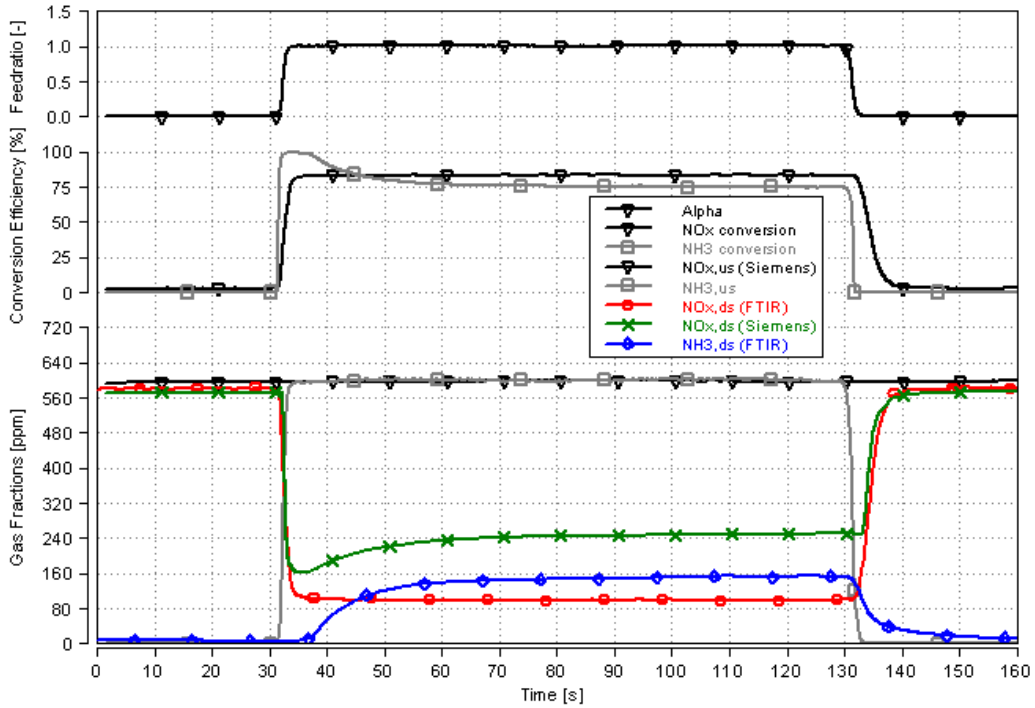

Figure A.12: Step response for $\alpha = 0 \rightarrow 1.0$ in OP 6

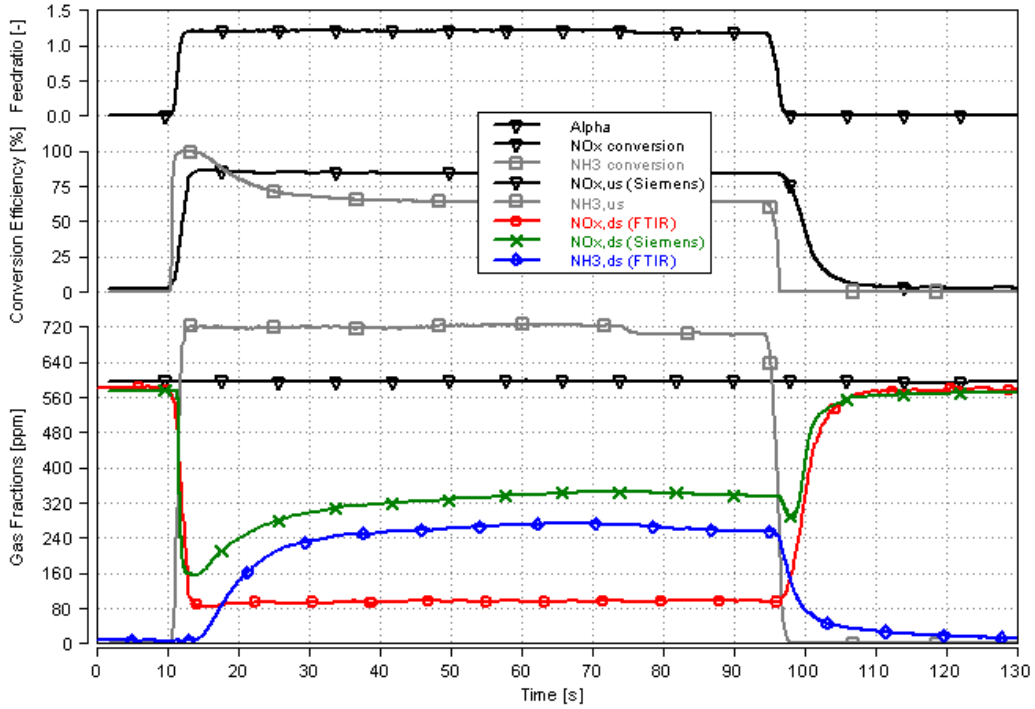

Figure A.13: Step response for $\alpha = 0 \rightarrow 1.2$ in OP 6

A.2 Verification of the SCR Model in FTP - 75

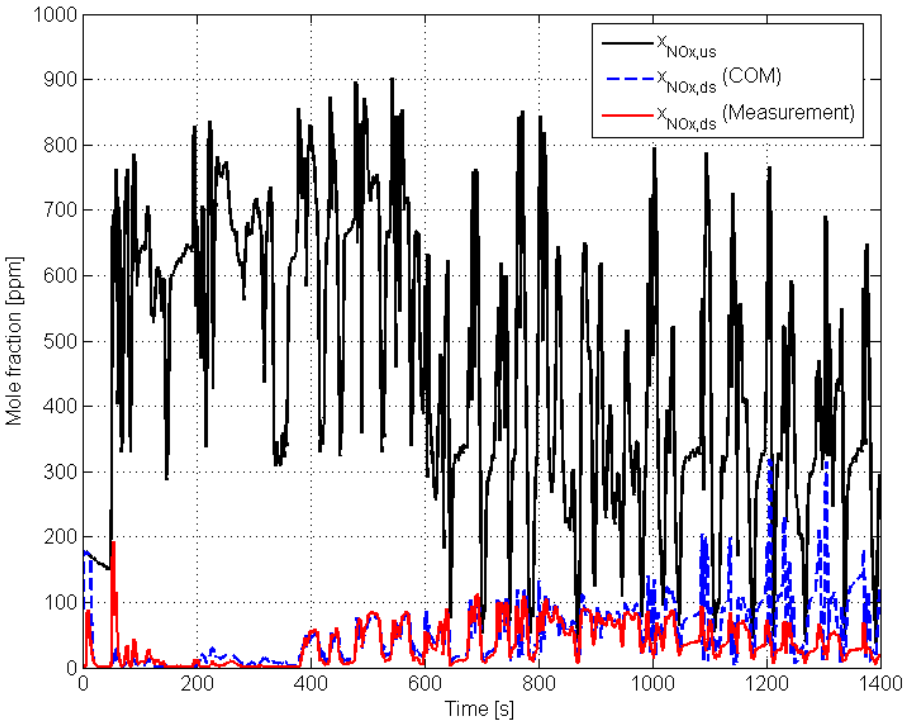

Figure A.14: NO_x fractions comparison in FTP ($\alpha = 1.6$)

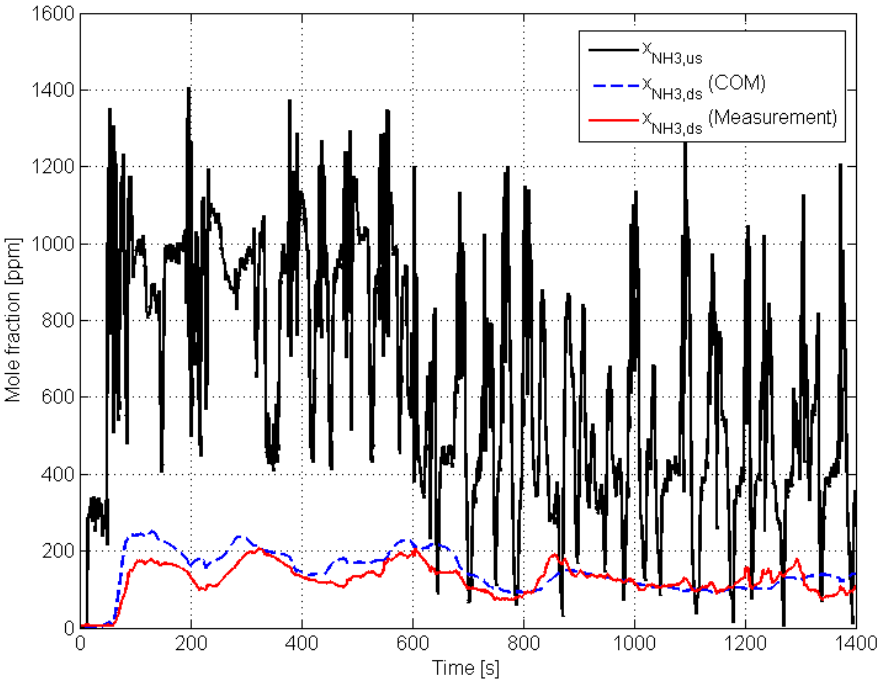

Figure A.15: NH_3 fractions comparison in FTP ($\alpha = 1.6$)

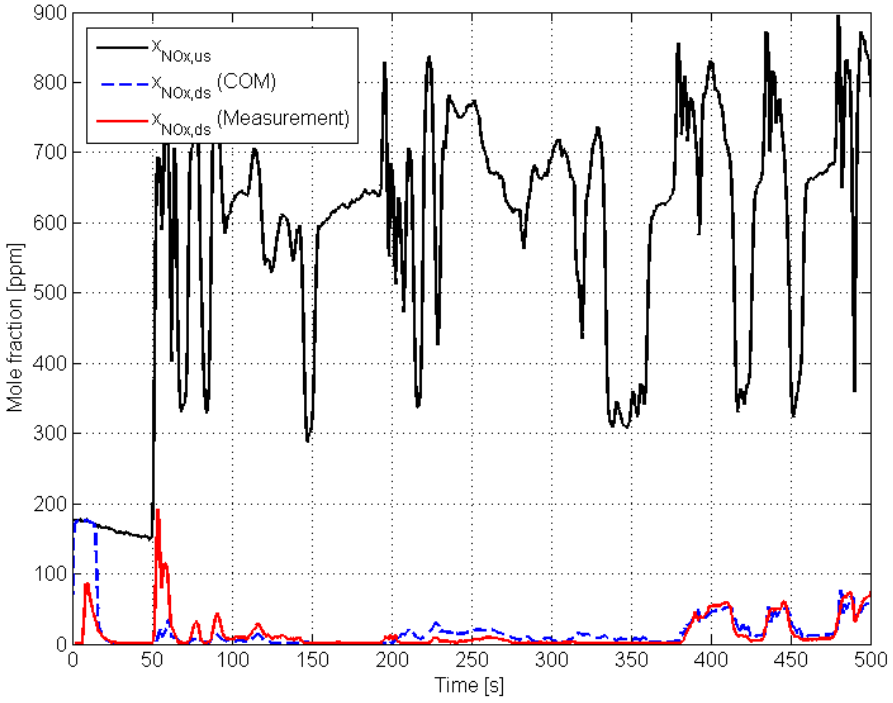

Figure A.16: NO_x fractions comparison in FTP ($\alpha = 1.6$) from $t = 0 \ldots 500\,\mathrm{s}$

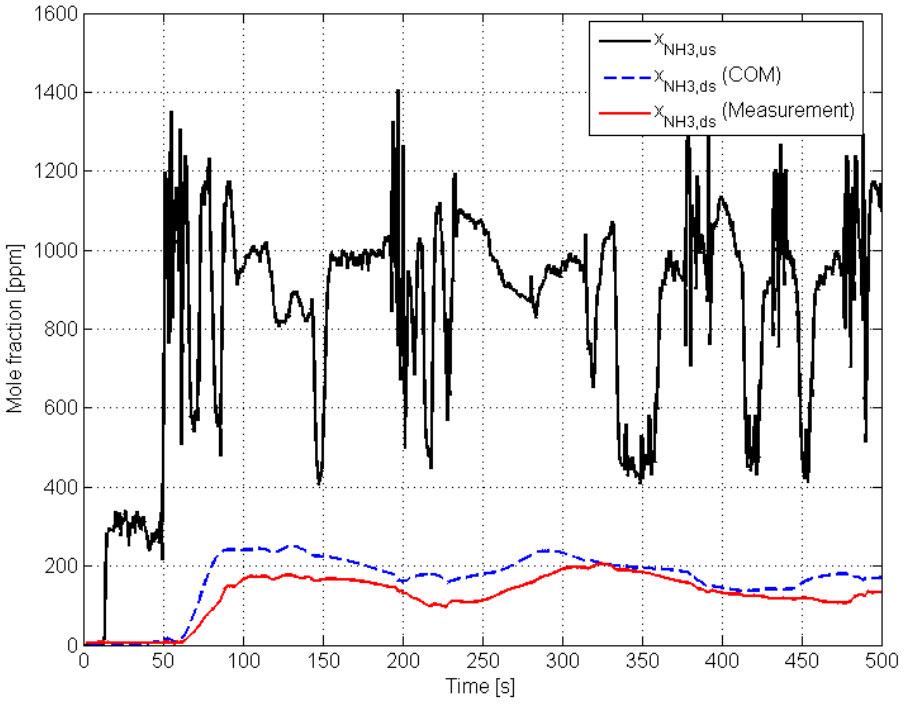

Figure A.17: NH_3 fractions comparison in FTP ($\alpha = 1.6$) from $t = 0 \ldots 500\,\mathrm{s}$

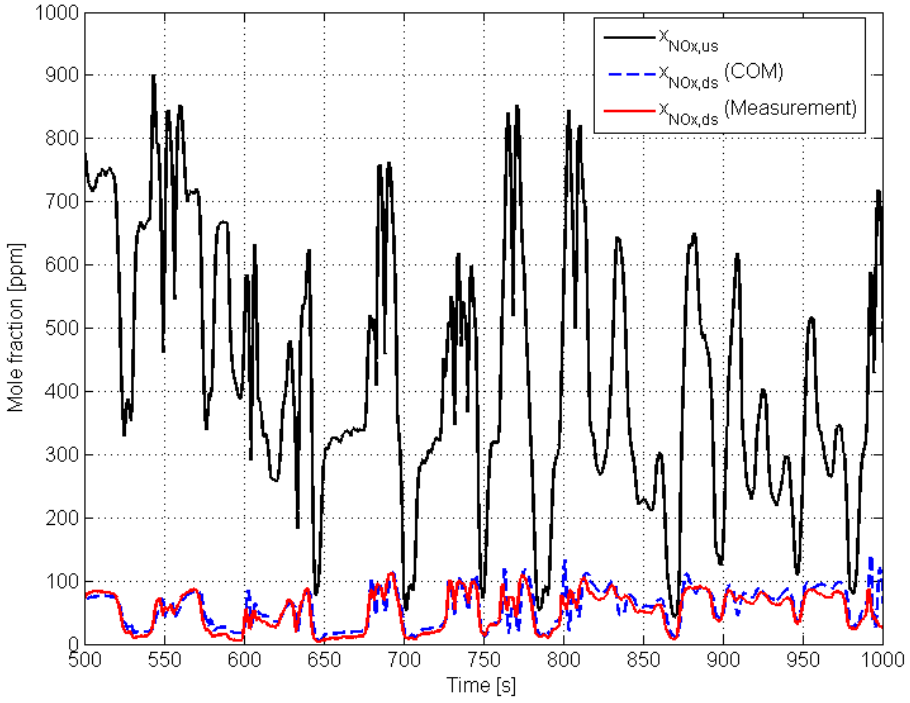

Figure A.18: NO_x fractions comparison in FTP ($\alpha = 1.6$) from $t = 500 \ldots 1000\,\mathrm{s}$

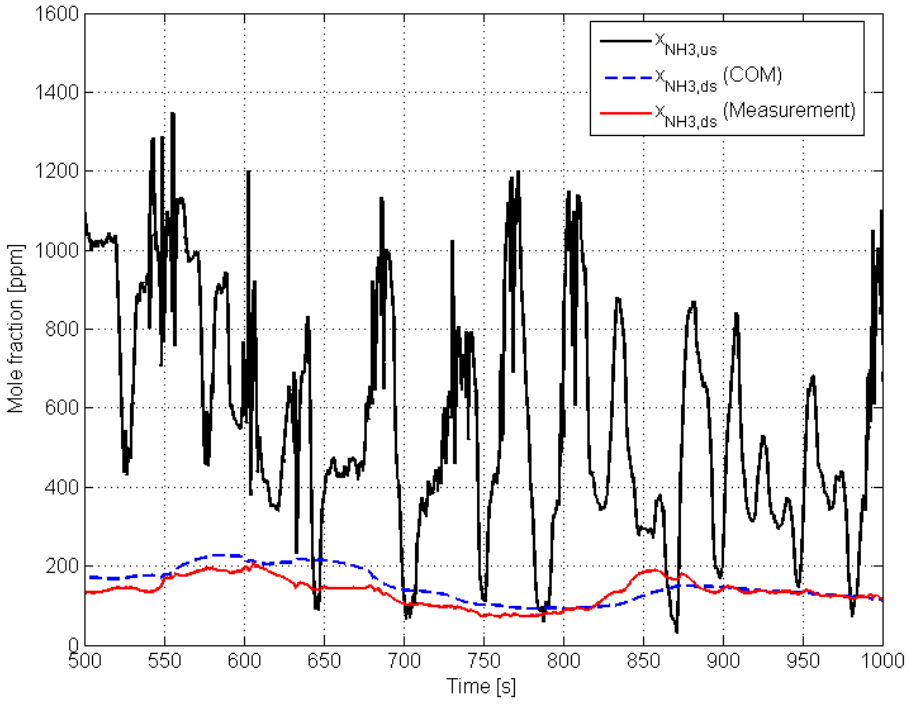

Figure A.19: NH_3 fractions comparison in FTP ($\alpha = 1.6$) from $t = 500 \ldots 1000\,\mathrm{s}$

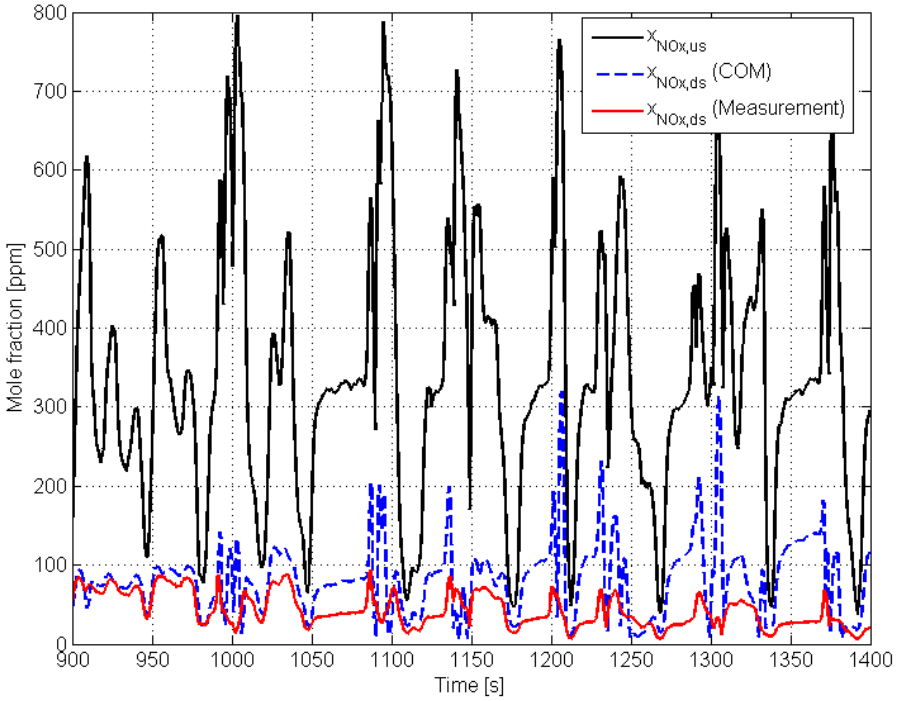

Figure A.20: NO_x fractions comparison in FTP ($\alpha = 1.6$) from $t = 900 \ldots 1400\,\mathrm{s}$

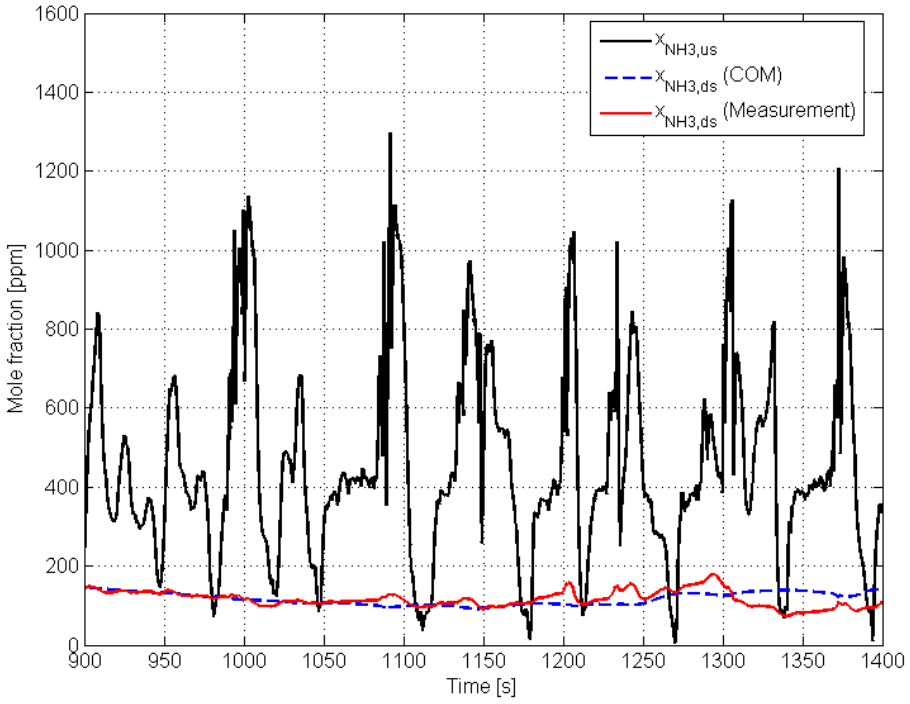

Figure A.21: NH_3 fractions comparison in FTP ($\alpha = 1.6$) from $t = 900 \ldots 1400\,\mathrm{s}$

Appendix B

Parameters, Curves and Maps

B.1 Characteristics of an 2^{nd} Order Systems

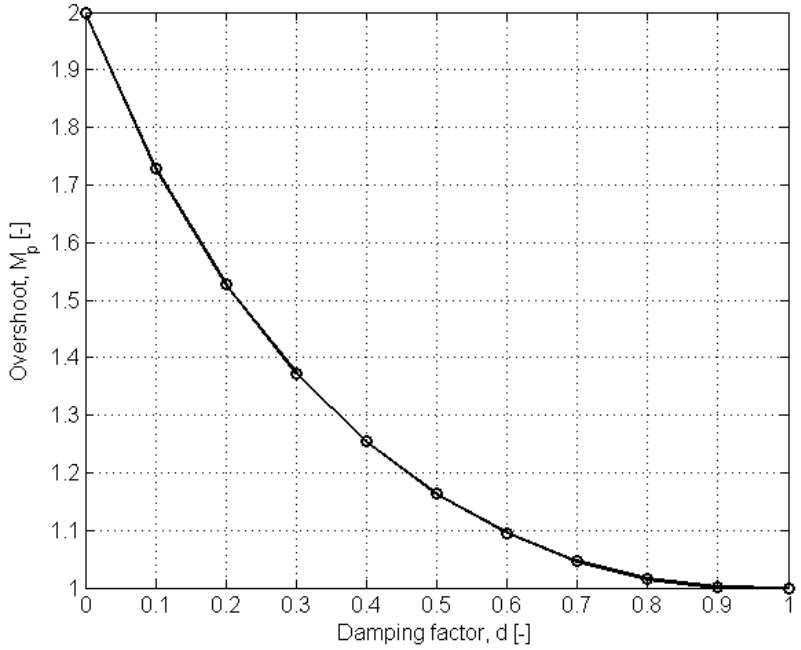

Figure B.1: Relationship between overshoot M_p and damping factor d

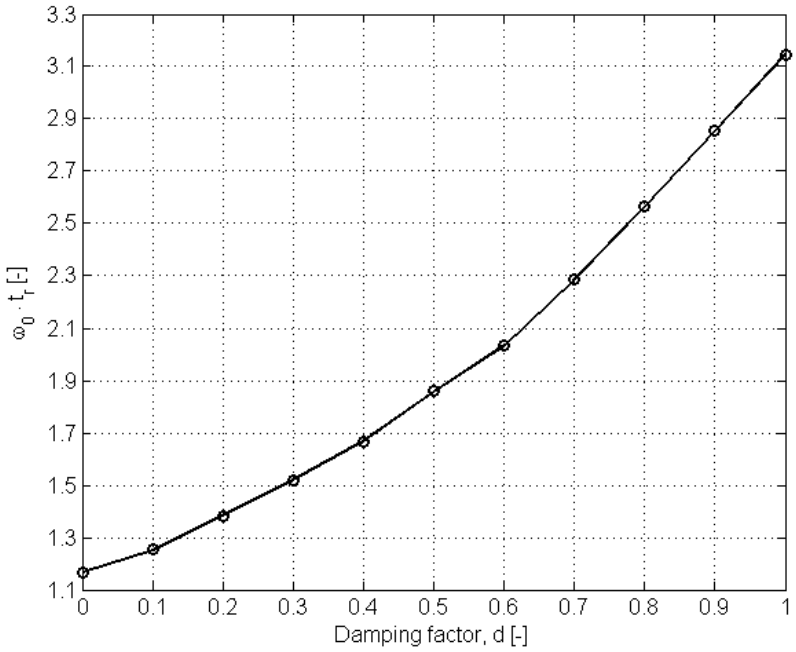

Figure B.2: Relationship between $\omega \cdot t_r$ and damping factor d

B.2 Parameter Maps of the *Loading Controller*

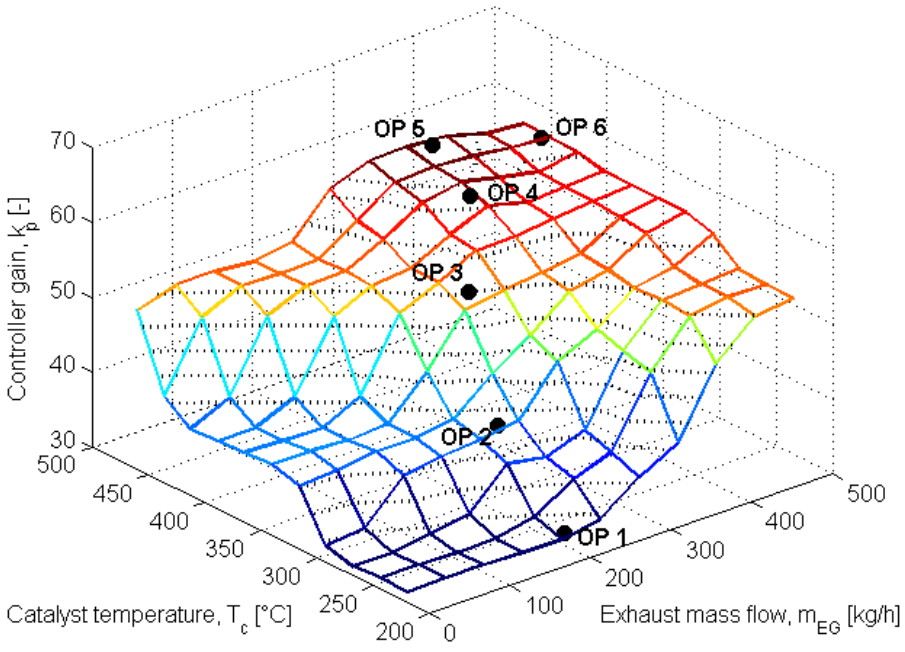

Figure B.3: Map of controller gain k_p

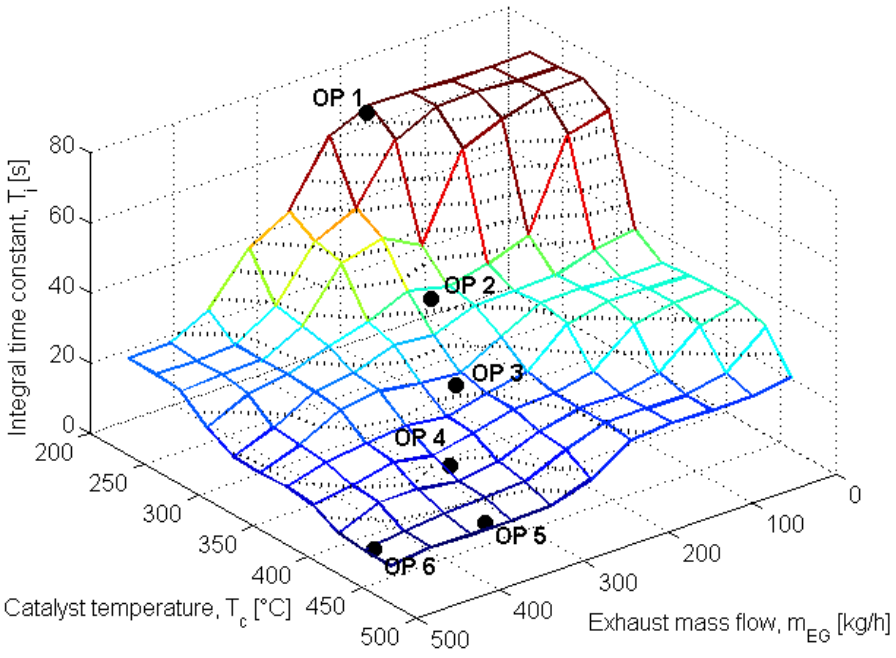

Figure B.4: Map of integral time constant T_i

Bibliography

[1] R. van Basshuysen and F. (Hrsg.) Schäfer. *Handbuch Verbrennungsmotor*. Vieweg-Verlag, 1st edition, 2002.

[2] Auto-Presse.de. *Weltweiter Kraftfahrzeugbestand: Milliardengrenze*. `www.auto-presse.de/news-auto.php?action=view\&newsid=22756`, January 2008.

[3] P. Hoffmann. *Hybridfahrzeuge*. TU-Wien, lecture notes edition, 2008.

[4] R. van Basshuysen and F. (Hrsg.) Schäfer. *Lexikon Motorentechnik*. Vieweg-Verlag, 1st edition, 2004.

[5] R. Bosch GmbH. *Automotive Handbook*. Springer-Verlag, 2nd edition, 1986.

[6] H. Eichelseder. *Kolbenmaschinen*. VKM-THM TU-Graz, lecture notes edition, 1999.

[7] L. Guzella and C. H. Onder. *Introduction to Modeling and Control of Internal Combustion Engine Systems*. Springer-Verlag, 1st edition, 2004.

[8] H. Eichelseder. *Verbrennungskraftmaschinen, Vertiefte Ausbildung*. VKM-THM TU-Graz, lecture notes edition, 2005.

[9] M. Decker. *Entwicklung eines schnellen Aufheizverfahrens fuer einen SCR-Katalysator beim Dieselmotor*. Master's thesis, VKM-THM TU-Graz, 2008.

[10] Dieselnet.com. *Emissions standards*. `www.dieselnet.com/standards/`, June 2009.

[11] Dieselnet.com. *Selective Catalytic Reduction*. `www.dieselnet.com/tech/cat_scr.html`, November 2003.

[12] M. Koebel and M. Elsener. *Vor- und Nachteile stickstoffhaltiger Reduktionsmittel beim Einsatz in mobilen SCR-Systemen*. In *3. Dresdner Motoren-Kolloquium*, 1999.

[13] O. Kröcher. *New challenges for urea-SCR systems: From vanadia-based to zeolite-based SCR catalysts*. Paul Scherrer Institute, 2007.

[14] Dieselnet.com. *SCR Systems for Mobile Engines*. `www.dieselnet.com/tech/cat_scr_mobile.html`, June 2005.

[15] J. Lunze. *Regelungstechnik 1*. Springer-Verlag, 5th edition, 2006.

[16] E. Müller-Erlwein. *Chemische Reaktionstechnik*. Teubner-Verlag, 1st edition, 1998.

[17] F Willems et al. *Is Closed - Loop SCR Control Required to Meet Future Emission Targets?* In *SAE 2007 - 01 - 1574*, 2007.

[18] R. Bosch GmbH. Denoxtronic. `www.rb-k.bosch.de/de/leistungverbrauchemissionen/dieselsysteme/dieselsysteme/pkw/abgasnachbehandlung/denoxtronic/index.html`, July 2009.

[19] C. Schär. *Control of a Selective Catalytic Reduction Process.* PhD thesis, ETH Zürich, 2003.

[20] AVL-List GmbH, Hans List Platz 1. *SESAM-FTIR Mehrkomponenten-Abgasmessystem.*

[21] L. Lietti et al. *Transient kinetic study of the SCR - DeNOx reaction.* In *Catalysis Today (1998) 85-92*, 1998.

[22] Siemens VDO. *Specification Smart NOx Sensor.*

[23] H. Schweiger. *Untersuchung des Einflusses von Kohlenwasserstoffen auf den NOx - Umsatz bei Selektiver Katalytischer Reduktion.* Master's thesis, VKM-THM TU-Graz, 2009.

[24] J. Wurzenberger and R. Wanker. *Multi - Scale SCR Modeling, 1D Kinetic Analysis and 3D System Simulation.* In *SAE 2005 - 01 - 0948*, 2005.

[25] C. Roduner. *H∞ - Regelung linearer Systeme mit Totzeiten.* PhD thesis, ETH Zürich, 1997.

[26] J. Lunze. *Regelungstechnik 2.* Springer-Verlag, 5th edition, 2008.

[27] D.G. Luenberger. *Observing the State of Linear Systems.* In *IEEE Transactions on Military Electronics*, 1964.

[28] D.G. Luenberger. *Observer for Multivariable Systems.* In *IEEE Transactions on Automatic Control*, 1966.

[29] O. Levenspiel. *Chemical Reaction Engineering.* John Wiley & Sons, 3rd edition, 1999.

[30] E. Fitzer, W. Fritz, and G. Emig. *Technische Chemie.* Springer-Verlag, 4th edition, 1995.

[31] AVL-List GmbH, Hans List Platz 1. *AVL Boost Aftertreatment Manual.*

[32] Dieselnet.com. *Emission Test Cycles: FTP - 75.* `www.dieselnet.com/standards/cycles/ftp75.html`.

[33] Dieselnet.com. *Emission Test Cycles: ETC.* `www.dieselnet.com/standards/cycles/etc.html`.

[34] C. Chen. *Analog & Digital Control System Design.* Saunders College Publishing, 1st edition, 1993.

[35] H. Lutz and W. Wendt. *Taschenbuch der Regelungstechnik*. Harri Deutsch Verlag, 5th edition, 2003.

[36] B. Friedland. *Advanced control system design*. Prentice - Hall Inc., 1st edition, 1996.

[37] H. Khalil. *Nonlinear systems*. Pearson Education, 3th edition, 2000.

[38] M. Horn and N. Dourdoumas. *Regelungstechnik*. Pearson Studium, 1st edition, 2004.

[39] AVL-List GmbH. *AVL DynoExact*. `www.avl.com/wo/webobsession.servlet.go/encoded/YXBwPWJjbXMmcGFnZT12aWV3JiZub2RlaWQ9NDAwMDEzMTgy.html`.

Statement

Herewith I affirm that I have written this thesis on my own. I did not enlist unlawful assistance of someone else. Cited sources of literature are perceptibly marked and listed at the end of this thesis. The work was not submitted previously in same or similar form to another examination committee and was not yet published.

(Place, Date) (Signature)